November 2016

Transit Preferential Treatments at Signalized Intersections: Person-based Evaluation and Real-Time Signal Control

Yashar Zeiynali Farid

TRANSIT PREFERENTIAL TREATMENTS AT SIGNALIZED INTERSECTIONS: PERSON-BASED EVALUATION AND REAL-TIME SIGNAL CONTROL

A Dissertation Presented

by

YASHAR ZEINALI FARID

Submitted to the Graduate School of the
University of Massachusetts Amherst in partial fulfillment
of the requirements for the degree of

DOCTOR OF PHILOSOPHY

September, 2016

Civil and Environmental Engineering

TRANSIT PREFERENTIAL TREATMENTS AT SIGNALIZED INTERSECTIONS: PERSON-BASED EVALUATION AND REAL-TIME SIGNAL CONTROL

A Dissertation Presented

by

YASHAR ZEINALI FARID

Approved as to style and content by:

Eleni Christofa, Chair

John Collura, Member

Ahmed Ghoniem, Member

Richard N. Palmer, Department Head
Civil and Environmental Engineering

ACKNOWLEDGMENTS

This work was partially funded by the US DOT through the New England University Transportation Center.

ABSTRACT

TRANSIT PREFERENTIAL TREATMENTS AT SIGNALIZED INTERSECTIONS: PERSON-BASED EVALUATION AND REAL-TIME SIGNAL CONTROL

SEPTEMBER, 2016

YASHAR ZEINALI FARID

B.S., URMIA UNIVERSITY

M.S., TARBIAT MODARES UNIVERSITY

Ph.D., UNIVERSITY OF MASSACHUSETTS AMHERST

Directed by: Professor Eleni Christofa

Efficient public transportation has the potential to relieve traffic congestion and improve overall transportation system performance. In order to improve transit services, Transit Preferential Treatments (TPT) are often deployed to give transit vehicles priority over other vehicles at an intersection or along a corridor. Examples of such treatments are exclusive bus lanes, queue jumper lanes, and signal priority strategies. The objective of this study is threefold: 1) perform a person-based evaluation of alternative TPTs when considered individually and in combination, 2) develop a bus travel time prediction model along a signalized arterial, and 3) develop a real-time signal control system, which minimizes total person delay at an isolated intersection accounting for stochasticity in transit vehicle arrivals. This study first develops analytical models to estimate person delay and person discharge flow when

various spatial and time TPTs are present at signalized intersections with and without near-side bus stops. This part of the research has contributed to the modeling of traffic along signalized arterials by improving the previous models to evaluate various TPT strategies with and without nearside bus stops. Next, a robust method to predict bus travel time along a signalized arterial is developed. This part of the research contributes to the bus travel time prediction models by estimating the status of traffic signals using automated vehicle location (AVL) data. The model decomposes bus travel time along signalized arterials and infers trajectories of the transit vehicles. Finally, the real-time signal control system is developed to provide priority to transit vehicles by assigning weights to transit vehicle delays based on their passenger occupancies as part of the optimization objective function. The system optimizes the movements by minimizing total person delay at the intersection. The system estimates bus arrival time at the intersection stopline and uses the developed analyitical models in the first part of the research to evaluate the person delay measure. This part of the research contributes to the real-time signal control systems by providing a priority window to account for the stochasticity in bus arrival times.

TABLE OF CONTENTS

LIST OF TABLES

LIST OF FIGURES

Figure **Page**

GLOSSARY

Chapter 3

C: cycle length [sec];

$D_{j,T}$: total delay of autos in lane group j during cycle T [veh-sec];

$d_{j,T}$: delay of a single vehicle in the platoon in lane group j during a cycle T [sec];

$d_{b,T}$: delay of a single bus b during a cycle T [sec];

$d_{b,f}$: bus dwell time at bus stop f for bus b [sec];

G_j^e: effective green time for the phase that serves lane group j [sec];

j: lane group index (movement);

K_j: jam density [veh/ft];

$N_{j,T-1}^i$: case i residual queue size of lane group j at the end of the previous cycle T -1 [veh];

$n_{b,T}$: position of bus b in the platoon during cycle T [veh];

$P_{j,T}$: total platoon size of lane group j during cycle T;

$P_{j,T}^i$: case i platoon size of lane group j during cycle T;

$Q_{j,T}$: auto vehicle discharge flow during cycle T [vph];

$R_j^{(1)}$: component of the red time from the beginning of the cycle until the start of the green time for lane group j [sec];

$R_j^{(1),Next}$: $R_j^{(1)}$ of the next cycle [sec];

$R_j^{(2)}$: component of the red time from the end of the green until end of the cycle for lane group j [sec];

s_j: total saturation flow of lane group j [vpm];

s_j^i: saturation flow for the vehicles in lane group j that belong to case i [vpm];

T: signal cycle index;

$t_{b,q}$: time it takes to serve the vehicles that are in queue in front of bus b [sec];

$t_{j,T}$: platoon arrival time at the intersection of lane group j during cycle T [sec];

$t_{b,T}$: arrival time of bus b at the intersection during cycle T if the bus does not dwell at a bus stop [sec];

$t_{b,T}^D$: arrival time of bus b at the intersection during cycle T if the bus dwells at a bus stop [sec];

$t_{l,T}$: waiting time before a lane change occurs for vehicles that change lanes during cycle T [sec];

X_b: bus position from the stopline when it arrives in queue [ft];

X_f: distance of bus stop f from the stopline [ft];

X_{qj}: queue jumper lane length [ft]; α^p: the portion of lanes serving vehicles associated with platoon p.

Chapter 4

$I_N = \{1, 2, .., N\}$: Set of network intersections,

$I_B = \{1, 2, .., B\}$: Set of buses traveling through the arterial segment,

$I_A = \{1, 2, .., i\}$: Set of ordered AVL records,

$I_K = \{1, 2, , K\}$: Set of bus stops,

$I_{N_{i,j}}$ is a subset of I_N that includes the signalized intersections between AVL records i and j,

I_b is a subset of I_A that includes the AVL records for bus $b \in I_B$,

$I_{K_{i,j}}$ is a subset of I_K that includes the bus stops between AVL records i and j,

$\bar{p}$: Average bus pace along a segment (sec/mile),

$\bar{v}$: Average bus speed along a segment (miles/sec),

t_{gr}^n: Beginning of the green signal indication for the direction of interest at intersection n as measured from the beginning of the cycle (sec),

t_b^n: Bus b arrival time at intersection n as measured from the beginning of the cycle (sec),

$tt_b^{u,n}$: Bus b travel time from the AVL record reported upstream of the intersection n to the intersection n stop line (sec),

$\hat{tt}_{b,i,j}$: Bus b travel time from AVL record i to j,

$\bar{w}^k$: Average dwell time at bus stop k (sec/bus),

$D_{b,1}^n$, $D_{b,2}^n$, $D_{b,3}^n$, $D_{b,4}^n$: Delay of bus b at intersection n for different cases (sec),

$\bar{D}^n$: Average bus delay at intersection n (sec),

D_b^n: Delay of bus b at intersection n (sec),

$\bar{a}^n$: Average lost time at intersection n (sec),

$\bar{ad}$: Average acceleration/deceleration lost time (sec),

$x_{b,1}^n$, $x_{b,2}^n$, $x_{b,3}^n$, $x_{b,4}^n$: Binary variables indicating the delay case that bus b at intersection n belongs to,

$y_{b,1}^n$, $y_{b,2}^n$: Binary variables indicating the bus arrival time case that bus b at intersection n belongs to,

$t_{b,i}$: Bus b AVL record i time stamp (sec),

$t_b^{u,n}$: Bus b most recent time stamp upstream of intersection n (sec) as measured from the beginning of a cycle (sec),

$l_{b,i,j}$: distance traveled by bus b between records i and j (miles),

$l_b^{u,n}$: distance between most recent record of bus b upstream of intersection n and intersection n stop line (miles),

$AD_{b,i,j}$: Number of acceleration/deceleration events from AVL record i to j for bus b, M: Big number,

C^n: Signal cycle length of intersection n (sec),

r^n: Signal red phase duration for the direction of interest at intersection n (sec),

g^n: Signal green phase duration for the direction of interest at intersection n (sec).

Chapter 5

$M_a = \{1, 2, .., 6\}$: Set of auto delay cases,

$M_b = \{1, 2, .., 16\}$: Set of transit delay cases,

$J = \{1, 2, .., j\}$: Set of lane groups,

$I = \{1, 2, .., i\}$: Set of signal phases,

$B = \{1, 2, .., b\}$: Set of total transit vehicles during cycle T,

$B_j = \{1, 2, .., b_j\}$Set of the transit vehicles traveling on the lane group j during cycle T,

G_j^e: effective green time for the phase that serves lane group j (sec),

za_j^m: variable introduced to defeat bilinearity in determining delay of autos traveling in lane group j for case m,

$zb_{j,b}^m$: variable introduced to defeat bilinearity in determining delay of transit vehicle b traveling in lane group j for case m,

x_j^m: Binary variable indicating the delay case that autos in lane group j belong to,

$y_{j,b}^m$: Binary variable indicating the transit vehicle sub-case that transit vehicle b in lane group j belongs to,

E_b^1, E_b^2, and E_b^3: Binary variable indicating the transit vehicle case (i.e., within, ahead, or behind the platoon) that transit vehicle b in lane group j belongs to,

C: cycle length (sec),

$N_{j,T-1}$: residual queue size of lane group j at the end of the previous cycle T -1 (veh),

$P_{j,T}$: total platoon size of lane group j during cycle T,

s_j: total saturation flow of lane group j (vpm),

$tb_{b,T}$: arrival time of transit vehicle b at the intersection during cycle T (sec),

$t_{j,T}$: platoon arrival time at the intersection of lane group j during cycle T (sec),

t_T: beginning of the cycle (sec),

$\bar{o}_a$ average auto occupancy (passenger/car),

$\bar{o}_b$ average transit vehicle occupancy (passenger/transit vehicle),

$Z_{\alpha/2}$ = the value from the standard normal distribution for the confidence level $(1 - \alpha)\%$,

σ = standard deviation of transit arrival time predictions,

$Da_{j,T}$: total delay of autos in lane group j during cycle T (veh-sec),

$Da^s mj, T$: delay of autos in lane group j during cycle T for delay case m $m \in M_a$ (veh-sec),

$Db_{j,T}$: total delay of transit vehicles in lane group j during cycle T (veh-sec),

$Db_{j,T}^m$: delay of transit vehicles in lane group j during cycle T for delay case m $m \in M_b$ (veh-sec),

$R_j^{(1)}$: component of the red time from the beginning of the cycle until the start of the green time for lane group j (sec),

$R_j^{(2)}$: component of the red time from end of the green until end of the cycle for lane group j (sec),

T: signal cycle index.

CHAPTER 1

INTRODUCTION

1.1 Motivation

Public transportation helps improve quality of life and is a crucial part of solutions to address economic, energy, and environmental challenges in urban areas. High quality public transportation improves mobility for people especially the ones that are unable to drive (elderly, teenagers, and the disabled), provides access to activity areas (e.g. work, school, and shopping centers), improves environmental and ecological sustainability, and reduces traffic congestion and fuel consumption. Improvements in transit performance provide additional incentives for travelers to switch modes and could potentially reduce traffic congestion. According to the Texas A&M Transportation Institute report (Schrank et al., 2012), if public transportation were not available in the urban areas that were studied, congestion related costs would have risen by nearly $21 billion for 2011.

Public transportation system performance can be improved by giving transit vehicles, which have higher passenger occupancy than cars, priority at the intersections or along corridors. These strategies may significantly increase the person throughput of the system. Thus, in recent years, urban traffic management policies have increasingly differentiated between transit vehicles and cars by providing priority to the transit vehicles.

In order to provide priority to transit vehicles, transit preferential treatments (TPTs) are deployed. TPTs give transit vehicles priority over other vehicles at an intersection or along a corridor. The primary objective of TPTs is to reduce transit

travel times by shortening or eliminating the time spent by transit vehicles waiting for a queue clearance or a green signal indication. Substantial delay reductions can further lead to improved transit operations and service reliability and consequently increased transit ridership.

Transit signal priority (TSP) is a TPT strategy which adjusts signal timings to favor transit vehicles approaching a signalized intersection. TSP strategies as well as other applications of intelligent transportation systems (ITS) including advanced traveler information systems (ATIS) rely on short-term travel time predictions. Accurate predictions can improve bus service reliability and traffic signal control efficiency while providing TSP.

Real-time signal control systems is an effective way of providing TSP. Real-time signal control systems with TSP are responsive to transit requests as well as the current traffic conditions in real-time. These systems provide priority while optimizing given traffic performance criteria such as vehicle delay, person delay, and transit delay. In general, real-time signal control systems with TSP require traffic detection (both transit and non-transit vehicles) and communication systems, estimation of appropriate performance measures, estimation of traffic demand and bus arrival time to stopline, and a decision system.

1.2 Problem Statement

The need for efficient and sustainable management of transportation systems is steadily increasing due to growing demand in urban networks. Urban congestion, higher fuel consumption and emissions are major problems of large urban areas, but can be mitigated by efficient transit systems. Transit preferential treatments are promising strategies for reducing transit delay and improving transit performance. Some treatments modify roadway segments (space priority strategies) such as dedicated bus

lanes, queue jumper lanes, and intermittent bus lanes while other treatments provide priority by adjusting signal timing settings (time priority strategies).

Implementing priority strategies are often expensive, especially space priority strategies. Pre-evaluation of these strategies would help planners and decision makers in assessing the advantages and disadvantages of the plans before their deployment. Currently, most of the agencies evaluate TPT plans using micro-simulation software packages which require considerable time and money. Accurate and reliable analytical models could be used for such assessments without the need for expensive simulations. The analytical models can also be used in real-time signal control systems to evaluate various performance measures.

Among various transit signal priority strategies, real-time TSP systems can potentially handle traffic movements through an intersection more efficiently, since they can adjust signal timing plans based on real-time data. Various real-time TSP models have been developed in recent years. These models often rely on predictions of bus arrival time. Accurate prediction of bus arrival time at an intersection stopline can improve the efficiency of the real-time TSP systems. Transit vehicle travel time is subject to traffic conditions as well as driver behavior. Also, bus dwell times at bus stops vary due to different factors such as the number of passengers boarding and alighting, the fare collection system as well as the bus and bus stop design. Variability in transit arrival times may affect the quality of priority timings, which in turn affects the effectiveness of the TSP system. Accurate bus travel time prediction as well as the stochasticity of bus arrival times and its impact on the real-time TSP systems require further investigation.

1.3 Research Questions

The question that motivates this research are:

- *What are the impacts of implementing individual or combined TPTs on person delay and person discharge flows along signalized arterials?*
- *How bus arrival time at intersection stopline can be estimated more accurately?*
- *How should real-time signal control systems be designed to minimize person delay while accounting for stochasticity in bus arrivals?*

1.4 Research Contributions

The objective of this study is threefold: First, this study performs a person-based evaluation of alternative TPTs when considered individually and in combination. This study develops analytical models based on kinematic wave theory as well as simulation models in order to perform a person-based evaluation of various spatial and time TPTs when near-side bus stops are present at signalized intersections. Second, a robust model to predict bus travel time using low resolution Automated Vehicle Location (AVL) data is presented. Finally, this study proposes a real-time signal control system which minimizes total person delay at an isolated intersection accounting for stochasticity in transit vehicle arrivals to provide priority to them. The contributions of this dissertation are as follows:

- Development of analytical models to evaluate various space (e.g., queue jumper lane and dedicated bus lane) and time (e.g., transit signal priority) priority strategies along signalized arterials with and without nearside bus stops. The analytical models evaluate person-based performance measures including person delay and person discharge flow using Kinematic Wave Theory. Vehicles approaching the signalized intersection are considered to travel within platoons.
- Development of a bus travel time prediction model using data obtained from AVL systems. The proposed model estimates traffic signal status using the AVL records of buses and provides more accurate predictions in comparison to

a simple linear regression model. The proposed model decomposes bus travel time into its components including running travel time, dwell times at bus stops, and delays at intersections. Unlike other studies, the developed model in this research estimates intersection delay for individual buses rather than estimating an average delay over all buses thus, improves prediction accuracy.

- Development of a real-time traffic signal control with TSP which takes into account stochasticity in bus arrivals and provides a priority window for buses. The control system minimizes total person delay at an intersection. The person delay measures are determined using the analytical models developed for the TPT evaluation. This study is unique since the developed control system provides a priority window to make sure that buses can pass the intersection (if arriving during the green phase) considering a certain confidence level to overcome the randomness in the bus arrival time predictions.

1.5 Dissertation Organization

The rest of the dissertation is organized as follows: In Chapter 2 previous studies on TPT evaluation, bus travel time prediction, and real-time signal control systems are reviewed. Chapter 3 presents the formulation of the analytical models for estimating different person-based measures of various TPT strategies and the model application. In Chapter 4, the development of the bus travel time prediction model using low resolution AVL data as well as the application of the model are presented. In Chapter 5, a real-time signal control plan development and its application are discussed. Finally, Chapter 6 includes a summary of the key findings, the dissertation's contribution, and future research directions.

CHAPTER 2

LITERATURE REVIEW

This chapter reviews previous studies on transit preferential treatments, bus travel time prediction, real-time signal control with TSP systems, and stoachasticity in transit vehicle arrivals. It concludes with the summary of the literature review that provides insights to motivate research.

2.1 Transit Preferential Treatments

TPTs can be categorized in space and time priority strategies. The impact of both space and time TPTs on traffic and transit operations has been extensively investigated through field, simulation, and analytical studies. In the field studies, before and after impacts associated with TPT deployment have been assessed. In the field studies, typically different measures of effectiveness (MOEs) are used to assess impacts associated with preferential treatment deployment. These MOEs commonly include travel time, number of stops, transit delay, schedule adherence, average person delay, and cross-street delays. Use of simulation models, including VISSIM, INTEGRATION, AIMSUN, and PARAMICS, is the most common TPT evaluation method. There are only a few studies that have utilized analytical models for TPT evaluation purposes.

2.1.1 Space Transit Preferential Treatments

Space priority considers special facilities such as dedicated bus lanes (DBL), queue jumper lanes (QJL), or intermittent bus lanes (IBL) for public transit vehicles that

allow them to bypass standing traffic queues. Delay due to congestion can be reduced by mitigating congestion and/or implementing space preferential treatments through the creation of dedicated space for transit vehicles. These treatments allow transit vehicles to bypass standing traffic queues, thereby reducing their travel times. Space priority strategies are often effective in reducing delays due to congestion, however these solutions can be expensive or even infeasible, especially in dense urban areas, due to inadequate or expensive urban space.

2.1.1.1 Dedicated Bus Lanes (DBL)

DBLs (also known as exclusive bus lanes, reserved bus lanes or just bus lanes) provide exclusive right-of-way to buses ensuring that they are not delayed by other traffic (Figure 2.1). The effectiveness of DBLs in increasing transit speed and improving transit reliability in arterials has been thoroughly investigated in the literature. However, in areas with intense commercial and residential developments, allocating a bus lane per direction could often be very expensive and in some cases infeasible due to space limitations. Thus, single reversible DBLs are often introduced to reduce deployment costs and increase in delays.

Figure 2.1: Dedicated bus lane (*source: Wikipedia*)

Field Studies

Surprenant-Legault and El-Geneidy (2011) analyzed a DBL that was implemented on Boulevard Saint-Michelusing, Montreal, Canada. The analysis of real-world data showed that the DBL had a substantial positive effect on the running time, reliability and on-time performance of the bus routes. Total running time for the buses decreased by 1.3% to 2.2%, and schedule adherence improved by 65%.

Sakamoto et al. (2007) evaluated the effects of a bus rapid transit (BRT) line implemented in Shizuoka City, Japan. The BRT line included a 3 km long DBL and a bus priority signal system. Before and after analysis indicated that the mean total bus travel time on the two studied lines dropped by 6.2% and schedule adherence improved by 17% to 58%.

Reserved lanes have also been implemented for rail transit systems such as trams. Currie et al. (2013) evaluated the effect of a dedicated transit way on tram performance in Melbourne, Australia. In this study regression models were developed using Automatic Vehicle Monitoring (AVM) data to measure the effect of implementing the dedicated transit way as well as transit signal priority. Before and after analysis indicate that the dedicated transit way deployment reduced tram run time by 1.6% and run time variability by 10.2%.

Simulation Studies

Iswalt et al. (2011) developed a micro-simulation model to evaluate a proposed single reversible DBL implementation on Stevens Creek Boulevard, San Jose, California, using the VISSIM micro-simulation software. Results of the study show that a single reversible DBL led to travel time savings of over 10%.

Arasan et al. (2010) analyzed the impact of DBL under highly heterogeneous traffic condition using the HETEROSIM simulation software. In this study the impact of the volume-to-capacity ratio on the non-transit vehicles level of service (LOS)

was analyzed. This study also estimated the probability of switching from a personal vehicle to transit when DBLs are provided.

Analytical Studies

Li et al. (2009) developed an analytical model to evaluate the impacts of a single DBL versus double DBLs implemented as part of a BRT system. In a single DBL, one lane is dedicated to buses in both directions. The study presented an optimization model to minimize the weighted sum of the dwell time and travel time of the buses in the BRT system. A case study analysis concluded that total travel time of the single DBL system is similar to that of a BRT system with double DBL when the headway is longer than 20 minutes. Shorter headways increase bus travel time for the single DBL system due to higher intersection delays.

2.1.1.2 Queue Jumper Lanes (QJL)

QJLs are intersection-specific treatments that allow buses that operate in mixed-traffic lanes to bypass the queue at a signalized intersection. This treatment is a short right-turn lane or a separate bypass lane implemented at the intersection approach. Two types of queue jumper lanes can be implemented depending on whether or not an extra bus signal phase is provided. In Type 1 QJLs (Figure 2.2), an advanced green phase is provided for the buses to pull ahead of through traffic before the signal phase for the rest of the through vehicles is activated. This type of QJL does not require an auxiliary lane for acceleration downstream, but it may lead to increases of through traffic delay. Type 2 QJLs (Figure 2.3), an auxiliary lane on the far-side of the intersection is available to allow buses to merge with the through traffic downstream of the intersection. In this case, a separate signal phase is not provided. Type 2 QJLs are also called queue bypass lanes.

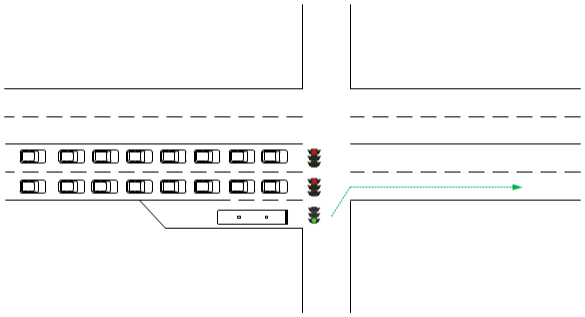

Figure 2.2: Queue jumper lane - Type 1

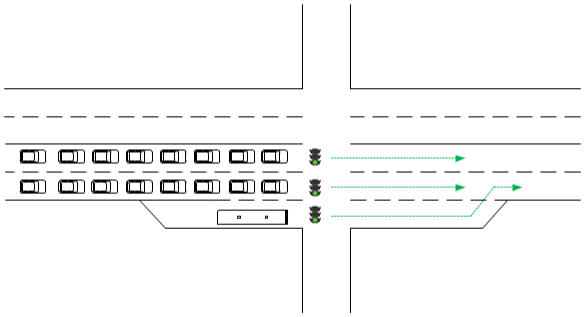

Figure 2.3: Queue jumper lane - Type 2

Field Studies

Reductions of 5% to 15% in bus travel time associated with the implementation of QJLs at intersections have been reported (Danaher et al., 2007) in the following case studies:

- Lincoln Street at 13th Avenue in Denver, 7- 10 second reduction in bus intersection delay;
- NE 45th Street route in Seattle, WA, 27-second, 12-second and 6-second reduction in bus travel time along the corridor during the morning peak, and afternoon peak periods, and across an entire day respectively.

The City of Portland and the Tri-County Metropolitan Transportation District of Oregon (Tri-Met) conducted the Powell Boulevard Bus priority Pilot Project (Kloos

et al., 1994). The test was designed to evaluate the application of TSP strategies as well as a QJL. The QJL was implemented on the 26th Avenue for the eastbound (EB) buses. It included an advanced green phase to enable the bus to pull in front of the eastbound through queued traffic (Type 1 QJL). The buses received a short advanced green phase when they were at the bus stop during a normal eastbound through red phase. Results indicated that generally bus travel times decreased by 5% for the inbound morning peak and decreased by 7.8% for the outbound evening peak directions. Total bus person delay decreased by 12.3%, however, total person delay did not change significantly. The method used in the study resulted in higher delays for the through traffic, especially the westbound one.

Simulation Studies

Several studies have investigated the effect of QJLs combined with TSP on transit performance using micro-simulation software packages. Zlatkovic et al. (2013) used a VISSIM micro-simulation model to evaluate individual and combined effects of queue jumper lanes and TSP on traffic performance of a BRT system in West Valley City, Utah. A QJL was modeled along with an exclusive 8 seconds signal phase at intersections (Type 2 QJL). The results of the study showed that the QJL combined with TSP reduced bus travel time by 13%-22% and increased bus speed by 22%. However, the strategy increased average delay for cross-street traffic by 15%. The individual QJL scenario reduced bus travel time by 6%-15% and increased cross-street traffic delay by 8%. The implementation of individual TSP reduced bus travel times by 9%-11% and increased cross-street traffic delay by 8%.

Lahon (2011) studied the effects of QJL combined with TSP using VISSIM. A QJL was modeled along with a special signal phase (type 2 QJL). Results indicated that the QJL with TSP reduced transit travel time by 30%. The author did not

report the impact of the TPTs on cross street traffic performance.

Anallytical Studies

To the extend of the author's knowledge, there is no study to-date investigating the impact of QJLs on person delays using analytical models.

2.1.1.3 Intermittent Bus Lanes (IBL)

Intermittent bus lanes reduce bus delay by temporarily clearing auto vehicle traffic from a lane for a section under consideration ahead of a bus. When a bus approaches a section where an IBL is implemented, the subject lane becomes a bus lane, and after the bus leaves that section, it becomes a mixed traffic lane again (Viegas and Lu, 2004). An example of IBL implemented in Lisbon, Portugal, is shown in Figure 2.4. The impact of intermittent bus lanes, bus lanes with intermittent priority and other strategies for sharing a lane between cars and buses on traffic operations has also been analyzed through field tests and the development of analytical and simulation models (Eichler and Daganzo, 2006, Viegas and Lu, 2004, Guler and Cassidy, 2012).

Field Studies

Viegas et al. (2007) studied a trial IBL treatment in Lisbon, Portugal (Figure 2.4), for a period of 6 months starting in September 2005. The study showed that the IBL treatment increased bus average speed by 20% with very limited impacts on general traffic operations.

Currie and Lai (2008) reviewed the performance of dynamic fairway (DF), a variation on the IBL concept, implemented in Melbourne, Australia. The system, which was initiated in 2001, is shown in Figures 2.5 and 2.6. When a tram approaches, the pavement lights start flashing and the variable message sign (VMS) changes to right-turn traffic only sign. When the tram passes, the pavement lights turn off and

(a) Vertical signalization- Variable Message Sign

(b) Horizontal signalization- LED's on the pavement

Figure 2.4: Intermittent bus lane (*source: Viegas et al. (2007)*)

Figure 2.5: Flashing lights of the intermittent bus lane in Melbourne, Australia (Currie and Lai, 2008)

the VMS reverts to through and right-turn traffic sign. The right turn movements are allowed to use the IBL unless congestion occurs. The results of the study indicated that the IBL increased transit speed between 1% and 10%.

Simulation Studies

Zyryanov and Mironchuk (2012) developed a simulation model to evaluate IBL treatment using the AIMSUN micro-simulation software. The study case was Scheboldaev Street, in Rostov-on-Don, Russia. Results indicate that IBL with TSP increases bus speed by 8%-10%.

Analytical Studies

Zhu (2010) proposed a two-lane traffic model with an IBL using the cellular automaton traffic flow model. DBLs strategy, IBLs and ordinary two-lane traffic alternatives were considered and comparisons were made by numerical simulation. The results indicated that the IBL strategy is more efficient in improving the bus flow than the ordinary two-lane traffic alternatives. In the IBL case, bus speed is more than the ordinary two-lane traffic when density is more than 0.2 veh/site.

(a) Right-turn traffic only sign when tram is approaching

(b) Through and right-turn when tram enters

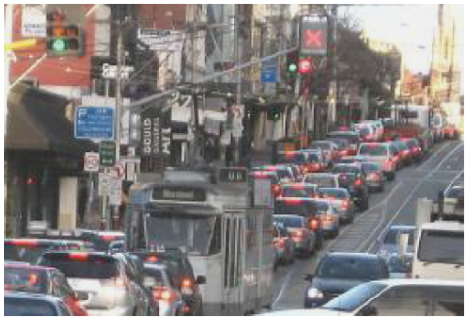

(c) No through or right turn when congestion occurs

(d) Right-turn traffic only when tram is approaching

Figure 2.6: VMS of the intermittent bus lane in Melbourne, Australia (*source: Currie and Lai (2008)*)

2.1.1.4 Bus Lanes with Intermittent Priority (BLIP)

BLIPs are similar to IBLs, but they force vehicles already in the bus lane to leave the lane. In the IBL case, vehicles already in the bus lane are not requested to leave the lane.

Simulation Studies

Carey et al. (2009) studied potential benefits and disadvantages of the BLIP and compared BLIP to other TPTs such as no-build, transit signal priority, and exclusive bus lanes using VISSIM. The study corridor was in Eugene, Oregon. The results indicated that bus travel time decreased by 14% and bus reliability improved by 28%. The BLIP alternative also showed minimal impact on overall delay and minimal change to the conflicting movements.

Analytical Studies

Eichler and Daganzo (2006) developed an analytical model using kinematic wave theory to study the feasibility, costs and benefits of BLIPs. In particular they developed analytical models to evaluate the auto capacity of BLIP systems, and to estimate the travel time savings of both the auto and bus occupants of an under-saturated BLIP system. The study has shown that BLIPs can reduce bus travel time, and can also reduce random fluctuations in travel and arrival times.

Chiabaut et al. (2012) studied the effects of BLIPs using kinematic wave theory. The study indicated that BLIP activation decreases capacity and increases bus travel time. The authors argue that the lane drop due to BLIP activation, reduces the capacity which negatively affects autos and consequently increases bus travel time.

2.1.2 Time Transit Preferential Treatments

In time priority strategies, signal timings can be set to favor approaches with public transit. Delay due to traffic signals can potentially decrease if time priority is

given to buses at intersections through Transit Signal Priority (TSP). TSP strategies dynamically adjust signal timings to prioritize the movement of transit vehicles and can be categorized as passive, active, or real-time (i.e., adaptive, traffic-responsive) strategies (Smith et al., 2005). Real-time signal control systems can be very effective in providing priority to transit vehicles while minimizing the impact on the rest of the traffic. TSP strategies often need negligible space for installing the required equipment and control system but might require signal controller upgrades.

Several studies have evaluated the effects of time priority strategies on the performance of different bus and light rail transit modes (Wahlstedt, 2013, Vlachou et al., 2010). Transit signal priority (TSP) strategies fall into the category of time preferential treatment and can be further classified in passive, active, and real-time.

2.1.2.1 Passive Priority Strategies

Passive priority strategies are developed based on historical data and do not require a transit detection system (Smith et al., 2005). Signal settings such as offsets, splits, and cycle lengths are modified to favor transit vehicles by considering traffic operations and geometric conditions. Passive priority strategies include adjustment of offsets, additional green time for the phases serving transit vehicles, and reduction in cycle length. These strategies can potentially reduce transit travel time with low implementation costs. However, the strategies may negatively affect cross-street traffic and allocate excessive green time to priority movements. Examples of such strategies include offset adjustment, longer cycle lengths and etc. Figure 2.7 shows an example of offset adjustment for TSP using time-space diagrams of vehicle trajectories traveling through two signalized intersections.

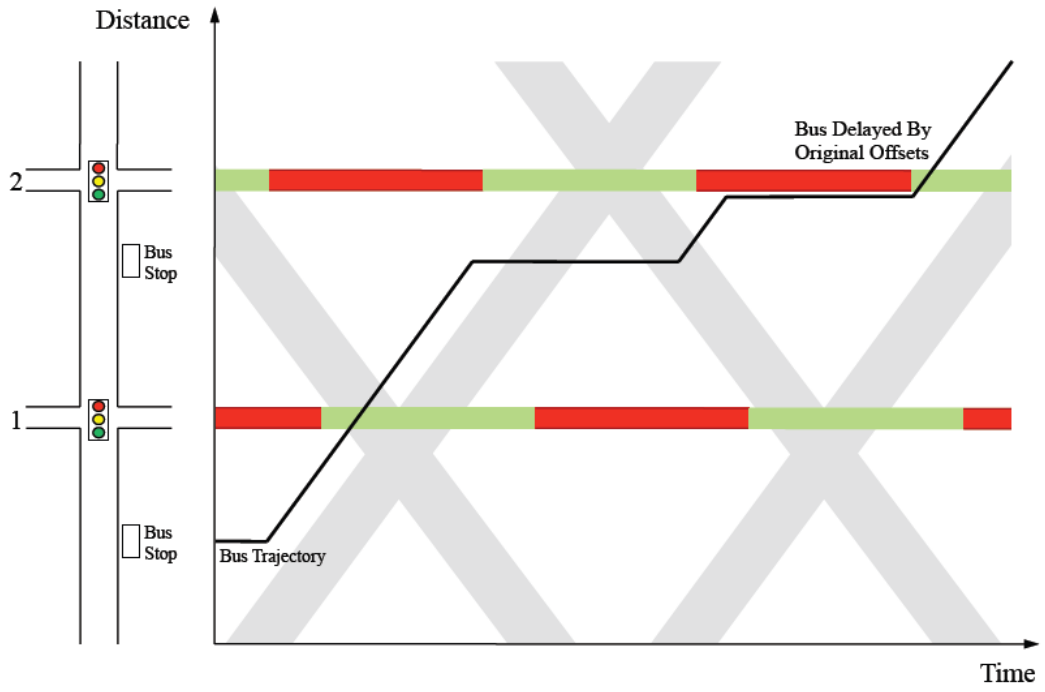

(a) Initial signal settings

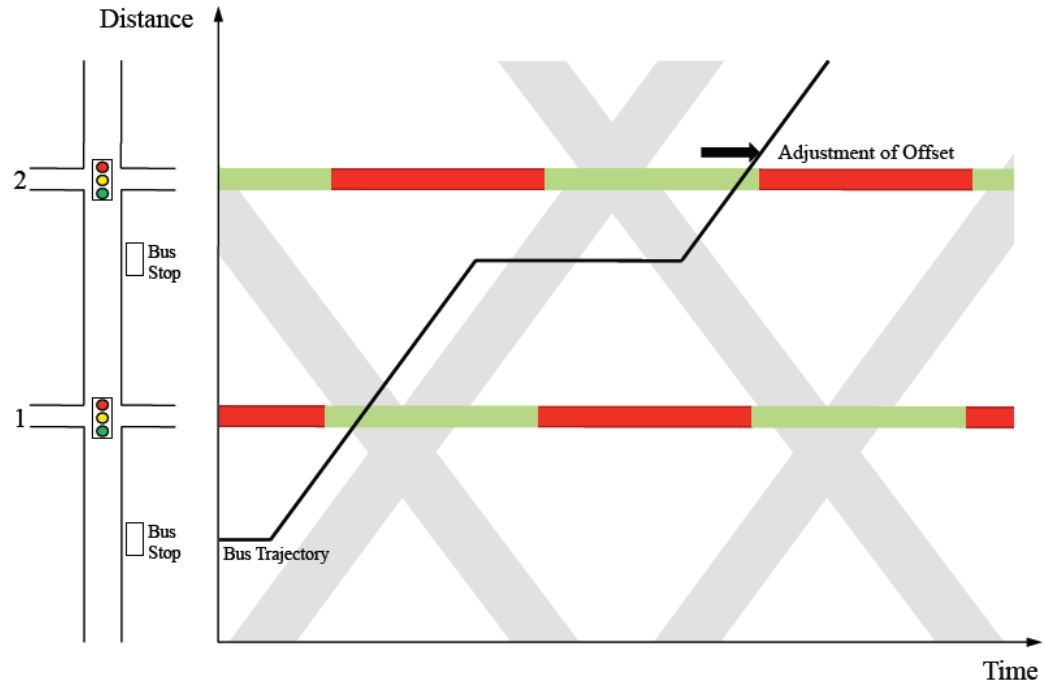

(b) Adjusted offset

Figure 2.7: Example of passsive TSP: offset adjustment (*source: Christofa (2012)*)

Field Studies

Oliveira-Neto et al. (2009) studied active and passive bus priority strategies in mixed traffic arterials. The study evaluated the operational performance of several scenarios with and without priority, during peak and off-peak traffic periods. The 13 de Maio Avenue in Fortaleza, Brazil, was selected as the case study. A field study of the various scenarios indicated that passive priority strategies have low effectiveness either under fixed- or real-time control, on heavy mixed traffic bus corridors. Passive bus priority under fixed-time scenario changed the mean stopped delay in seconds per vehicle and per traffic direction by -3.7% to 9.4% in comparison to the well-adjusted fixed-time scenario.

Simulation Studies

Skabardonis (2000) developed passive priority strategies and determined optimal signal timings by minimizing a weighted combination of delays and stops offline. Weighting factors accounted for passenger loads and as a result the system favored the buses. A 6.7 km (4.2 mi) long segment of San Pablo Avenue, in the San Francisco Bay Area, which includes 21 signalized intersections, was selected as the test site for evaluation of the proposed strategies. The study site was modeled in TRANSYT and CORSIM. The optimal signal settings in the passive priority strategy resulted in a 14% decrease in bus delay without significant negative effect on the rest of the traffic.

Oliveira-Neto et al. (2009) tested passive and active signal priority strategies on a 1.5 mile long segment of the 13 de Maio Avenue arterial in Fortaleza, Brazil, that included 10 signalized intersections. The passive TSP strategy was modeled in TRANSYT. The results of the study did not favor the adoption of the passive priority techniques for this specific case study. The authors also tested the SCOOT adaptive control on the same site.

Analytical Studies

There are no models analyticaly evaluating the impact of passive TSP strategies, however, analytical evaluation can be performed with existing models that evaluate delay when fixed-time signal control is in place. In the Highway Capacity Manual (HCM, 2010), the average delay per vehicle for a lane group is given as the sum of the uniform delay, random delay, and initial queue delay. Since vehicles are not detected in real-time to provide passive priority, the method for analytically evaluating MOEs is the same as for fixed-time signals. The MOEs can be calculated simply by replacing the calculated signal phases duration with the ones designed for the passive TSP strategies.

2.1.2.2 Active Priority Strategies

Active priority strategies provide priority to a transit vehicle based on real-time information of traffic conditions and transit arrivals. These strategies may change regular traffic signal settings in response to detection of a transit vehicle. Active TSP strategies use real-time transit vehicle information and consequently are more effective than passive strategies in improving transit performance. In addition they may cause fewer negative effect on cross street traffic operations. However, active TSP strategies may negatively affect signal coordination and require vehicle detection and communication systems, which are often expensive. Different types of active priority strategies are as follows:

- Phase extension (green extension): when a transit vehicle is detected to be approaching an intersection, a phase extension strategy extends the green time for the phase that serves the transit vehicle to provide the right-of-way to the transit vehicle as soon as possible (Figure 2.8).

- Phase advance (red truncation): when the signal is red for an approaching transit vehicle, this strategy may expedite the return to green for the transit

phase by shortening the non-transit green phases and therefore truncating the red for the subject transit phase (Figure 2.8).

- Phase insertion: when a transit vehicle is detected, a special phase may be inserted (Figure 2.9).
- Phase rotation: the order of the signal phases may be rotated to prioritize transit vehicle movement (Figure 2.9).

Field Studies

The City of Portland and the Tri-County Metropolitan Transportation District of Oregon (Tri-Met) conducted the Powell Boulevard Bus priority Pilot Project (Kloos et al., 1994). The test was designed to evaluate the application of phase extension and phase advance TSP strategies. A 2-mile four-intersection segment of SE Powell Boulevard between Milwaukie and 50th Avenues in southeast Portland was selected as the test site. The amount of green extension or early green allowed was up to 10 seconds per cycle during off-peak periods and up to 20 seconds during peak periods. Overall, the TSP strategy decreased delay for bus passengers by more than 12% and decreased bus travel times by 5%-8% during the peak period. However, the change in total intersection person delay was insignificant during the peak periods, although the person delay did increase slightly in the off-peak period. The TSP's effect on total vehicle delay was insignificant.

In Northern Virginia (Rakha and Ahn, 2006) an 8.06 miles long corridor from Fairfax County Parkway to North King/Shields intersection including 27 signalized intersections was analyzed. A 10-second green extension resulted in 3% to 6% reduction of the overall bus travel time. During peak periods, intersection bus delays decreased between 9.26% and 23%. Bus delay reduction during off peak hours was 10.17%, while a 13.3% reduction was observed during the entire morning analysis

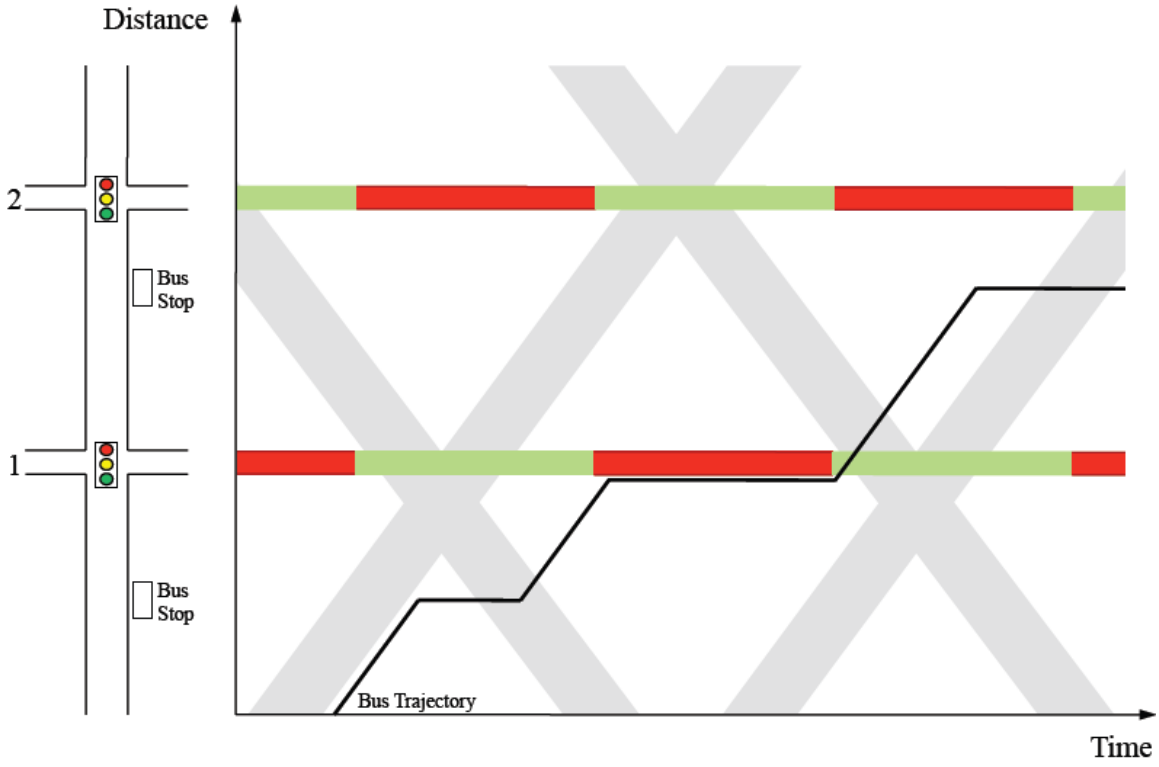

(a) Initial signal settings

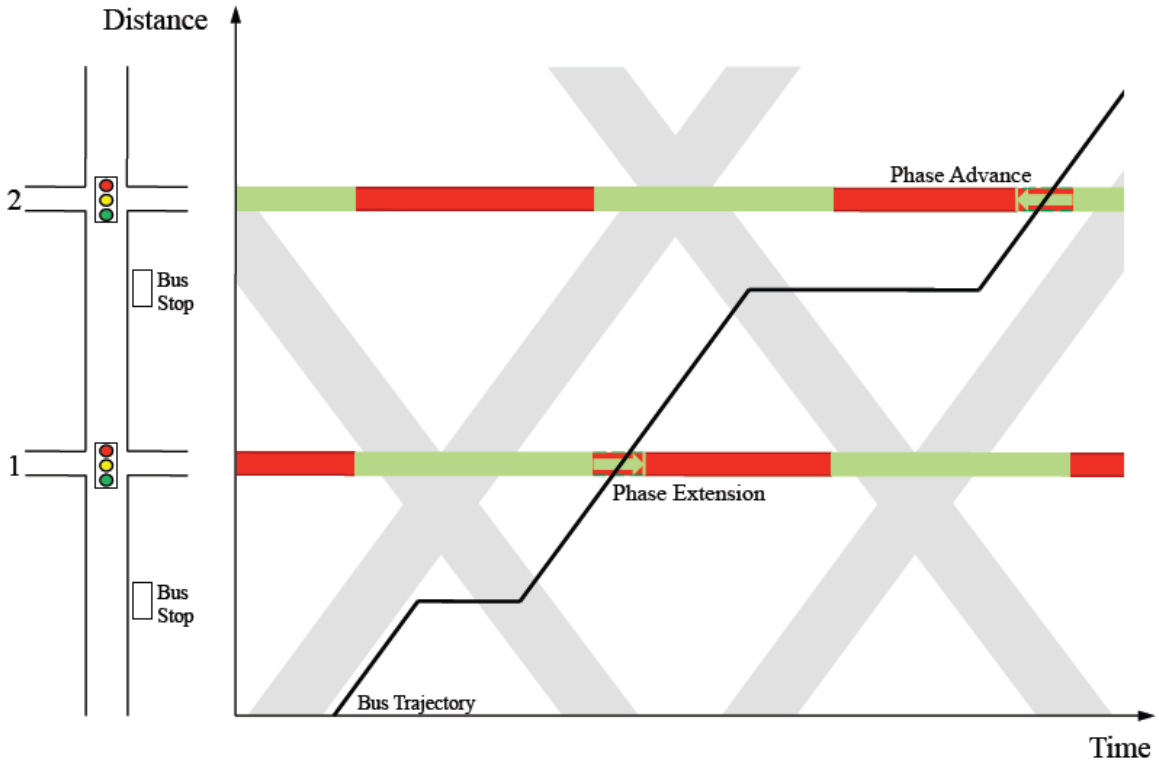

(b) Phase advance and phase extension

Figure 2.8: Phase advance and phase extension (Christofa, 2012)

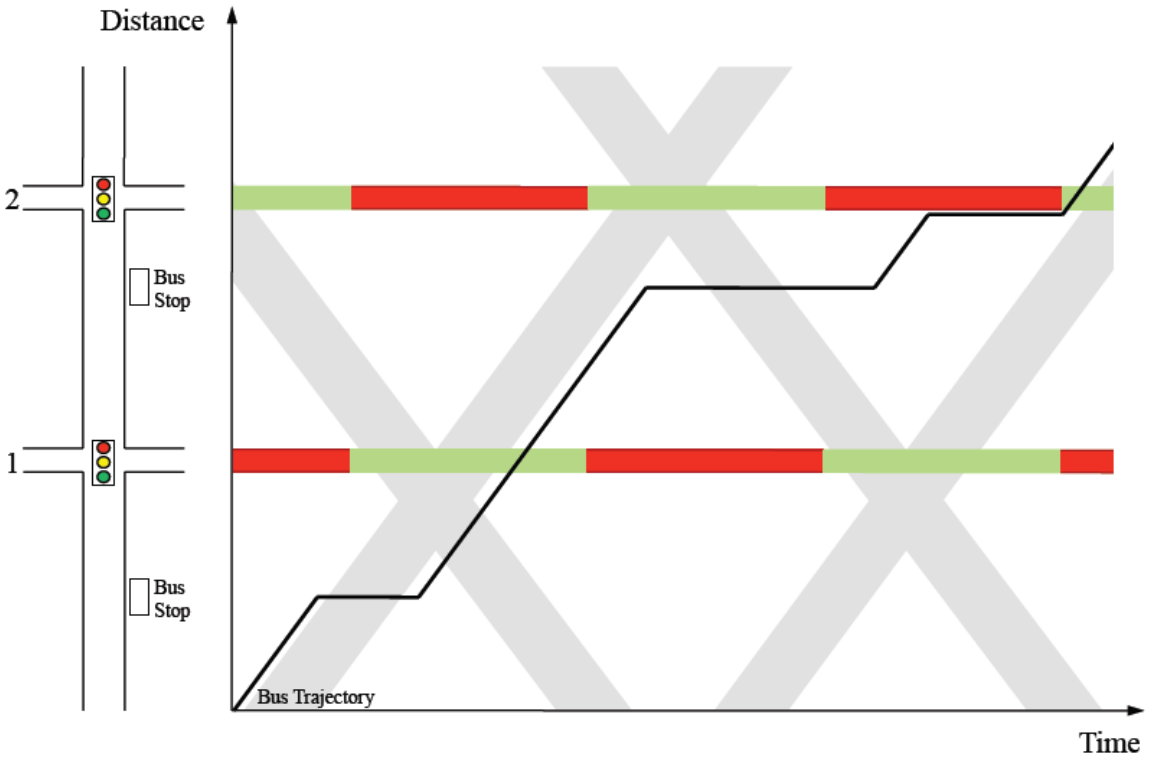

(a) Initial signal settings

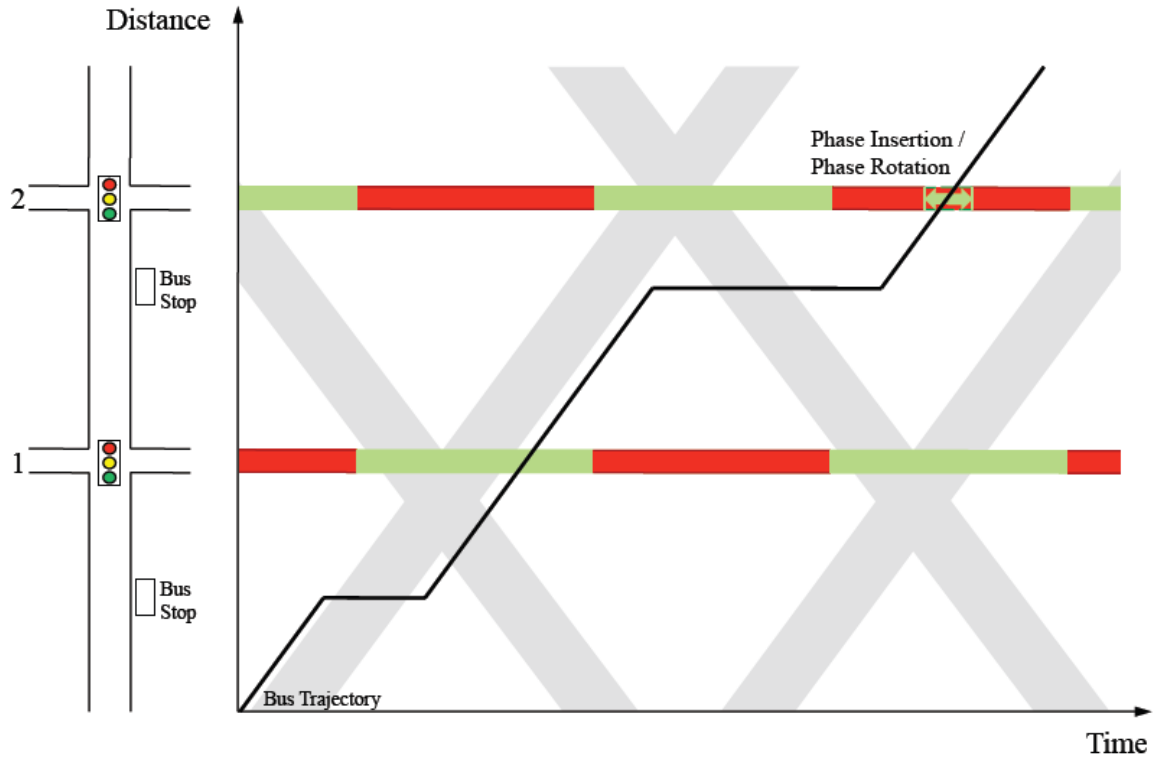

(b) Phase insertion/phase rotation

Figure 2.9: Phase insertion and phase rotation (*source: Christofa (2012)*)

period.

Simulation Studies

Kamdar (2004) used VISSIM to evaluate the impacts of TSP at twenty-six signalized intersections along U.S. 1 corridor in Northern Virginia during the morning peak period. The MOEs used were transit travel time, bus control delay, and queue length on side streets. The results showed that on the priority approach bus travel time decreased by 0.8%-4%, bus control delay decreased by 5%-16% and total queue length on the side streets increased by about 1.23%.

Analytical Studies

A thorough literature review indicates that very few studies have used analytical models to evaluate TSPs. Jacobson and Sheffi (1981) developed an approximate stochastic analytical model to evaluate the bus priority impact on person delay at a signalized intersection. For simplicity, an isolated intersection with a one-way main street and a one-way cross-street, where the buses operated only on the main street, was considered. Both phase extension and phase advance strategies were applied. Based on the probability density functions and an expression for the mean vehicle delay, impacts of the priority strategies on the total person delay were estimated.

Liu et al. (2008) developed a model to estimate the impact of the phase extension and phase advance priority strategies on vehicle delay at an intersection. In this study it was assumed that TSP implementation does not significantly affect the randomness of the traffic flow arrivals to the intersection; consequently, the random delay was assumed to remain unchanged before and after the implementation of the TSP strategies. Therefore, the impact of TSP was evaluated by assuming deterministic arrivals and service rates considering a D/D/1 queuing system. Vehicle arrival

and departure rates were assumed to be constant. The analytical model results were compared to the simulation models results obtained using VISSIM.

Abdy and Hellinga (2011) developed an analytical model to evaluate the impacts of phase extension and phase advance priority strategies on vehicle delay. The model is applicable to individual intersections. It was assumed that the intersection can be modeled as a D/D/1 queuing system with constant arrival rates. The results obtained from the analytical model closely matched those obtained from the micro-simulation analysis for volume-to-capacity ratios up to 0.8. VISSIM was used for the micro-simulation modeling analysis.

Overall previous analytical studies did not perform a comprehensive analysis the impact of TPT alternatives on person delay and person discharge flow when implemented individually or in combination. Also, previous analytical models did not capture the effect of platooned vehicle arrivals at intersections.

2.1.3 Impacts on Other Traffic

Previous studies have confirmed that TSP implementation will increase the delay for vehicles traveling on conflicting phases. TSP with IBL implementation increased cross-street delay by 17% to 58% (2007). Almost all real-time signal control with TSP studies have considered TSP impacts on other than the priority vehicles in their mathematical formulations. These formulations mainly consider vehicle delays for the conflicting approaches. Although delays for traffic on the conflicting phases will increase, appropriate TSP design may reduce total person-delay of the system.

2.1.4 Near-side Bus Stops Presence

In addition to the implementation of TPTs, the presence of bus stops can play a very important role in traffic and transit performance. The most common type of bus stop is the curbside stop where buses block a travel lane while stopping (Fitzpatrick and Nowlin, 1997). These stops are often located at a short distance from the stop line of

signalized intersections (so called near-side stops) to eliminate the spillback effect that occurs when a bus stops at the far side of the intersection and to provide convenient crosswalk access for passengers (Fitzpatrick et al., 1996). However, buses dwelling at near-side bus stops may block the through and right-turn lane on the intersection approach, reducing intersection capacity and potentially disrupting traffic flow.

Several studies have investigated the impact of bus stops on the performance of signalized intersections. Wong et al. (1998) developed a microscopic simulation model to investigate the delay at a signalized intersection for near-side bus stops based on factors such as the distance between the bus stop and the stop line, car and bus flows, bus dwell time, and signal settings. Furth and San Clemente (Furth and SanClemente, 2006) modeled the influence of bus stop location and roadway grade on bus delay based on vehicle characteristics such as acceleration and bus dwell time. Other studies investigated the effect of bus stops on the capacity of signalized intersections. Zhao et al. (2007) used a two-lane cellular automaton (CA) model to evaluate roadway capacity based on factors such as stop location, signal timing and bus dwell time. Most recently, Gu et al. (2013) investigated the impacts of near-side bus stops on residual queue length and car delays using kinematic wave theory. While several studies have examined the impact of bus stops on vehicle delay and capacity of signalized intersections, there is a gap in determining how the presence of bus stops affects the performance of TPTs with regard to person-based measures of effectiveness (MOEs).

2.2 Bus Travel Time Prediction

Short-term travel time predictions include prediction of travel times after a few seconds to possibly a few hours using current and past traffic information (Vlahogianni et al., 2014). Several applications of intelligent transportation systems (ITS) rely on short-term travel time predictions including advanced traveler information systems

(ATIS) and transit signal priority (TSP) strategies. ATIS provides information to travelers to decide on their destination and reach them quickly and safely (Noonan and Shearer, 1998). Inaccurate transit travel time prediction can increase traveler waiting times at bus stops and therefore, reduce system reliability. When active and real-time TSP strategies are implemented, the system detects the presence of a bus approaching the intersection and places a priority request to the traffic signal controller. By predicting the bus arrival time at the intersection stop line, the signal controller decides whether to provide priority or not and at what time. Since a few seconds of green extension or red truncation are provided (e.g., 5 or 10 seconds), the predicted arrival time at an intersection stop line must be accurate and within a required strict level of tolerance (e.g., within a 5-second error bound). Inaccurate bus arrival predictions can restrict real-time signal control systems with TSP from realizing their full potential in improving car and transit operations (Christofa et al., 2016).

Automated vehicle location (AVL) systems have been widely adopted by transit operators since they allow bus tracking and gathering of vehicle location and time data that can be used for scheduling and management purposes. AVL data sampling can be categorized in distance/location-based, time-based, and event-based sampling (Jenelius and Koutsopoulos, 2012). In location-based sampling, data are polled at fixed locations such as bus stops or intersections while in distance-based sampling data are sampled at specific distances from the previous record. In time-based polling, data are stored at fixed-time intervals (e.g. every 1 second or every 60 seconds) and in the event-based sampling data are polled when specific events occur (e.g., when a stop is requested).

While AVL systems offer an abundance of information to be used for improved transit operations and management, they have a number of limitations. Low resolution data sampling often caused by communication constraints, is one of the most

important challenges when using AVL data. In this case the actual bus trajectories are not available and should be inferred from sparse data. Inferring trajectories can be challenging specially in signalized urban arterials due to heterogeneous traffic conditions.

The literature on travel time prediction models is extensive. Existing models can be broadly categorized into parametric and non-parametric models. Parametric models include an assumption about their functional form and unknown parameters are estimated by fitting the model to the training dataset (James et al., 2013). Functional forms are often determined based on certain theories and then, unobserved variables are estimated by various techniques including norm approximation such as least-squares method (Tan et al., 2006), maximum likelihood (Hellinga et al., 2008, Jenelius and Koutsopoulos, 2013) and Bayesian estimation (Hofleitner et al., 2012). Parametric models investigated in previous studies include linear regression (Nikovski et al., 2005, Tan et al., 2006), Kalman filtering (Cathey and Dailey, 2003, Hans et al., 2014, Kumar et al., 2015, Liu et al., 2012), auto regressive integrated moving average (ARIMA) models (Ma et al., 2015), and accelerated failure-time survival models (Gayah et al., 2016).

Non-parametric models have also been used for short-term travel time prediction. Non-parametric models do not make assumptions about the functional form of the model, but they try to estimate a functional form that fits the data points as well as possible (James et al., 2013). Various machine learning techniques have been used with this type of models including support vector regression (SVR) with non-linear kernel (Yu et al., 2011, 2012, Hu et al., 2016) artificial neural network (ANN) (Chien et al., 2002, Jeong and Rilett, 2005, Khosravi et al., 2011, Mazloumi et al., 2011, Jeong and Rilett, 2004, Ma et al., 2015), k-nearest neighbors (KNN) (Myung et al., 2011, Baptista et al., 2012, Tak et al., 2014), additive model (Kormaksson et al., 2014), Gaussian process regression (Idé and Kato, 2009), and ensembles (van

Hinsbergen et al., 2009, Zhang and Haghani, 2015). Non-parametric models are powerful tools in predicting bus travel times to specific locations when AVL records are available at those locations; however, these models might result in inaccurate travel time predictions of locations where AVL records are not available to train the model. That is because for such locations in-between records, assumptions need to be made to estimate arrival times (e.g., travel time is a linear function of traveled distance). Parametric models can be used to decompose travel time into its components and provide estimates for each component. As a result, parametric models provide a more powerful tool for inferring vehicle trajectories between two specific locations for which AVL records are not available.

The vast majority of previous studies have investigated bus travel time between fixed locations (e.g., bus stops) with the use of both parametric and non-parametric models (Jeong and Rilett, 2004, Chen et al., 2005, Lin et al., 2013, Hernandez, 2014). In the absence of data for a specific location, interpolation is performed to infer travel time to that point (Sinn et al., 2012). Interpolation is reasonable for relatively high-resolution data polling; however, reduction in the sampling frequency can significantly reduce prediction accuracy and precision.

Since the main factors affecting bus travel time uncertainty are dwell times at bus stops and intersection delays, improvements in the dwell time and intersection delay estimates can enhance prediction accuracy (Baptista et al., 2012). While most studies consider bus dwell times in estimating bus arrival time, few studies have taken into account the intersection delay component. For instance, Bie et al. (Bie et al., 2011) developed analytical models to estimate bus arrival time at the intersection stop line, which can be used to estimate bus delay at the intersection. Bus stops were not taken into account and the model required detailed data on speed and signal settings. Average intersection delay has been estimated in previous studies (Tan et al., 2006, Gibson et al., 2015, Farid et al., 2016); however, expected intersection

delay values over all buses in the training data set were estimated instead of individual bus intersection delay. Modeling intersection delay by an average value can reduce accuracy of the models in predicting bus travel time sufficiently accurately for use in TSP systems.

2.3 Real-time Signal Control Systems with Transit Priority

Real-time signal control systems with transit priority are responsive to transit requests as well as the current traffic conditions in real-time. Real-time signal control systems with TSP provide priority while optimizing given traffic performance criteria such as vehicle delay, person delay, and transit delay. In general, real-time signal control systems with TSP require traffic detection (both transit and non-transit vehicles) and communication systems, estimation of appropriate performance measures, estimation of traffic demand and bus arrival time to stopline, and a decision system as shown in Figure 2.10.

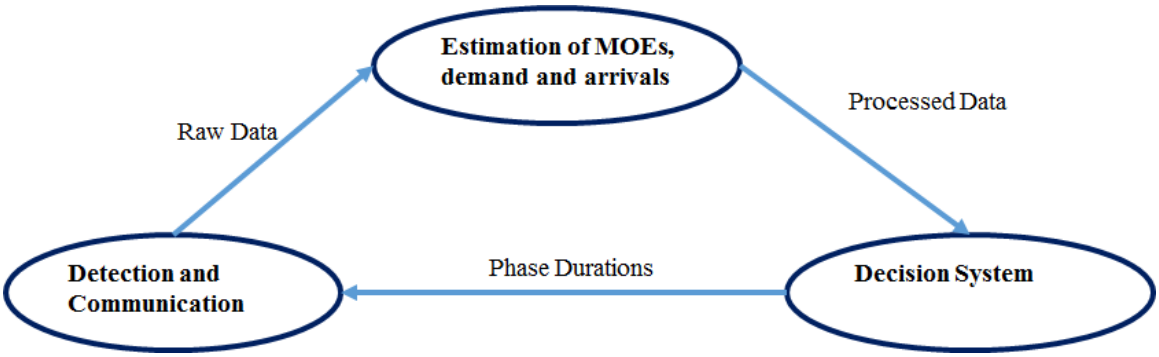

Figure 2.10: Simplified real-time signal control architecture

Vehicle detection can be performed at the local level or at the network level. At the local level, vehicles may be detected approaching an intersection through the use of various sensing technologies (e.g. inductive loops, active infrared sensors, etc.) that do not look beyond a certain distance from the intersection (a few hundred feet). De-

tection at the network level is accomplished through automatic vehicle location (AVL) system, where vehicles communicate their position to a centralized transit or traffic management center through the use of Global Positioning System (GPS) or other automated vehicle location technologies. The communication system is responsible for linking the detection system to the traffic signal control system.

Macroscopic, mesoscopic, or microscopic models are used to estimate the current state of traffic conditions based on raw data obtained from the detectors. Vehicle arrival times at intersections are estimated as well. Finally, optimal values for the decision variables (green phases, and cycle times) are calculated by optimizing selected performance measure(s) such as total vehicle delay.

Real-time traffic signal control systems that have incorporated TSP are as follows:

- **SCOOT**

  Split Cycle Offset Optimization Technique (SCOOT) was originally developed in England (Hunt et al., 1982). SCOOT is a centralized traffic signal control system which works both on arterials and grid networks and automatically responds to variations in traffic demand. The performance of SCOOT relies on traffic flow data obtained from detectors. The system needs a large number of detectors which should be located at pre-determined upstream locations on every link (usually at the upstream end of the link). Downstream detectors are used to determine left turning movements and optimize left turning phase.

  The SCOOT algorithm estimates vehicle delays and number of stops on each link and determines the system's performance index (PI). The PI is typically the sum of the average delay and the number of stops at all approaches in the network. SCOOT incrementally adjusts signal control parameters such as phase durations, cycle lengths, and offsets of pre-timed signal plans based on the actual traffic flow fluctuations (Bretherton et al., 2002). The Split optimizer

equalizes saturation and congestion, offset optimizer minimizes delay, number of stops and congestion, and cycle optimizer minimizes delay.

Transit signal priority is provided through phase extension or phase advance. In SCOOT 4.4, different priority levels between 0 and 6 can be provided for buses based on some mechanisms outside SCOOT. When an AVL system is present, the priority level can be determined based on the bus headway or timetable (Bretherton et al., 2002).

In London, SCOOT operation began in early 1984. An assessment of bus priority field trials in the areas of Camden Town and Edgware Road in London in 1996 showed that SCOOT reduced bus delay by 1% to 71% depending on the selected strategy (e.g. central extensions, local extensions, etc.) and saturation ratio (SCOOT, 2015).

- **SCATS**

  The Sydney Coordinated Adaptive Traffic System (SCATS) was developed by the Roads and Traffic Authority of New South Wales, Australia (Sims and Dobinson, 1980). SCATS adjusts phase duration and offsets in response to variations in traffic flow and system capacity, using some predefined plans. For each intersection, SCATS distributes its computations between the field controller and a regional computer at the operations center. The computer makes incremental adjustments to traffic signal timings based on minute by minute changes in traffic flow at each intersection. SCATS divides the network into smaller sub-networks and designs signal settings for each of them independently. Data is obtained by detectors which are located at the intersection stop lines.

  SCATS has three control levels: central, regional, and local. The central computer is responsible for communications and the database function while the

regional computer and local traffic controllers handle the strategic and tactical controls respectively.

In the strategic control, the algorithm selects suitable signal timings on a cycle by cycle basis for the target area and sub-areas based on average prevailing traffic conditions. The algorithm uses car equivalent flow, degree of saturation and signal phase timings information. The tactical control, may modify the plan provided by the strategic control taking into account the demand.

Slavin et al. (2013) conducted a before and after study of SCATS implementation with TSP along Powell Boulevard, Portland, Oregon. The study reports both negative and positive effects of the SCATS implementation on travel speed. Four tests were conducted at two intersections for both east and west bound approaches. One of the tests indicated a 22% increase in general traffic travel speed, however, on the other three tests, general traffic travel speed was reduced by 7% to 21%. During peak periods, transit travel time in the eastbound direction was improved, however, in the westbound direction transit travel time did not improve.

- **RHODES**

  The Real-Time, Hierarchical, Optimized, Distributed, and Effective System for traffic control (RHODES) was developed at the University of Arizona (Mirchandani and Head, 2001). Using a dynamic programming approach, this system finds the optimum signal phasing and timing for an intersection while taking into account delay, number of stops, and queue lengths. RHODES was developed to estimate arrival of vehicles on all approaches and optimize phase durations based on the user-defined objectives, such as minimizing average delay or number of stops.

The intersection control strategy of RHODES treats each vehicle alike by assigning an identical weight to it. To predict future arrivals at the intersection, RHODES uses data obtained from detectors on the approach of each upstream intersection, and takes into account the traffic state and signal phase timings of the upstream signals.

RHODES control was studied in a field-test in the City of Tempe, Arizona (Mirchandani and Lucas, 2001). The results indicated that RHODES performed as well as Tempeś existing finely-tuned semi-actuated coordinated control system. In this study, TSP strategies were not implemented, however, it has been mentioned that RHODES can be expanded to include TSP as shown in Figure 2.11.

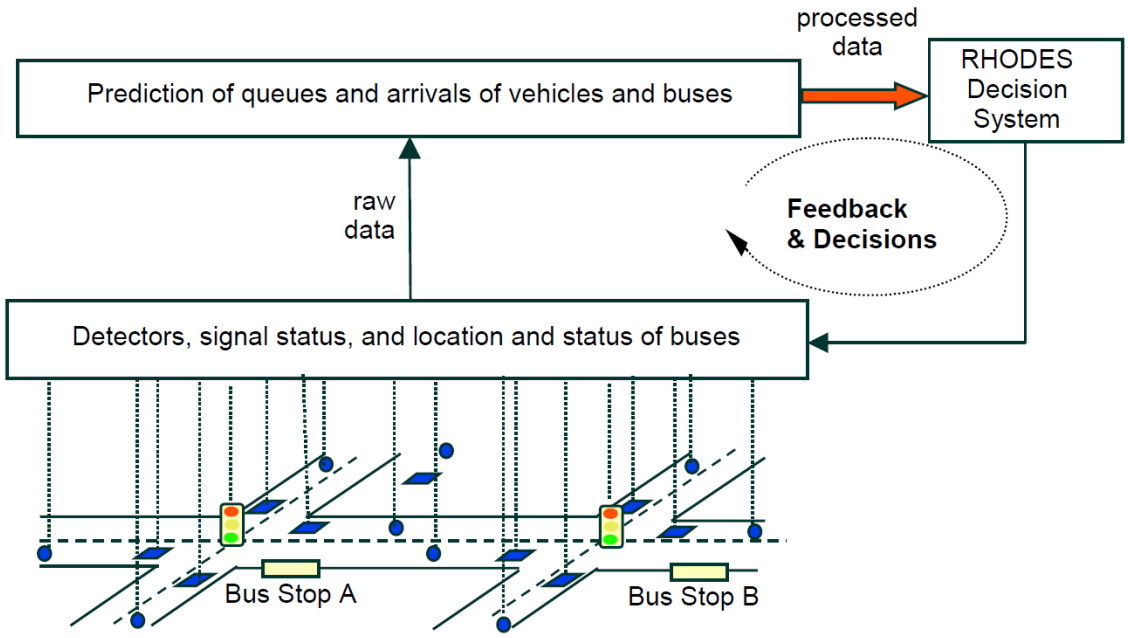

Figure 2.11: TSP implementation in RHODES (*source: Mirchandani and Lucas (2001)*)

In RHODES each detected vehicle is treated equally and consequently buses can not get priority over other vehicles. Mirchandani and Lucas (2004) presented Categorized Arrivals-based Phase Reoptimization at Intersections (CAPRI) which integrated TSP and rail/emergency preemption with RHODES. In RHODES-

CAPRI TSP is provided either by giving each bus a variable weight which depends on how late the bus is and on the bus passenger occupancy, or by providing a constraint to set signal phase to a desirable phase at a specified or scheduled time. A simulation test using CORSIM along an arterial was conducted and the RHODES control was implemented at a single intersection. In comparison to standard semi-actuated control (SAC), for low cross-street volumes (550 vehicles per hour per direction), RHODES without TSP reduced bus delay and cross-street delay by 0.23% and 43.69% respectively. RHODES with TSP (RHODES-BP) decreased bus delay and cross-street traffic delays by 0.66% and 39.77% respectively. For high cross-street volumes (1100 vehicles per hour per direction), RHODES-BP reduced bus delay by 4.46% and increased cross-street traffic delay by 4.8%.

- **UTOPIA**

  The Urban Traffic Optimization by Integrated Automation system (UTOPIA) is an adaptive signal control system that was first developed and implemented in Italy in 1985. The objective of the system was to integrate real-time traffic control with transit priority needs. The controllers determine the signal control settings based on local traffic demands, transit priority, and coordination requirements (Shepherd, 1992).

  UTOPIA can provide absolute, weighted, and selective priority to buses and trams at signalized intersections and also can be extended to emergency and very important person (VIP) vehicles. UTOPIA needs detectors only on the intersection approaches with significant traffic volumes and where traffic fluctuates significantly. UTOPIA was first implemented in a large area in Turin, Italy (Donati et al., 1984). Field results indicated that both private and public vehicles' travel times reduced on the order by about 9%-15%.

- **SPPORT**

  The Signal Priority Procedure for Optimization in Real Time (SPPORT) is a rule-based model that provides transit priority. The system evaluates the individual priority levels of all incoming requests and determines the aggregated priority level for each phase. A set of possible signal plans is determined for a planning horizon based on the current signal status. The plan with the lowest delay is selected for the next implementation period (e.g., 5 seconds). (Yagar and Han, 1994)

  The objective of SPPORT is to minimize total intersection delay. In SPPORT detectors are located about 150 and 1000 meters upstream from an intersection. Information on the current queue lengths and the future arrivals of vehicles is provided by these detectors. Given this information, SPPORT generates a short term (5 second) plan. This plan is then re-evaluated after a 5-second duration and a new plan is implemented (Garrow and Machemehl, 1997).

  SPPORT was tested through simulation for the Queen and Bathurst Street intersection in Toronto, Canada. The simulation results indicated that the delay per person was reduced by about 50% with SPPORT. Delay per vehicle for both private vehicles and streetcars was also reduced by roughly 50% in comparison to the existing conditions (Garrow and Machemehl, 1997).

- **MOTION**

  The Method for the Optimization of Traffic Signals In On-line controlled Networks (MOTION) is a decentralized and hierarchical signal control system which was developed in Germany (Bielefeldt and Busch, 1994). The system minimizes delays and stops in the network by optimizing phase durations and sequences, cycle lengths, and offsets (Busch and Kruse, 2001). MOTION provides special priority to public transport vehicles both on the network and the local level. It

can provide absolute and relative priority. In the absolute priority, bus delay at all intersections will be zero regardless of the general traffic conditions. In the relative priority, priority is given to transit vehicles only if the auto delay does not exceed predefined thresholds. The detectors are located near stopline.

- **PAMSCOD**

  The Platoon-based Arterial Multi-modal Signal Control with Online Data (He et al., 2012) is a unified platoon-based mathematical formulation which considers multiple travel modes in a vehicle-to-infrastructure communications environment to perform arterial traffic signal control. Its objective function is to minimize the sum of slack variables representing the total green rest time as well as the total weighted delay. Green rest happens when green reaches maximal in one ring while the other ring does not reach the barrier which causes the ring to rest on the barrier. Using mixed-integer linear programming, the algorithm determines signal timings for four cycles in the future based on the predicted platoon sizes and locations, current traffic controller status, online platoon data and priority requests every 30 seconds. Transit signal priority can be applied using weighting factors which can be adjusted for individual vehicles based on vehicle characteristics, such as vehicle occupancy. Microsimulation using VISSIM showed that PAMSCOD was able to improve vehicle and bus delay at degrees of saturation greater than 0.8 but often experienced higher delays at saturation rates of less than 0.6.

- **Person-based Real-time Signal Control System** Christofa et al. (2013) presented a person-based traffic responsive signal control system for implementing TSP on conflicting transit routes at an isolated intersection. A mixed-integer nonlinear program was used with the objective of minimizing total person delay. The proposed method was tested both analytically using deterministic arrival

tests and with micro-simulation tests (stochastic arrival tests) using Aimsun. The deterministic test results for the intersection flow ratio of 0.90, indicated that the person-based optimization in comparison to the vehicle-based optimization reduces total person delay at the intersection by 5% by decreasing bus delay by 26% and increasing auto delay by 2%. Results from the simulation test for an intersection flow ratio of 0.6, showed that the person-based approach in comparison to the vehicle-based approach reduced bus delay by 31%. In another study, Christofa et al. (2013) presented the formulation of an arterial-level person-based traffic responsive signal control system.

2.4 Stochasticity in Transit Vehicle Arrivals

Early detection of a transit vehicle is key in allowing more time to adjust the signals to provide priority while minimizing impacts on the rest of the traffic (Smith et al., 2005). Another critical issue in designing real-time signal control system with TSP is the ability to accurately predict vehicle arrival times at intersections as well as "optimal" times to place priority requests (Liu et al., 2007). Efficient real-time signal control highly depends on the availability and precision of vehicle arrival time estimation (Liu et al., 2007).

Bus dwell time at a bus stop plays an important role in predicting transit arrival times. If dwell times were perfectly predictable, transit vehicle arrival times could be predicted more accurately. However, dwell times generally exhibit some variability, which creates uncertainty in arrival predictions. Dwell time variability is mainly because of the variable number of passengers boarding/alighting, the boarding and fare collection process, etc. Other factors such as traffic conditions and driver behavior may also affect variability of bus travel time and therefore transit vehicle arrival time.

Regression analysis has been used to estimate bus dwell time at bus stops as a function of various variables such as passenger loads and bus headway (Kim and

Rilett, 2005, Tan et al., 2008, Ekeila et al., 2009). Linear regression models are based on a set of assumptions such as: the error terms are independent of each other, have a zero mean, and have a constant variance across all values of the predictor variables. If one or more of these assumptions does not hold, the analysis is invalid (Gujarati, 2003). Also, regression models depend highly on historical data to develop a prediction model, which will reduce their efficiency in real-time predictions, especially where traffic conditions may change significantly.

Due to randomness in transit dwell time and delay at intersections, transit arrival time prediction is highly uncertain. To overcome this uncertainty, the arrival time window concept has been introduced. Signal settings are adjusted so that the transit phase is green for an arrival time window within which the bus is expected to arrive. Based on the phases that contain the start and end points of the priority window, an appropriate TSP strategy, green extension, early green, or phase insertion can be selected as shown in Figure 2.12.

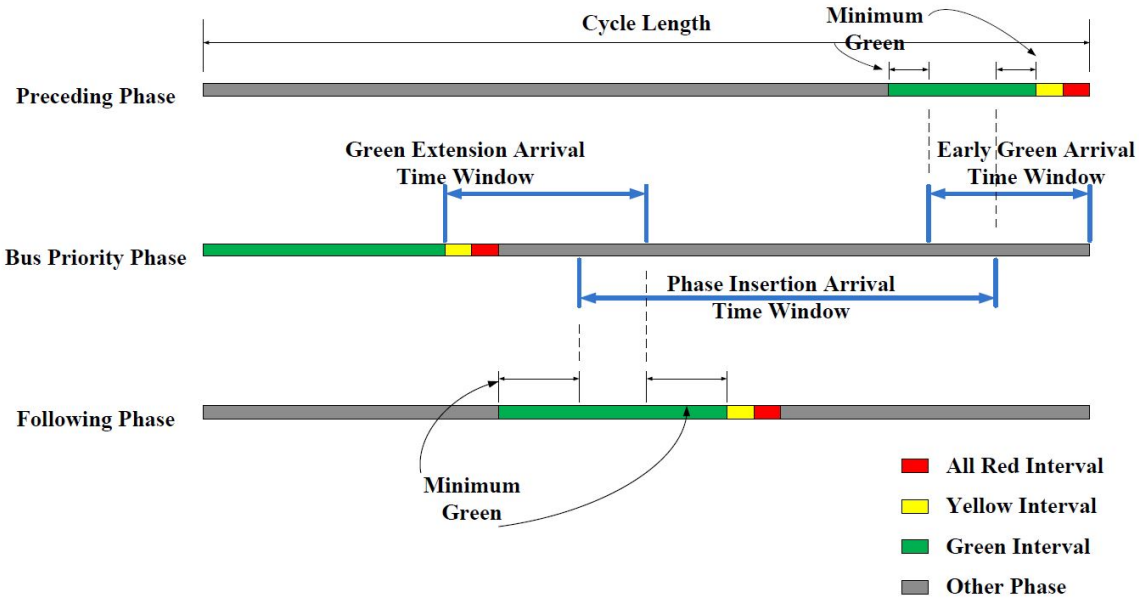

Figure 2.12: Priority windows for TSP (*source: Wen et al. (2012)*)

Kim and Rilett (2005) used weighted-least-squares regression modeling to estimate bus stop dwell time and its arrival time at the stop line. The study proposed a TSP algorithm which accommodates the bus dwell time as well as its variability. The algorithm provides a priority phase wide enough to accommodate the 100(1-α)% estimated interval of dwell time at the nearside stop (Figure 2.13). The proposed algorithm was tested on an urban arterial section of Bellaire Boulevard in Houston, Texas, using VISSIM. Results indicated that the proposed TSP algorithm decreased bus delay without significantly affecting auto delays in comparison to the existing deployed TSP algorithm.

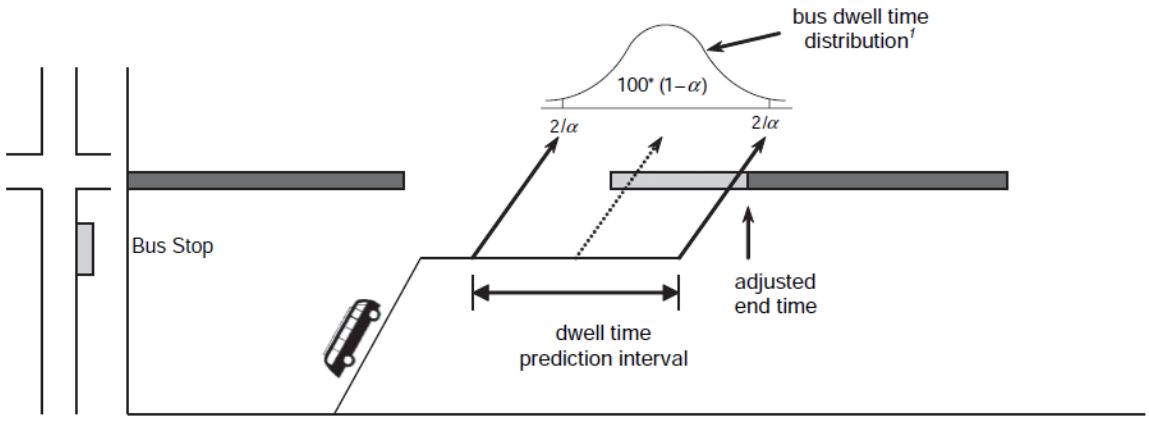

Figure 2.13: Prediction interval in TSP (*source: Kim and Rilett (2005)*)

Wadjas and Furth (2003) developed a TSP algorithm in which transit vehicles are detected two to three cycles in advance of their arrival at an intersection stopline, and the transit-serving phase is green for a 40-second predicted arrival window. The algorithm was tested on a light-rail system on Massachusetts' Huntington Avenue corridor, Boston. The algorithm resulted in 82% of the trains arriving during the green phase, and substantially improved the transit travel time with negligible impacts on auto vehicles.

2.5 Summary of the Literature

Table 2.1 summarizes the MOEs that have been used in TPT (space TPTs and time TSP) field studies. These studies suggest that TPTs may, depending on the strategy implemented as well as other factors, decrease transit travel time by 1% to 12% with minor to major negative impacts on other vehicles travel times. Table 2.2 summarizes simulation studies that have focused on TPT evaluation. These studies indicate that the results of the simulation models have been inconsistent and project-specific. Effects of TPTs on different MOEs vary among studies due to other factors influencing the effectiveness of TPTs such as traffic conditions, and transit characteristics (e.g., bus volume, transit routes, and bus and geometric configuration) (Skabardonis, 2000).

Very few studies have comprehensively evaluated the combined effects of time priority and space priority strategies on traffic and transit performance. Even the ones that have studied combined effects (Currie et al., 2013) have not incorporated person-based MOEs, such as person delay and person discharge flow in their evaluation, therefore, ignoring the contribution of transit vehicles in serving more people than private vehicles. In addition, very few studies have developed analytical models for TPT evaluation in general and none of them have compared TPTs using person-based measures. A comprehensive person-based evaluation of different spatial TPTs in the presence of near-side bus stops at intersections is missing.

Effective implementation of the TPTs is highly dependent on accurate bus arrival time predictions especially when the only available data is low frequency AVL data sampling. One of the objectives of this study is to develop a model that predicts bus travel time at signalized urban arterials under the assumption of pre-timed signal control and existence of dedicated bus lanes. A review of the literature indicates that the majority of previous studies have studied bus arrival time at fixed locations like bus stops using location-based or high resolution time-based data sampling protocols. Very little research has been devoted to estimating bus travel time to any location

by inferring trajectories using low resolution AVL data. In addition, few studies have investigated the intersection delay component of the bus travel time and even those who have taken into account, they have either assumed perfect information about signal status and timings or have considered average values for intersection delays over all buses for travel time predictions purposes.

While traditional traffic signal control systems rely on historical data to develop optimal signal timing plans, recent systems increasingly rely on real-time data to provide real-time control that automatically adapts to changes in traffic conditions. Adjustments of signal timings to traffic conditions can potentially improve system efficiency. Various real-time TSP systems have been designed, however, to the best of the auhor's knowledge, no studies have taken into account the stochastic bus arrival times while providing priority window for buses.

Table 2.1: Field Studies on Transit Preferential Treatments

Study	TPT	Transit System	Test Site	Average Person Delay	Cross-Street Delays	Number of Stops for Transit	Schedule Adherence	Transit Intersection Delay	Transit Speed	Transit Travel Time
Seattle, WA (Zheng et al., 2009)	TSP	Bus	Corridor	↓ 0.02 - 0.05 s		Not Significant	↑ 3.9%-27.4%			↓ 1%-5%
Portland, OR (Kittelson et al., 2003)	TSP	Bus	Corridor							↓ 2%-11 %
Portland, OR (Kimpel et al., 2005)	TSP	Bus	Corridor				5% (Total)			
Helsinki, Finland (Lehtonen and Kulmala, 2002)	TSP	Bus	Corridor					↓> 40%		
Miami, FL (Pessaro and Van Nostrand, 2011)	TSP	Bus	Corridor				↑ 8.3%	↓ 4%		↓ 1.4% 12.1%
Shizuoka City, Japan (Sakamoto et al., 2007)	TSP & IBL	Bus	Corridor		↑ 17% - 58%					↓ 6.2%
Lisbon, Portugal (Viegas et al., 2007)	IBL	Bus	Corridor						↑15% - 25%	
Melbourne, Australia (Currie and Lai, 2008)	IBL	Streetcar	Corridor						↑ 1% to 10%	

Table 2.2: Simulation Studies on Transit Preferential Treatments

Study	TPT	Transit System	Test Site	Average Person Delay	Cross-Street Delays	Number of Stops for Transit	Schedule Adherence	Transit Intersection Delay	Transit Speed	Transit Travel Time
Minneapolis, MN (Liao and Davis, 2007)	TSP	Bus	Corridor							↓ 4% -15%
Arlington, VA (Dion et al., 2004)	TSP	Bus	Corridor	↑8.7% ↓1.64% (Total)		↑0.94% ↓1.04%				↑2.82% ↓3.17%
Boston, MA (Furth et al., 2010)	TSP	Bus	4 Intersections Network					↓22 s (50%)		
Arlington, VA (Chang et al., 2003)	TSP	Bus	Corridor	↑0.6%			↑3.2%			
Fairfax, VA (Kamdar, 2004)	TSP	Bus	Corridor					↓5%-16%		↓0.8%-4%
Berkeley, CA (Skabardonis, 2000)	TSP	Bus	Corridor			↓1%		↓2-6 s	↑4%	
Vancouver, Canada (Ekeila et al., 2009)	TSP	Light rail	Intersection		Not Significant					↓6%- 8%
West Valley City, (Zlatkovic et al., 2012)	TSP	Bus	Corridor			↓10%-23%		↓20%-	↑7%-13%	↓6%-14%
UT (Zlatkovic et al., 2012)	& QJL							70%		
Pleasanton, CA (Lahon, 2011)	TSP & QJL	Bus	Corridor							↓30%
Rostov-on-Don,Russia (Zyryanov and Mironchuk, 2012)	IBL	Bus	Corridor						8%-20%	

CHAPTER 3

TPT EVALUATION

Extensive literature exists on the impact of transit preferential treatments on traffic and transit operations, however, very few studies have evaluated TPTs using analytical models. In addition, there is limited research on investigating the impact of space and time TPTs, individually and in combination, on traffic and transit operations. Furthermore, existing studies have used various performance measures such as: vehicle delay, schedule adherence, travel time and queue length; but, very few studies have used person-based measures in their evaluation. This chapter presents an analytical model to evaluate TPTs using person-based measures, which could be used for such assessments without the need for expensive simulations.

3.1 Transit Preferential Treatment Alternatives

Three types of space TPTs and one type of time TPT have been selected for evaluation with regards to their impact on person delay and person discharge flow at signalized intersections. These TPTs are first implemented and evaluated individually. Then, three space priority strategies are combined with the one time priority strategy to investigate their impact when implemented together. TPTs that are studied consist of:

- Space TPTs
  - Queue Jumper Lane Addition: Queue jumper lanes are modeled according to the TCRP Report 19 guidelines (Fitzpatrick et al., 1996). The report

provides guidelines for locating and designing bus stops in various operating environments. Right lane near-side and far-side open bus bays are added for bus deceleration and acceleration on the direction of interest at all intersections. Right-turning vehicles are allowed to use queue jumper lanes. The second type of QJL (see section 2.3) is studied as part of this dissertation.

  - Bus Lane Addition: A dedicated bus lane is added on the direction of interest. The lane's width is the same as for the rest of the lanes, and right-turning vehicles are allowed to use it.
  - Bus Lane Substitution: The right most existing lane is substituted for a dedicated bus lane on the direction of interest, which can be used by right-turning vehicles.

- Time TPTs
  - Transit Signal Priority: Phase extension is applied for a chosen transit movement at all intersections when needed. When a TSP-equipped vehicle passes the priority request detector during the green phase, the strategy extends the green time for 10 seconds for that movement. Early green, as well as phase rotation or insertion, are not considered in this study.

3.2 Analytical Model for Evaluation of the MOEs

The analytical model presented in this chapter is an improvement to a model previously developed by Christofa et al. (2013). The model estimates vehicle delay and consequently person delay accounting for passenger occupancy of vehicles at signalized intersections when vehicles arrive in platoons and when transit vehicles are present during some of the cycles. In this study, the previously published model is extended to estimate vehicle discharge flow and therefore, person discharge flow and

estimate transit vehicles delays when space TPTs are in place. In addition, the current study addresses shortcomings of the previous research, as the former model could not evaluate the DBL or QJL performance with respect to various person-based MOEs. In addition, the impact of nearside bus stops on traffic operations and performance measures was not accounted for in previous research efforts.

The addition of a QJL, addition of a DBL, and substitution of a mixed-traffic lane for a DBL are the three spatial TPTs selected for evaluation in this study. For the base case, no TPTs are considered to be available. Analytical models both in the presence and absence of near-side bus stops are presented. In cases where bus stops are available, right lane near-side stops are added at the intersection approaches. For the existing conditions, a curbside bus stop located near-side the intersection are considered. When DBLs or QJLs are available, it is assumed that the bus stop is located within those lanes, not blocking general traffic. The impact of time TPTs (TSP) is also investigated both individually (implemented on the base case) and combined with each space TPT alternative.

For the development of the analytical model, it is assumed that vehicle operations can be described by kinematic wave theory (KWT) (Lighthill and Whitham, 1955, Richards, 1956) . Since the intersection under consideration is part of a larger signalized arterial, it is also assumed that autos travel in platoons. Platoon dispersion is considered negligible, so the autos are served at capacity and arrive at the same capacity flow at the downstream intersection. Therefore, all vehicle trajectories in a platoon are parallel, as shown in Figure 3.1(a). It is also assumed that vehicles are distributed equally between the lanes. In order to estimate the delay for a bus, it is assumed that it behaves as a platoon of size one after it joins the queue (Figure 3.1(b)). Compared to autos, the estimation of bus delay is different in that its arrival at the queue depends on the dwell time it experiences at a potential bus stop located upstream of the subject approach.

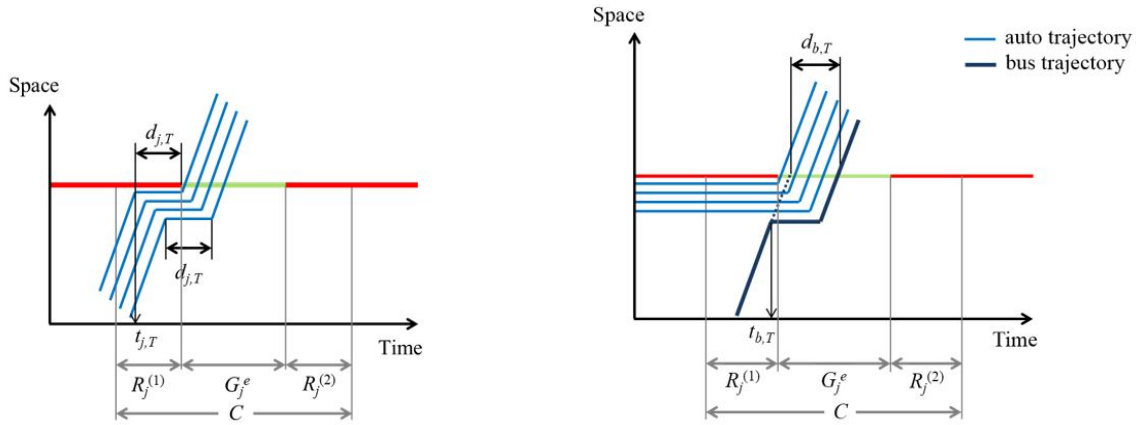

(a) Delay illustration for platooned autos

(b) Delay illustration for bus b

Figure 3.1: Vehicle delay estimation for platoon arrivals and transit vehicles

The following list presents the notation utilized for the development of the analytical model:

C: cycle length [sec];

$D_{j,T}$: total delay of autos in lane group j during cycle T [veh-sec];

$d_{j,T}$: delay of a single vehicle in the platoon in lane group j during a cycle T [sec];

$d_{b,T}$: delay of a single bus b during a cycle T [sec];

$d_{b,f}$: bus dwell time at bus stop f for bus b [sec];

G_j^e: effective green time for the phase that serves lane group j [sec];

j: lane group index (movement);

K_j: jam density [veh/ft];

$N_{j,T-1}^i$: case i residual queue size of lane group j at the end of the previous cycle T -1 [veh];

$n_{b,T}$: position of bus b in the platoon during cycle T [veh];

$P_{j,T}$: total platoon size of lane group j during cycle T;

$P_{j,T}^i$: case i platoon size of lane group j during cycle T;

$Q_{j,T}$: auto vehicle discharge flow during cycle T [vph];

$R_j^{(1)}$: component of the red time from the beginning of the cycle until the start of the green time for lane group j [sec];

$R_j^{(2)}$: component of the red time from the end of the green until end of the cycle for lane group j [sec];

s_j: total saturation flow of lane group j [vpm];

s_j^i: saturation flow for the vehicles in lane group j that belong to case i [vpm];

T: signal cycle index;

$t_{b,q}$: time it takes to serve the vehicles that are in queue in front of bus b [sec];

$t_{j,T}$: platoon arrival time at the intersection of lane group j during cycle T [sec];

$t_{b,T}$: arrival time of bus b at the intersection during cycle T if the bus does not dwell at a bus stop [sec];

$t_{b,T}^D$: arrival time of bus b at the intersection during cycle T if the bus dwells at a bus stop [sec];

$t_{l,T}$: waiting time before a lane change occurs for vehicles that change lanes during cycle T [sec];

X_b: bus position from the stopline when it arrives in queue [ft];

X_f: distance of bus stop f from the stopline [ft];

X_{qj}: queue jumper lane length [ft]; α^p: the portion of lanes serving vehicles associated with platoon p.

To estimate auto and bus delays, various possible cases that may occur are considered. Possible cases are introduced for each TPT alternative tested. The vehicle discharge flow is calculated based on the number of vehicles served by the intersection in each case. All things equal, a higher discharge flow would indicate lower delays since there are no changes in the signal settings. However, both delay and discharge flow are estimated and presented since different applications might require different measures of effectiveness for their analysis.

3.2.1 Auto Delay

3.2.1.1 Base Case

The term base case refers to all cases where no TPT is implemented. Auto delays for the base case are analyzed in two cases N and B. Case N represents the situation in which there are no buses traveling during the cycle while in case B a bus travels within the auto platoon and could stop at a bus stop or not. Bus delays for the base sub-cases are evaluated using sub-case T equations.

Case *N*

Based on the platoon arrival time, platoon size, residual queue length, and signal timing, different cases are considered. Note that for case N, $P_{j,T}^N$ and s_j^N are equal to the total number of vehicles in the platoon, $P_{j,T}$, and total saturation flow for the approach, s_j, respectively.

- Sub-Case $N1$: Platoon arrival before residual queue served, entire platoon served in green

  Vehicles in the residual queue, $N_{j,T-1}^N$, will be delayed by an amount of time equal to the red time from the beginning of the cycle until the start of the green time, $R_j^{(1)}$. All vehicles in the platoon will be served after the residual queue is served and they will be delayed by the time interval between the arrival time of the platoon and the time when the last vehicle in the residual queue is served.

  Total Auto Delay, $D_{j,T}$:

$$D_{j,T} = N_{j,T-1}^N R_j^{(1)} + P_{j,T}^N \left((T-1)C + R_j^{(1)} + \frac{N_{j,T-1}^N}{s_j^N} - t_{j,T} \right) \tag{3.1}$$

  Total Vehicle Discharge Flow $Q_{j,T}$:

$$Q_{j,T} = \frac{N_{j,T-1}^N + P_{j,T}^N}{C} 3600 \tag{3.2}$$

- Sub-Case $N2$: Platoon arrival before residual queue served, insufficient green to serve entire platoon

  Vehicles in the residual queue, $N_{j,T-1}^{N}$, will be delayed by an amount equal to the red time from the beginning of the cycle until the start of the green time, $R_j^{(1)}$. A portion of vehicles in the platoon will be served after the residual queue is served and they will be delayed by the time interval between the arrival time of the platoon and the time when the last vehicle in the residual queue is served. The rest of the vehicles in the platoon will be delayed an additional time interval equal to the red time interval until the end of the cycle, $R_j^{(2)}$.

  Total Auto Delay, $D_{j,T}$:

$$D_{j,T} = N_{j,T-1}^{N} R_j^{(1)} + P_{j,T}^{N} \left((T-1)C + R_j^{(1)} + \frac{N_{j,T-1}^{N}}{s_j^{N}} - t_{j,T} \right) + (P_{j,T}^{N} + N_{j,T-1}^{N} - G_j^{e} s_j^{N}) R_j^{(2)} \quad (3.3)$$

  The calculation of the discharge flow is based on the fact that the full green time is utilized to serve vehicles

  Total Vehicle Discharge Flow $Q_{j,T}$:

$$Q_{j,T} = \frac{G_j^{e} s_j^{N}}{C} 3600 \quad (3.4)$$

- Sub-Case $N3$: Insufficient green to serve residual queue

  All vehicles in the residual queue will be delayed by an amount equal to the red time from the beginning of the cycle until the start of the green time, $R_j^{(1)}$, and the ones that will not be served during cycle T will be delayed an additional time until the end of the cycle, (C-$R_j^{(1)}$). All vehicles in the platoon will be

delayed by the time interval between the platoon arrival and the end of the cycle.

Total Auto Delay, $D_{j,T}$:

$$D_{j,T} = N^N_{j,T-1}R^{(1)}_j + P^N_{j,T}(TC - t_{j,T}) + (N^N_{j,T-1} - G^e_j s_j)(C - R^{(1)}_j) \tag{3.5}$$

The calculation of the total vehicle discharge flow is based on the fact that the full amount of green time is utilized to serve vehicles.

Total Vehicle Discharge Flow, $Q_{j,T}$:

$$Q_{j,T} = \frac{G^e_j s^N_j}{C} 3600 \tag{3.6}$$

- Sub-Case $N4$: Platoon arrival after residual queue served, entire platoon served in green

  All vehicles in the residual queue will be delayed by an amount equal to the red time from the beginning of the cycle until the start of the green time that serves their lane group, $R^{(1)}_j$. The platoon will be served with no delay.

  Total Auto Delay, $D_{j,T}$:

$$D_{j,T} = N^N_{j,T-1}R^{(1)}_j \tag{3.7}$$

  The calculation of discharge flow is based on the fact that the whole residual queue and platoon are being served.

  Total Vehicle Discharge Flow $Q_{j,T}$:

$$Q_{j,T} = \frac{P^N_{j,T} + N^N_{j,T-1}}{C} 3600 \tag{3.8}$$

- Sub-Case $N5$: Arrival after residual queue served, insufficient green to serve entire platoon

  All vehicles in the residual queue will be delayed by an amount equal to the red time from the beginning of the cycle until the start of the green time, $R_j^{(1)}$, and the ones that will not be served during cycle T will be delayed an additional time until the end of the cycle, $(R_j^{(2)})$. All vehicles in the platoon will be delayed by the time interval between the platoon arrival and the end of the cycle.

  Total Auto Delay, $D_{j,T}$:

$$D_{j,T} = N_{j,T-1}^N R_j^{(1)} + \left(P_{j,T}^N - ((T-1)C + R_j^{(1)} + G_j^e - t_{j,T})s_j^N\right) R_j^{(2)} \quad (3.9)$$

  Total Vehicle Discharge Flow $Q_{j,T}$:

$$Q_{j,T} = \frac{N_{j,T-1}^N + ((T-1)C + R_j^{(1)} + G_j^e - t_{j,T})s_j^N}{C} 3600 \quad (3.10)$$

- Sub-Case $N6$: Arrival after the green, entire residual queue is served

  All vehicles in the residual queue will be delayed by an amount equal to the red time from the beginning of the cycle until the start of the green time, $R_j^{(1)}$. All vehicles in the platoon will be delayed by the time interval between the platoon arrival and the end of the cycle.

  Total Auto Delay, $D_{j,T}$:

$$D_{j,T} = N_{j,T-1}^N R_j^{(1)} + P_{j,T}^N (TC - t_{j,T}) \quad (3.11)$$

  The discharge flow is calculated based on the size of the residual queue since those are the only vehicles being served during the current cycle.

Total Vehicle Discharge Flow $Q_{j,T}$:

$$Q_{j,T} = \frac{N_{j,T-1}^{N}}{C} 3600 \tag{3.12}$$

3.2.1.2 Effect of Near-side Bus Stop

When a bus traveling within the auto platoon dwells at the near-side bus stop, as shown in Figure 3.2, the auto platoon can be divided into four separate sub-platoons A, B, C, and D. Sub-platoon A consists of the autos traveling in the lane(s) other than the lane that has the bus stop. Sub-platoon B includes autos in the bus stop lane that are ahead of the bus. Sub-platoon C involves autos waiting behind the bus and sub-platoon D includes autos behind the bus that decide to change their lane to avoid waiting behind the bus. Sub-platoons A and B will continue their regular trip while autos in sub-platoon C will stop and wait for the bus to finish loading and unloading passengers and then leave the intersection; thus, autos in sub-platoon C will experience additional delay due to the bus stop. Autos in sub-platoon D are those vehicles behind the bus that will attempt to change lanes to avoid waiting behind the bus while it dwells at the bus stop. Lane changing is possible when there is enough free space in the lane adjacent to the bus stop lane. It is assumed that autos in sub-platoon D will wait for sub-platoon A to clear, which is when the queue in sub-platoon A's lane is shorter than the distance from the stop line to the upstream end of the bus stop. As a result, the autos that want to change lanes will experience extra delay. If during a cycle, sub-platoon A does not allow enough free space for lane changes, then autos in sub-platoon D will not be able to change lanes and the size of sub-platoon D will be effectively zero.

In this study, the arrival time of the bus at bus stops is calculated assuming that the near-side bus stop is located very near the stop line. As a result, the free flow travel time from the bus stop to the intersection stop line is considered to be

negligible, or that short time may be assumed to be part of the dwell time used for the analytical calculations.

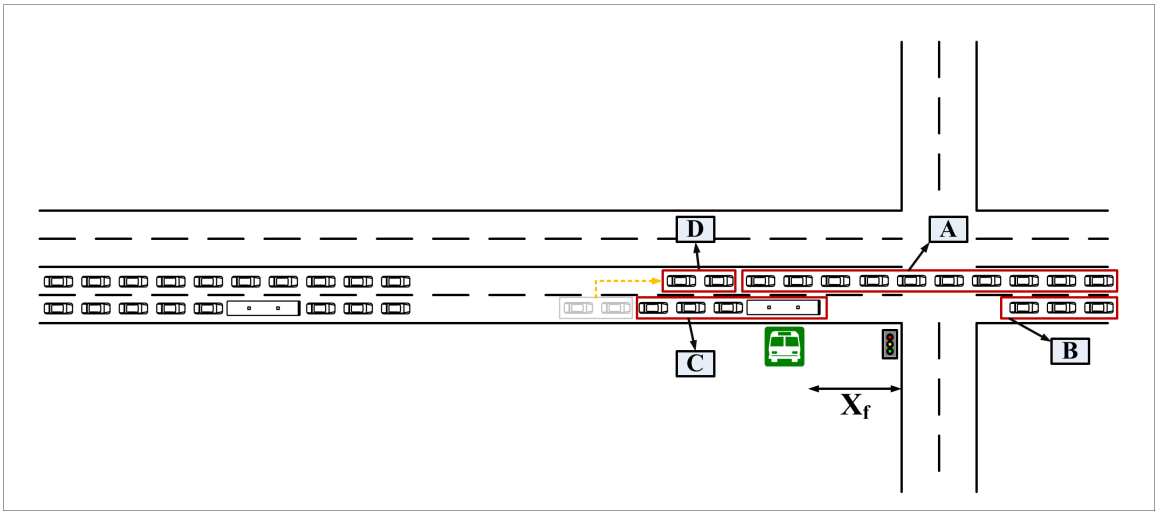

Figure 3.2: Platoons formed at an intersection approach with a near-side bus stop

Four sub-cases for the calculation of delay and discharge flow (BA, BB, BC, and BD) are considered for platoons A, B, C, and D as follows:

- Sub-Case BA:

$$P_{j,T}^{BA} = \alpha^{A} * P_{j,T} \tag{3.13}$$

$$s_{j}^{BA} = \alpha^{A} * s_{j} \tag{3.14}$$

In Figure 3.2, the portion of lanes serving vehicles of platoon A, α^{i} , is 0.5, indicating that the size of platoon A is half of the total platoon size for that lane group, because it includes vehicles that were originally in one lane of traffic. Therefore, the saturation flow is also half of the total saturation flow of that approach. Note that in this case, the residual queue of the previous cycle ($N_{j,T-1}^{BA}$) represents the residual queue of the previous cycle for platoon A, so it is again half the size of the residual queue for the whole approach. By replacing $P_{j,T}^{N}$, s_{j}^{N}, and $N_{j,T-1}^{N}$ with $P_{j,T}^{BA}$, s_{j}^{BA}, and $N_{j,T-1}^{BA}$ to the corresponding case N

equations (equations 3.1-3.12), auto delay and discharge flow for Sub-Case BA can be calculated.

- Sub-Case BB: The size of platoon B is equal to the number of autos in front of the bus, which is:

$$P_{j,T}^{BB} = n_{b,T} = max(0, (t_{b,T} - t_{j,T}) * s_j^{BB}) \tag{3.15}$$

and the associated saturation flow is:

$$s_j^{BB} = \alpha^B * s_j \tag{3.16}$$

where α^B represents the portion of lanes serving vehicles associated with platoon B, which is 0.5 for the case in Figure 3.2. The residual queue in front of platoon B is the residual queue of platoon C from the previous cycle, $N_{j,T-1}^{B}C$. Similar to Sub-Case BA, auto delay and discharge flow for Sub-Case BB can be calculated by replacing $P_{j,T}^{N}$, s_j^N, and $N_{j,T-1}^{N}$ with $P_{j,T}^{BB}$, s_j^{BB}, and $N_{j,T-1}^{BC}$ to the corresponding case N equations (equations 3.1-3.12).

- Sub-Case BC: The size of platoon C is the portion of the total number of vehicles behind the bus that will not change lanes. The total number of vehicles behind the bus is the total platoon size of the subject lane group minus the sizes of platoons A and B. So, the size of platoon C, $P_{j,T}^{BC}$, is:

$$\begin{aligned} P_{j,T}^{BC} &= (1-\beta) * (P_{j,T} - P_{j,T}^{BA} - P_{j,T}^{BB}) \\ &= (1-\beta) * (\alpha^C * P_{j,T} - max(0, (t_{b,T} - t_{j,T}) * s_j^{BB})) \end{aligned} \tag{3.17}$$

where β represents the portion of vehicles that change lanes. In cases where lane changing is not possible due to lack of free space, β is zero. The associated saturation flow for platoon C is:

$$s_j^{BC} = \alpha^C * s_j \tag{3.18}$$

In Sub-Case BC the bus is considered to be the first vehicle in platoon C and therefore, the arrival time of the first vehicle in platoon C at the intersection is equal to the arrival time at the bus stop plus the dwell time at the bus stop and is calculated as follows:

$$t_{j,T}^C = t_{b,T} + d_{b,f} \tag{3.19}$$

The residual queue in front of platoon C is the residual queue of platoon B in the same cycle, $N_{j,T}^{BB}$. Similar to Sub-Cases BA and BB, auto delay and discharge flow for Sub-Case BC can be calculated by replacing $P_{j,T}^N$, s_j^N, $t_{j,T}$, and $N_{j,T-1}^N$ with $P_{j,T}^{BC}$, s_j^{BC}, $t_{j,T}^C$ and $N_{j,T}^{BB}$ to the corresponding case N equations (equations 3.1-3.12).

- Sub-Case BD: The size of platoon D is the portion of the vehicles behind the bus that will change lanes. So, the size of platoon D, $P_{j,T}^{BD}$, is:

$$P_{j,T}^{BD} = \beta*(P_{j,T} - P_{j,T}^{BA} - P_{j,T}^{BB}) = \beta*(\alpha^D * P_{j,T} - max(0, (t_{b,T} - t_{j,T}) * s_j^{BB})) \tag{3.20}$$

and the associated saturation flow is:

$$s_j^{BD} = \alpha^D * s_j \tag{3.21}$$

In Sub-Case BD, the arrival time of the first vehicle in platoon D, $t^D_{j,T}$, at the intersection is the arrival time of the bus at the intersection stop line, $t_{b,T}$, plus the waiting time before a lane change occurs, $t_{l,T}$.

$$t^D_{j,T} = t_{b,T} + t_{l,T} \tag{3.22}$$

Lane changing waiting time is equal to the time platoon D is waiting behind the bus before it is capable of changing lanes, therefore, it depends on platoon Aś movement. The residual queue in front of platoon D is the residual queue of platoon A in the same cycle. Auto delay and discharge flow for Sub-Case BD can be calculated by replacing $P^N_{j,T}$, s^N_j, $t_{j,T}$, and $N^N_{j,T-1}$ with $P^{BD}_{j,T}$, s^{BD}_j, $t^D_{j,T}$ and $N^{BA}_{j,T}$ to the corresponding case N equations (equations 3.1-3.12).

3.2.2 Bus Delay

3.2.2.1 Mixed Traffic Lane

In this case, it is assumed buses travel within the auto platoon. For a bus to be within a platoon, its arrival time at the intersection stopline, $t_{b,T}$, should satisfy the following conditions:

$$t_{b,T} \geq t_{j,T} \tag{3.23}$$

and

$$t_{b,T} \leq t_{j,T} + P_{j,T}/s_j \tag{3.24}$$

and its position in the platoon can be estimated as follows:

$$t_{b,T} = max\{0, (t_{b,T} - t_{j,T}) * s_j\} \tag{3.25}$$

Based on the bus arrival time, platoon arrival time, platoon size, residual queue length, and signal timing, eight different cases are considered as follows:

- Sub-Case $TM1$: Platoon arrival before residual queue served, entire platoon served in green, bus is served during the green phase

  This case corresponds to case $N1$ of auto delay.

  Bus Delay, $d_{b,T}$:

$$d_{b,T} = (T-1)C + R_j^{(1)} + \frac{N_{j,T-1}^N}{s_j^N} - t_{j,T} \tag{3.26}$$

- Sub-Case $TM2$: Platoon arrival before residual queue served, insufficient green to serve entire platoon, bus is served during the green phase

  This case corresponds to case $N2$ of auto delay when the bus can be served during the green phase.

  Bus Delay, $d_{b,T}$:

$$d_{b,T} = (T-1)C + R_j^{(1)} + \frac{N_{j,T-1}^N}{s_j^N} - t_{j,T} \tag{3.27}$$

- Sub-Case $TM3$: Platoon arrival before residual queue served, insufficient green to serve entire platoon, bus is not served during green phase

  This case corresponds to case $N2$ of auto delay when the bus can not be served during the green phase.

  Bus Delay, $d_{b,T}$:

$$d_{b,T} = (T-1)C + R_j^{(1)} + \frac{N_{j,T-1}^N}{s_j^N} - t_{j,T} + R_j^{(2)} + R_j^{(1)} \tag{3.28}$$

- Sub-Case $TM4$: Insufficient green to serve residual queue

  This case corresponds to case $N3$ of auto delay.

Bus Delay, $d_{b,T}$:

$$d_{b,T} = TC + R_j^{(1)} + \frac{N_{j,T-1}^N - G_j^e s_j^N}{s_j^N} - t_{j,T} \tag{3.29}$$

- Sub-Case $TM5$: Platoon arrival after residual queue served, entire platoon served in green

  This case corresponds to case $N4$ of auto delay.

  Bus Delay, $d_{b,T}$:

$$d_{b,T} = 0 \tag{3.30}$$

- Sub-Case $TM6$: Arrival after residual queue served, insufficient green to serve entire platoon, bus is served during green phase

  This case corresponds to case $N5$ of auto delay when the bus can be served during the green phase.

  Bus Delay, $d_{b,T}$:

$$d_{b,T} = 0 \tag{3.31}$$

- Sub-Case $TM7$: Arrival after residual queue served, insufficient green to serve entire platoon, bus is not served during green phase

  This case corresponds to case $N5$ of auto delay when the bus can not be served during green phase.

  Bus Delay, $d_{b,T}$:

$$d_{b,T} = R_j^{(1)} + R_j^{(2)} \tag{3.32}$$

- Sub-Case $TM8$: Arrival after green, entire residual queue is served

  This case is corresponds to the case $N5$ of auto delay

  Bus Delay, $d_{b,T}$:

$$d_{b,T} = TC + R_j^{(1)} - t_{b,T} \tag{3.33}$$

3.2.2.2 Dedicated Bus Lane

Bus delays for the cases that dedicated rights-of-way are utilized by buses are estimated as follows:

- Sub-Case $TD1$: Bus arrival before the beginning of green

  The bus will experience delay equal to the time interval between the beginning of the green time interval and the bus arrival:

$$d_{b,T} = (T-1)C + R_j^{(1)} - t_{b,T} \tag{3.34}$$

- Sub-Case $TD2$: Bus arrival during the green phase

  The bus will get served as soon as it arrives at the intersection so it will not experience any delay:

$$d_{b,T} = 0 \tag{3.35}$$

- Sub-Case $TD3$: Arrival after the end of green

  The bus will experience delay equal to the time interval between the bus arrival time at the intersection in the current cycle and the beginning of the green time in the next cycle.

$$d_{b,T} = TC - t_{b,T} + R_j^{(1)} \tag{3.36}$$

3.2.2.3 Queue Jumper Lane

For the QJL alternative, auto delays can be calculated using the sub-case N equations. Bus delays will be estimated using two different sub-cases based on the location of the buses when they join the queue, as follows:

- Sub-Case $TQ1$: The distance between the intersection and the location of a bus when it joins the queue is longer than the queue jumper length ($X_b \geq X_{qj} or n_{b,T} \geq K_j * X_{qj}$). An example is shown in Figure 3.3. In this case the

bus cannot move to the queue jumper lane; thus, the bus will travel with auto traffic. The delay of the bus can be calculated using the equations presented in Sub-Cases $TM1$ - $TM8$.

- Sub-Case $TQ2$: The distance between the intersection and the location of a bus when it joins the queue is shorter or equal to the queue jumper length ($X_b \leq X_{qj} or n_{b,T} \leq K_j * X_{qj}$). An example is shown in Figure 3.4. In this case the bus moves to the queue jumper lane; thus, its delay can be calculated as if it were traveling on a DBL using equations provided for the $TD1$, $TD2$ and $TD3$ sub-cases.

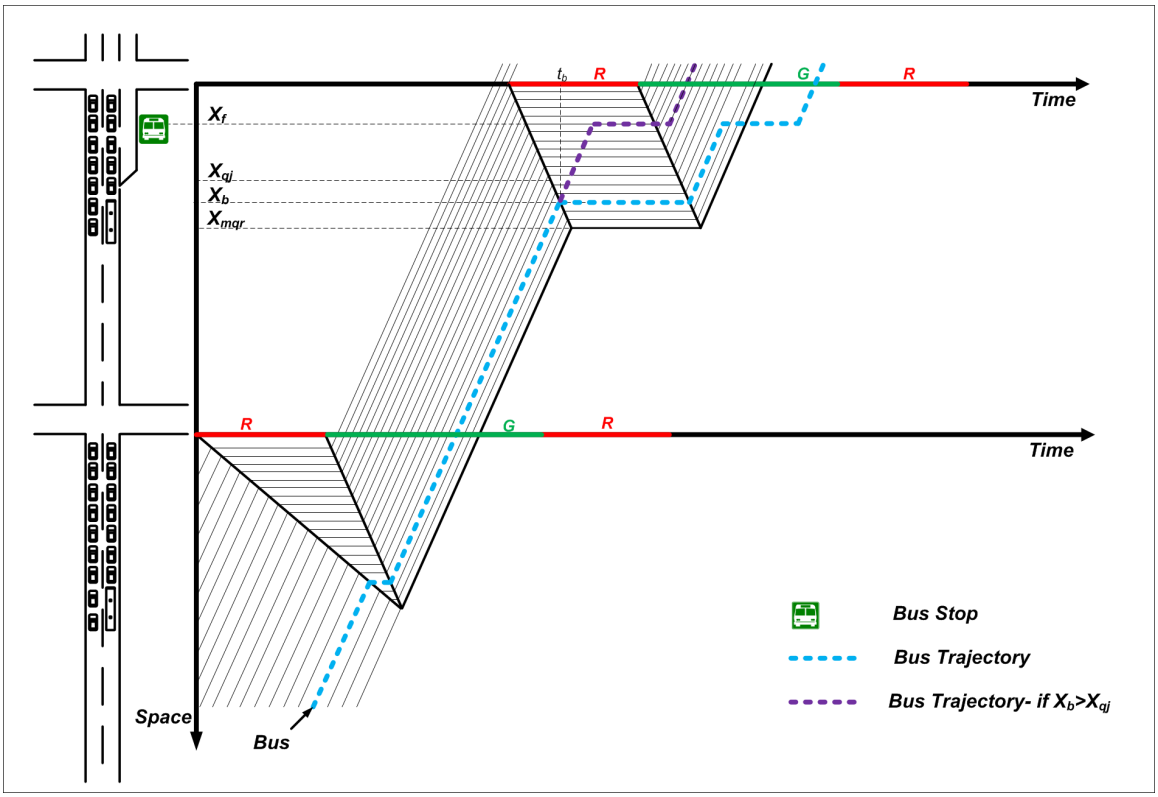

Figure 3.3: Time-space diagrams for a bus not utilizing the queue jumper lane

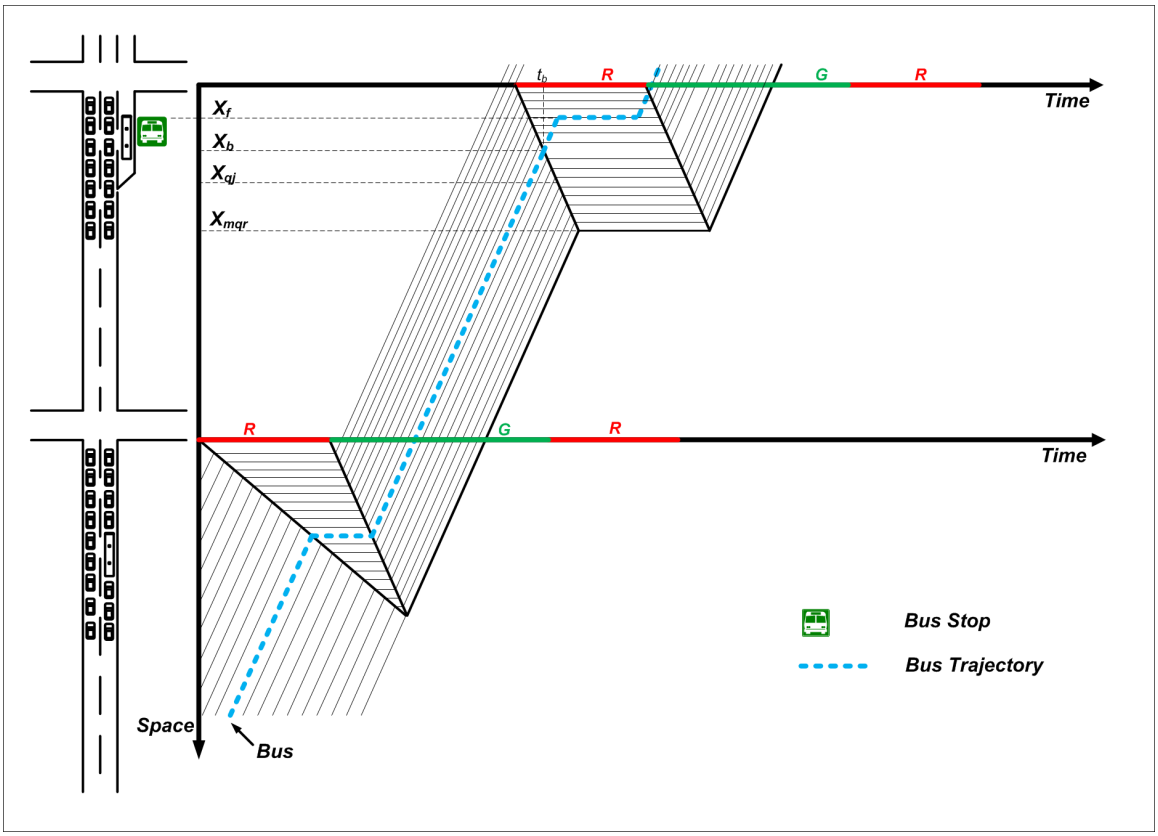

Figure 3.4: Time-space diagrams for a bus utilizing the queue jumper lane

3.3 Evaluation

Two types of space TPTs, DBLs and QJL, and one time TPT, green extension have been selected for evaluation with regards to their impact on person delay and person discharge flow at signalized intersections. For the QJLs, 240 feet deceleration lane at the upstream end and 420 acceleration lane and taper at the downstream end of the intersections are added according to the Transit Cooperative Research Program (TCRP) Report 19 guidelines (Fitzpatrick et al., 1996). Dedicated bus lanes are included in two types of scenarios: 1) DBL addition (a DBL is added on the direction of interest and has the same width as the mixed use lanes), and 2) DBL substitution (the right most existing lane is substituted for a DBL on the direction of interest). The time TPT scenario consists of providing a green extension of 10 seconds for a chosen transit movement at the intersection when needed, meaning

when it will result to reduced and ideally zero delay for the transit vehicle. These TPTs are first implemented individually. Then, each of the space priority strategies is combined with the time priority strategy to investigate their impact on person delay and person discharge flow when implemented together.

Two types of tests are performed and their results are compared with the help of the two types of models that have been developed: 1) analytical tests, and 2) microsimulation tests. An emphasis is placed on evaluating TPTs in terms of person delay and person discharge flow at signalized intersections. Vehicle discharge flow is also used in the evaluation.

3.3.1 Test Site

A four-intersection segment of San Pablo Avenue, in Berkeley, California, is used as the test site. The arterial section under consideration includes four signalized intersections: University Avenue, Delaware Street, Cedar Street, and Gilman Street. Figure 4.4 shows the arterial segment layout, bus stop locations, traffic volumes, and the bus routes along this segment during the evening peak hour (5-6pm). The distance between the intersections of San Pablo and University Avenues and San Pablo Avenue and Addison Street, which is the immediately upstream one, is 0.8 miles. In addition, emergency vehicles are not taken into account.

San Pablo Avenue is a signalized arterial accommodating vehicles and bus traffic in mixed traffic lanes. It has two lanes in each direction, 35 mph posted speed limit, permitted on-street parking, and left turning pockets at all intersections. The volumes and signal timings have been obtained by previous studies. The signals operate under a fixed-time coordinated signal control scheme with a common cycle length of 80 seconds. Ten bus lines travel through the corridor and on cross streets with headways that vary between 10 and 45 minutes during the evening peak hour that was used for the analysis. The northbound through movement, which is the heaviest

direction during the evening peak hour, has the following degrees of saturation for the four intersections moving from University Avenue towards Gilman Street: 0.94, 0.64, 0.70, and 0.84. Saturation flows were assumed to be 1,800 vph per lane. Data on individual buses departure times have been obtained from the Alameda-Contra Costa Transit Districts website (ACTransit, 2014).

3.3.2 Analytical Model Tests

To evaluate TPTs with the proposed analytical model, a one-hour microsimulation is performed with deterministic input for the platoon and bus vehicle arrival times, as well as for the platoon size at all northbound through approaches of the selected test site. Thirty bus arrival time scenarios are considered to capture the variability in the arrivals of transit vehicles and the average results of those thirty runs are presented. Platoon sizes and arrival times were assumed to be constant for all cycles of all scenarios. Since no information is available on the average car and bus passenger occupancies they have been assumed to be 1.25, and 30 persons per vehicle respectively. The developed analytical models are evaluated using MATLAB.

3.3.3 Microsimulation Tests

The microsimulation model used in the evaluation was developed using the AIMSUN software. The test site was modeled and calibrated during previous research studies by the authors (Christofa et al., 2013). The assumptions on the bus arrival times and auto and bus passenger occupancies were the same as for the analytical model. For the QJL alternative, right lane near-side and far-side open bus bays were added for bus deceleration and acceleration on the direction of interest at all intersections In addition, the right-turning vehicles were allowed to use the QJL or the DBL to turn right, which was not the case for the analytical model tests.

Green extension at signalized intersections was applied for transit vehicles. All northbound through buses were allowed to request priority as they approached an

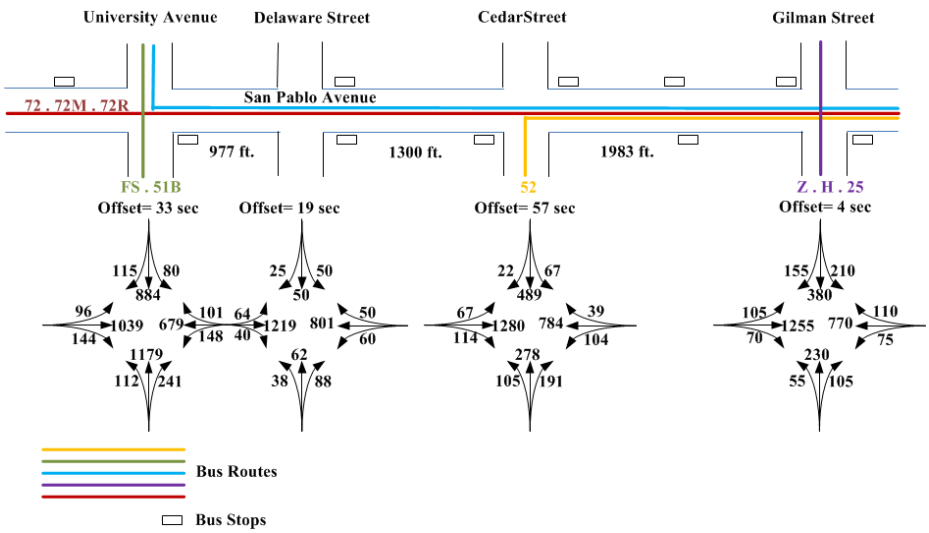

(a) Arterial layout, bus lines, and volumes (vph)

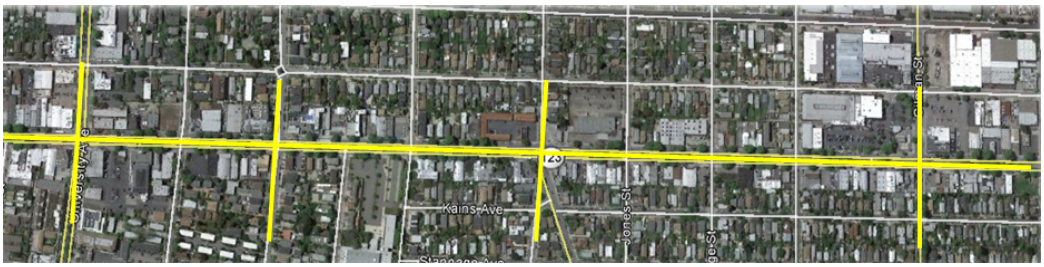

(b) Arterial map (*Source: Google Map*)

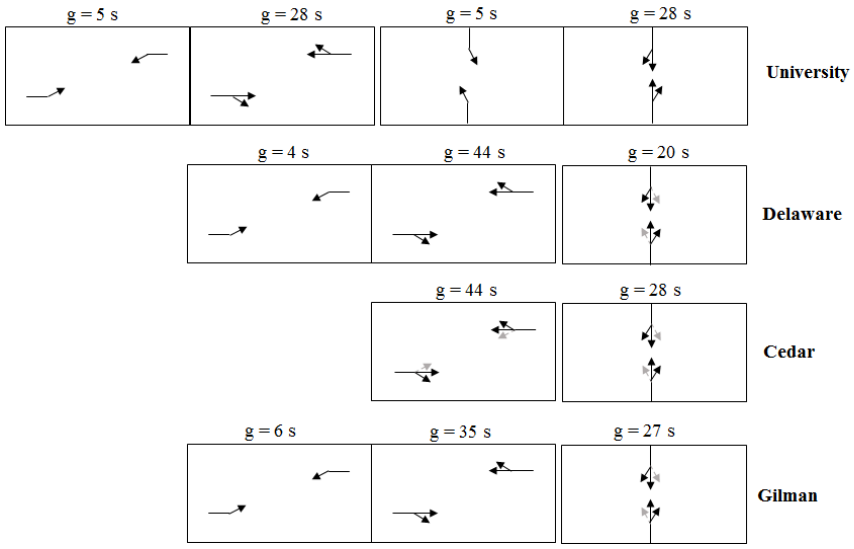

(c) Signal phases

Figure 3.5: Test site for TPT evaluation

intersection. The green time was extended by 10 seconds every time a bus was detected during the green phase for the transit movement. Priority request detectors were located upstream of each intersection stop line providing 5 seconds of travel time between the detector and stop line. To overcome the stochastic nature of microsimulation results, thirty replications were performed and the average outcome is presented. Each replication was run for one hour and it included 10 minutes of warm-up period.

3.3.4 Results

The microsimulation and analytical models are tested for both without and with nearside bus stops presence conditions. For the without nearside bus stop case, space and time priority strategies when implemented individually or in combination are tested. For the with nearside bus stop case, only space priority strategies are tested on the intersection of San Pablo Avenue and Cedar street.

3.3.4.1 Without Nearside Bus Stop

Figure 3.6 to 3.11 present the results provided by the analytical and microsimulation models for all eight alternative scenarios tested for the northbound through approaches of San Pablo Avenue with Cedar Street and Gilman Street. The focus was on the northbound direction since that is the heaviest one for the evening peak that was studied. While both the analytical and the microsimulation models have evaluated all four intersections, this study presents only results for Cedar Street and Gilman Street intersections, since they are the ones presenting the highest and lowest degree of saturation respectively, therefore allowing for a comparison of the TPT performance on congested (i.e., oversaturated) versus uncongested (i.e., close to saturation) approaches.

The results from the analytical model tests Figure 3.6 indicate that for the intersection of San Pablo with Cedar Street , there is a reduction in bus person delay

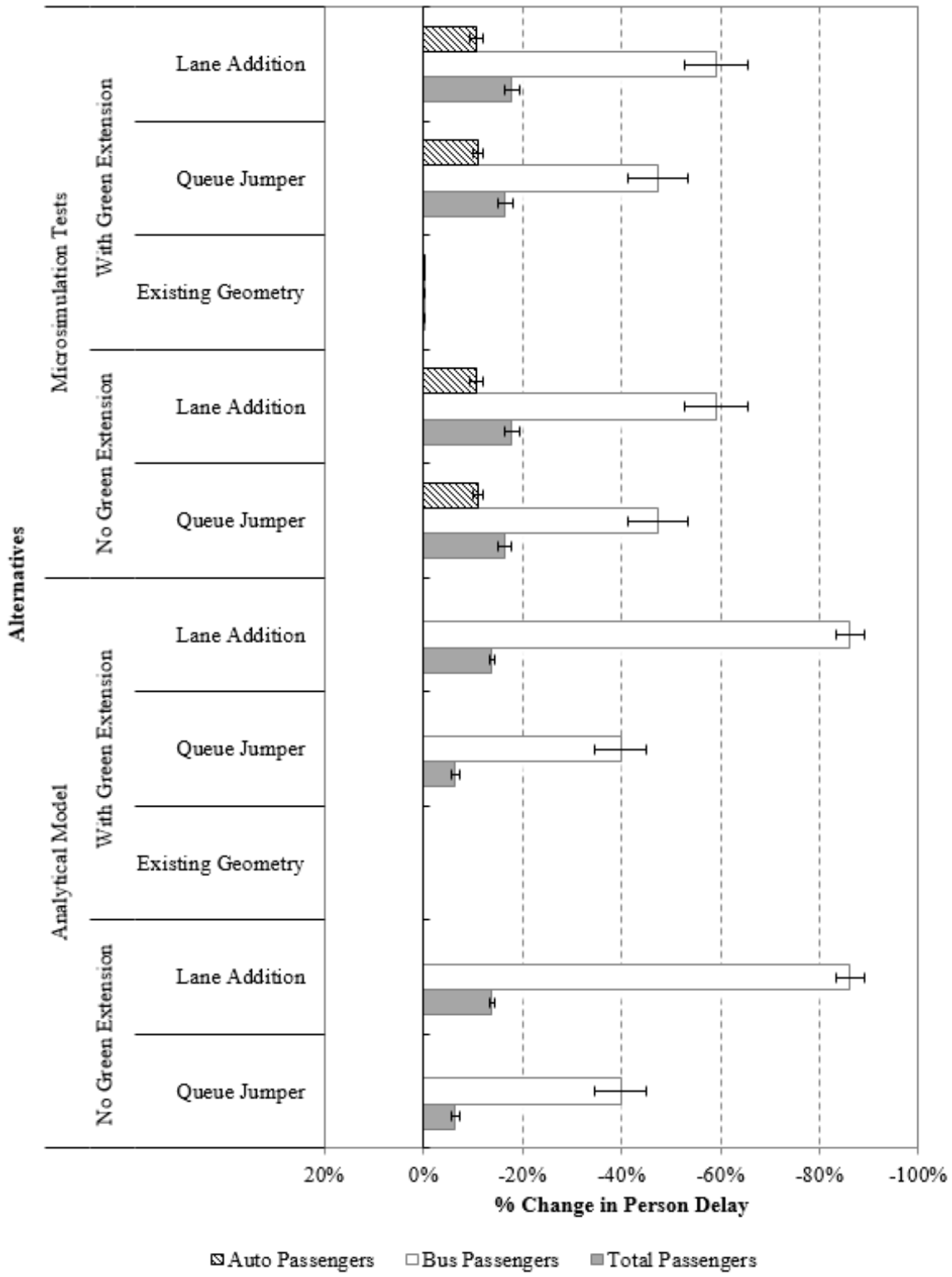

Figure 3.6: Percent change in person delay for the northbound direction at the intersection of San Pablo Avenue and Cedar Street with 30 passengers per bus (without bus stop)

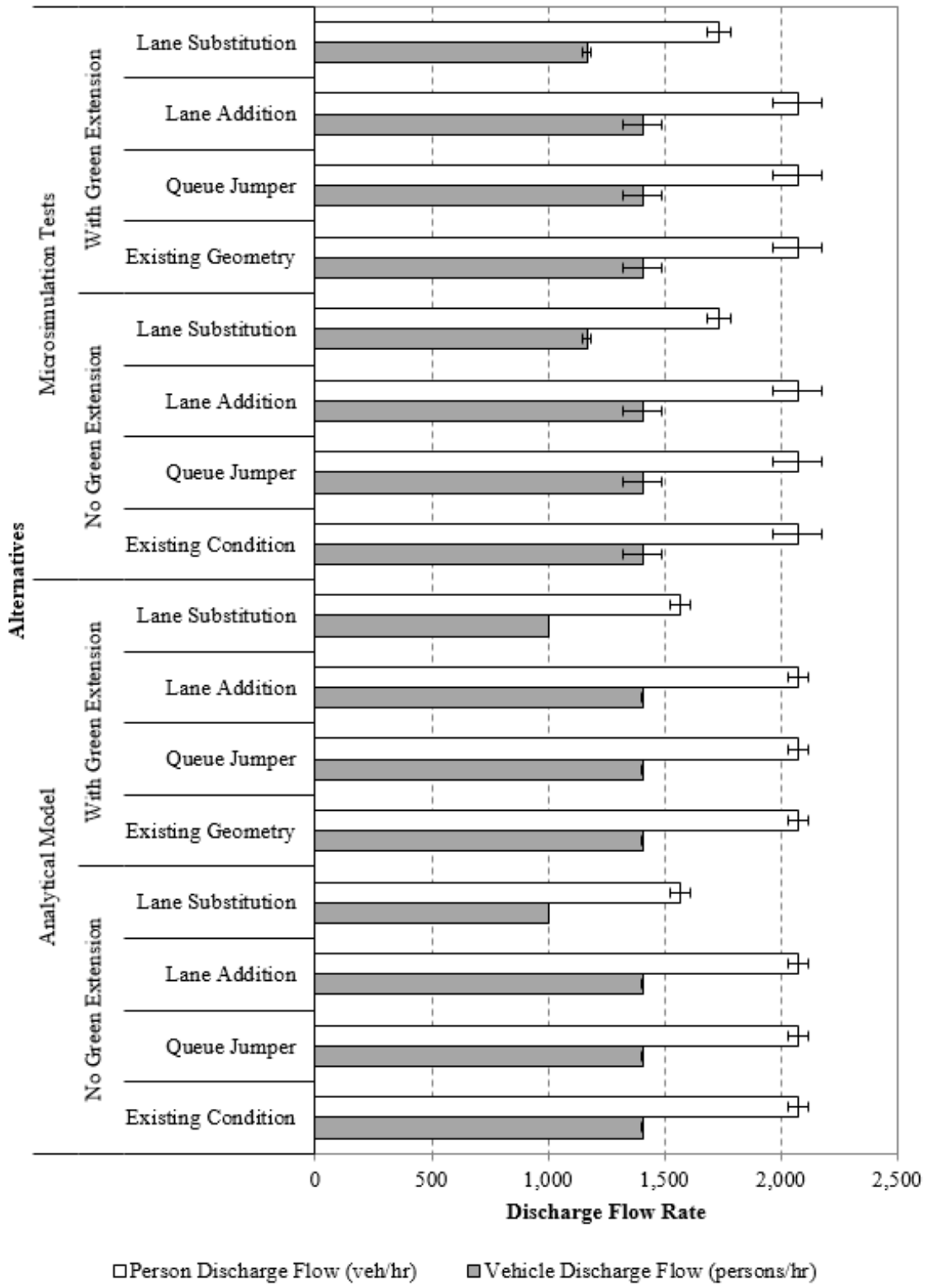

Figure 3.7: Discharge flow rate for the northbound direction at the intersection of San Pablo Avenue and Cedar Street with 30 passengers per bus (without bus stop)

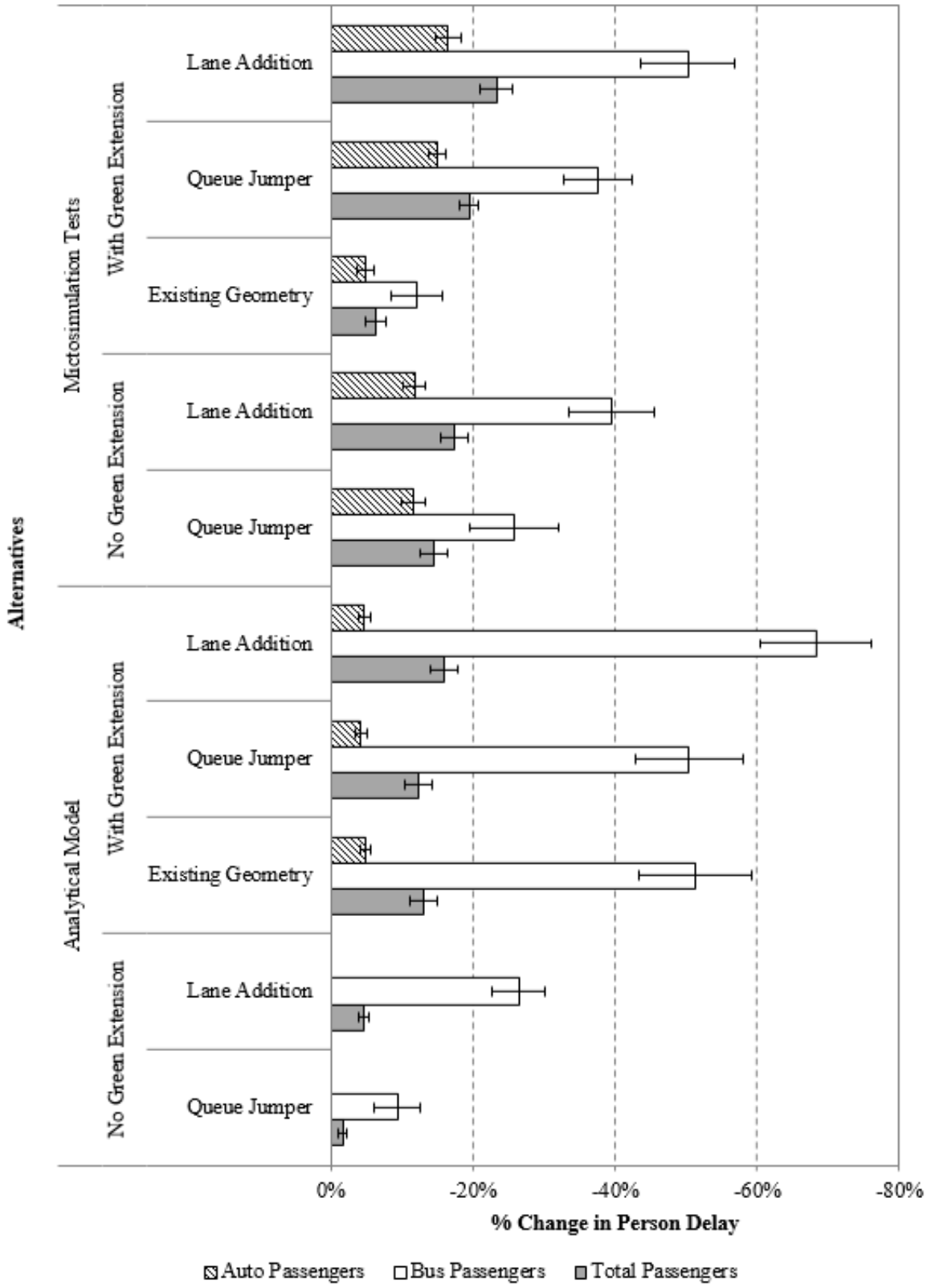

Figure 3.8: Percent change in person delay for the northbound direction at the intersection of San Pablo Avenue and Gilman Street with 30 passengers per bus (without bus stop)

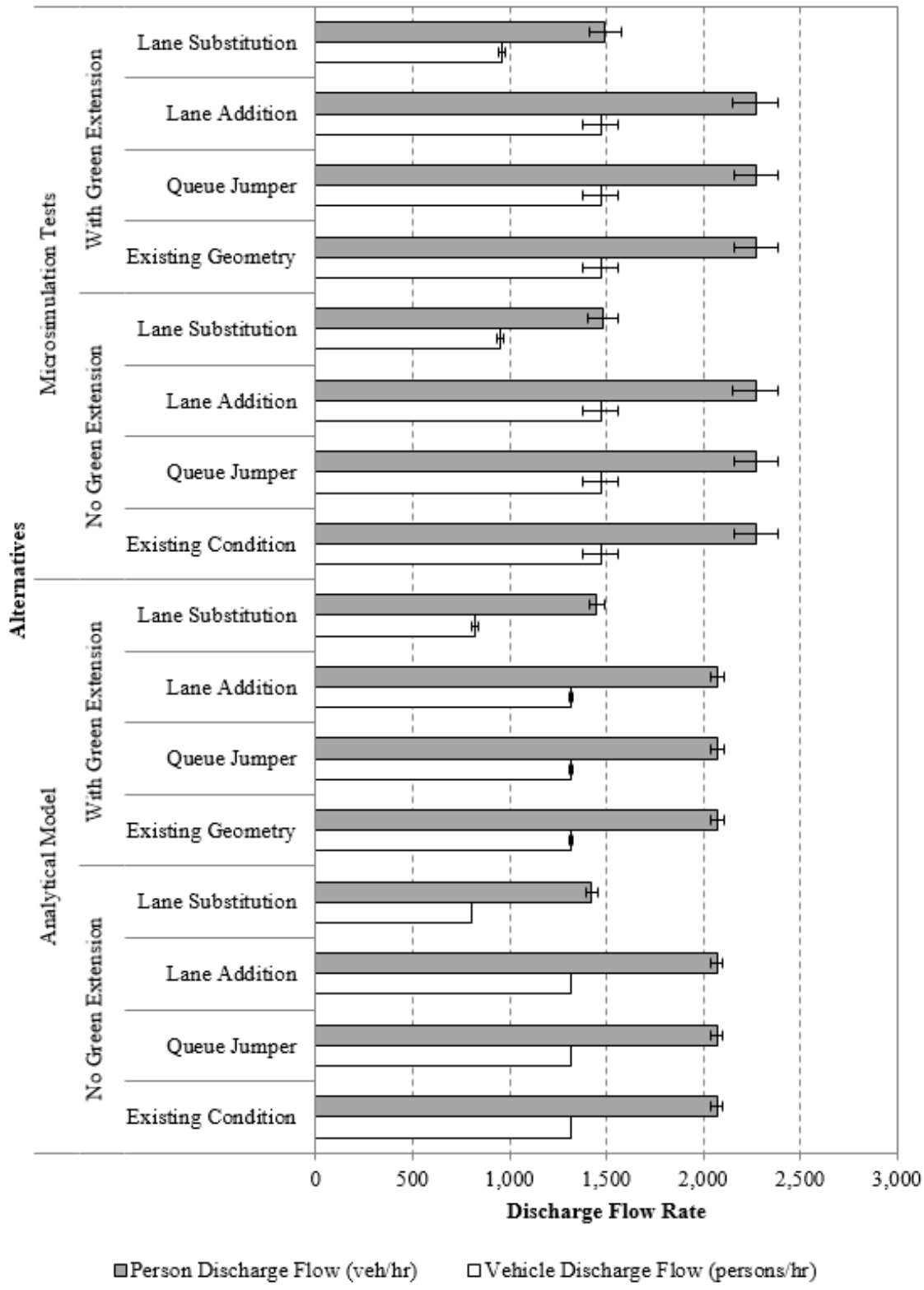

Figure 3.9: Discharge flow rate for the northbound direction at the intersection of San Pablo Avenue and Gilman Street with 30 passengers per bus (without bus stop)

by about 40% and 89% when QJL and DBL treatments are introduced respectively. When those treatments or existing conditions are combined with green extension, additional reductions are not observed. Bus lane substitution leads to a significant reduction in bus person delay, however, the total person delay increases since the intersection becomes oversaturated. Note that due to the big percent changes in person delay measure when bus lane substitution is implemented, the results of this alternative are not presented in Figure 3.6. Auto person delay does not significantly benefit from the green extension provision since all autos can pass the intersection during the regular green.. Person and vehicle discharge flows seem to remain at the same levels for all alternatives tested (Figure 3.7) and for both types of tests with the exception of the lane substitution alternative with and without green extension for which person discharge flow decreases by 29%. Similar results for person and vehicle discharge flows are observed for the microsimulation tests.

Microsimulation test results for the intersection of San Pablo with Cedar Avenue (Figure 3.6) indicate that when space TPTs are individually implemented bus person delay is reduced by about 47% and 59% with QJL and DBL addition treatments respectively. When no space TPT is implemented, green extension decreases bus person delay by about 0.1%. Total person discharge flow decreases by about 17% for bus lane substitution with and without green extension. Note that when space TPTs are combined with green extension the reductions in total, auto, and bus person delay are not significant as shown by the 95% confidence intervals in Figure 3.6.This is due to the higher variability in person delays observed in the microsimulation tests.

The analytical model results for the intersection of San Pablo Avenue and Gilman Street (Figure 3.8) show that implementation of individual space TPTs significantly decreases bus person delay by 9% and 26% for the QJL and DBL alternatives respectively. Combination of green extension and space TPTs results in extra 50% to 68% bus person delay reductions. For the bus lane substitution alternative the approach

becomes oversaturated and auto person delay increases by 2028%. As before, the lane substitution scenario is not presented in Figure 3.8. For the same scenario a significant reduction is observed in the vehicle and person discharge flow (Figure 3.9).

Microsimulation test results indicate that for the intersection of San Pablo Avenue and Gilman Street bus person delay decreases by about 26%, and 39% with QJL, and DBL alternatives respectively. Green extension implementation, individually or combined with space TPTs, significantly decreases bus person delay. When QJL, and DBL alternatives are combined with green extension the additional reductions of 11% and 12% in bus person delay are achieved. In addition, when no space TPT is implemented, green extension significantly reduces bus person delay by 12%.

There is consistency between the results of the analytical model and the AIMSUN microsimulation results for the space TPTs. In both the analytical and microsimulation results bus lane substitution significantly reduces vehicle and person discharge flow while QJL and DBL addition do not significantly change person discharge flow. In addition, space TPTs substantially decrease bus person delay. The significant differences observed between the analytical and the microsimulation results for the bus substitution alternative and in particular for the auto and total person delay on the Gilman Street intersection are due to the short length of the subject link. As a consequence of the short link vehicles are being kept upstream at the intersection, and thus delays are not captured in the microsimulation tests because microsimulation results are presented only for the link directly upstream of the intersection of San Pablo and Gilman Avenue.

The effects of green extension on the cross-street traffic is also examined in this study. Analytical model and microsimulation tests results of the San Pablo and Cedar Street intersection indicate that green extension does not increase total person delay for the cross street. Analytical model and microsimulation tests results for the intersection of San Pablo with Gilman Street show that green extension increases total

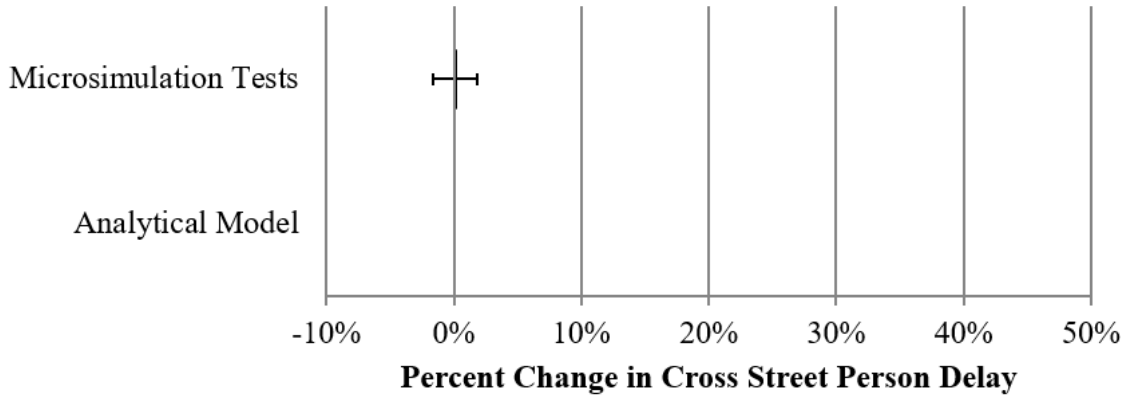

Figure 3.10: Percent change in total person delay for cross-streets at the intersection of San Pablo Avenue and Cedar Street (without bus stop)

person delay for the cross street by 4% and 11% respectively. While for both types of tests there is increase in the cross-street delay due to the reduced green time allocated to those approaches when green extension is provided in the northbound approach, the reductions are lower in the analytical model results due to the simplifying assumptions and the lack of stochasticity that accompany the analytical model.

Sensitivity Analysis

Sensitivity analysis is performed to investigate how the frequency of buses and their passenger occupancy affects the performance of the TPT alternatives with respect to person delay and person discharge flow.

Effect of Bus Frequency

For the sensitivity analysis bus frequencies in the studied direction (northbound) are doubled and the performance of the TPT alternatives is examined for the intersection of San Pablo Avenue and Gilman Street. Analytical results shown in Figure 3.13 reveal that with higher bus frequencies, higher person delay reduction is achieved when green extension is implemented in combination with space TPTs. In particular an extra 10% and 11% reduction in total person delay, in comparison to the case with regular bus frequency, is achieved when green extension strategy is combined

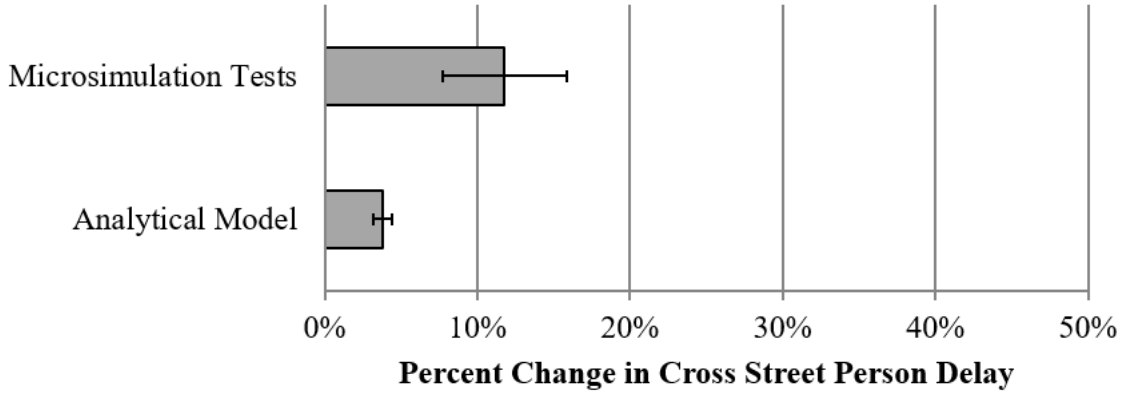

Figure 3.11: Percent change in total person delay for cross streets at the intersection of San Pablo Avenue and Gilman Street (without bus stop)

with QJL and DBL addition respectively Similar to the analytical models, microsimulation results show that green extension strategy is more effective with higher bus frequencies since an extra 1% and 2% reduction in total person delay, in comparison to the case with regular bus frequency, is achieved when green extension is combined with QJL and DBL addition respectively.

Effect of Bus Passenger Occupancy

The effect of various bus occupancies on the person delay is tested by increasing the bus passenger occupancy to 40 passengers per vehicle, compared to 30 passengers that were used in the previous tests. The auto passenger occupancy remained at 1.25 passengers per auto and the frequency was equal to the frequency of the initial tests performed. Results show that higher bus occupancy has insignificant effect on the person delay.

3.3.4.2 With Nearside Bus Stop

Nearside bus stop at the intersection of San Pablo Avenue and Cedar Street has been taken into account. Figures 3.15 and 3.16 represent the person delay evaluation of the alternatives using the analytical and simulation models for the northbound

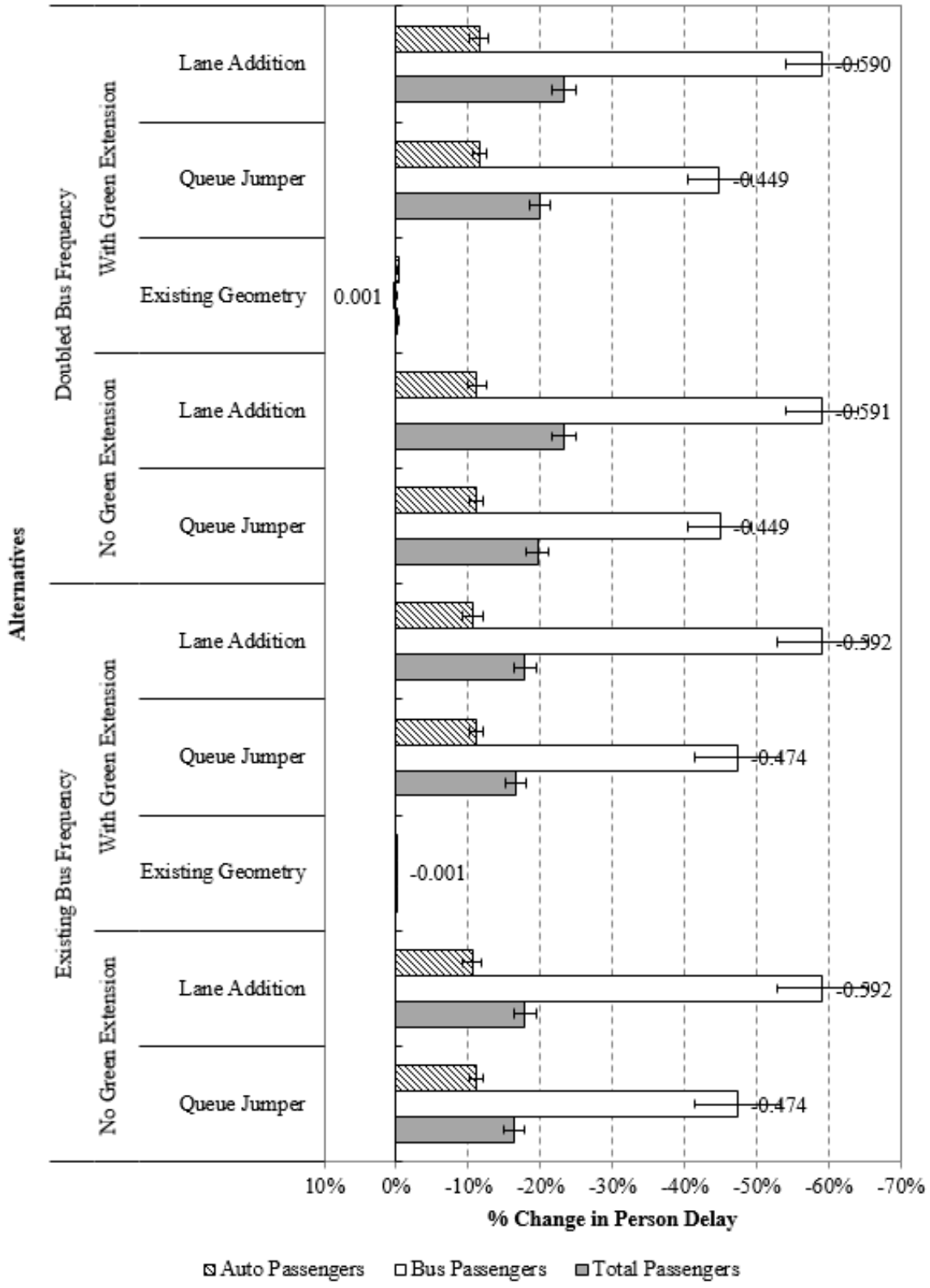

Figure 3.12: Microsimulation results for the percent change in person delay of the northbound direction at the intersection of San Pablo Avenue and Cedar Street with double bus frequency (without bus stop)

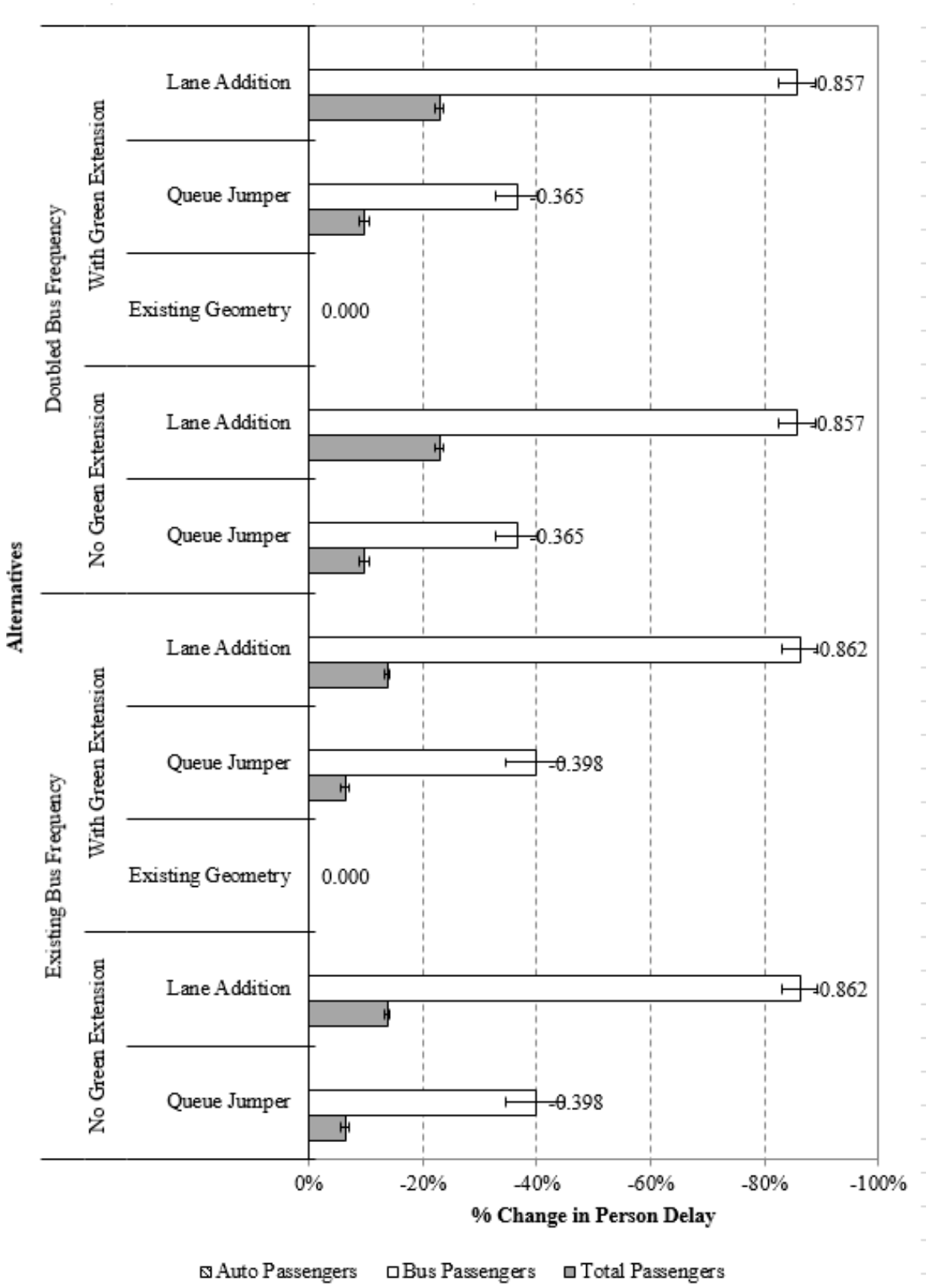

Figure 3.13: Analytical model results for the percent change in person delay of the northbound direction at the intersection of San Pablo Avenue and Cedar Street with double bus frequency (without bus stop)

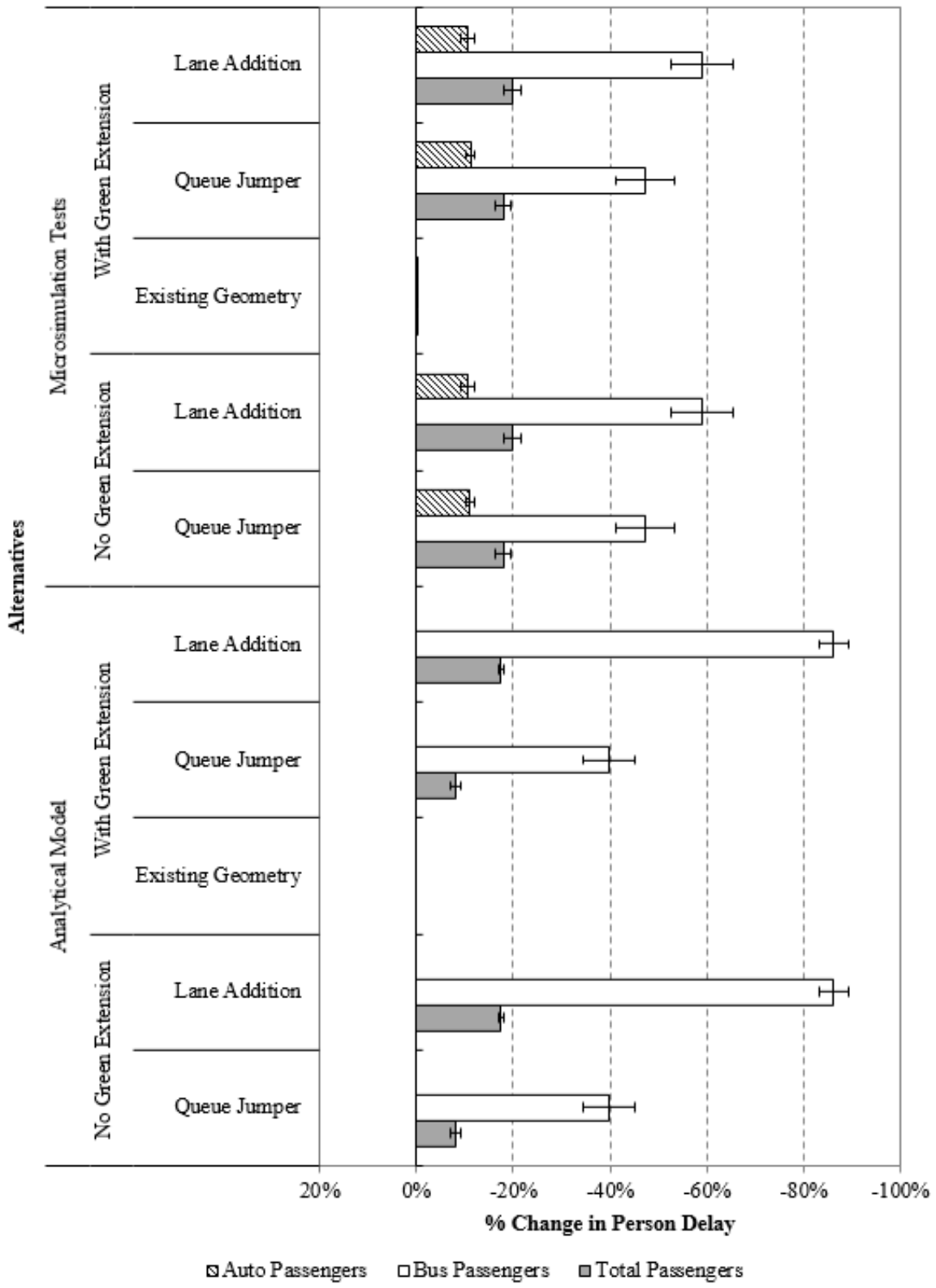

Figure 3.14: Percent change in person delay for the northbound direction at the intersection of San Pablo Avenue and Cedar Street with 40 passengers per bus (without bus stop)

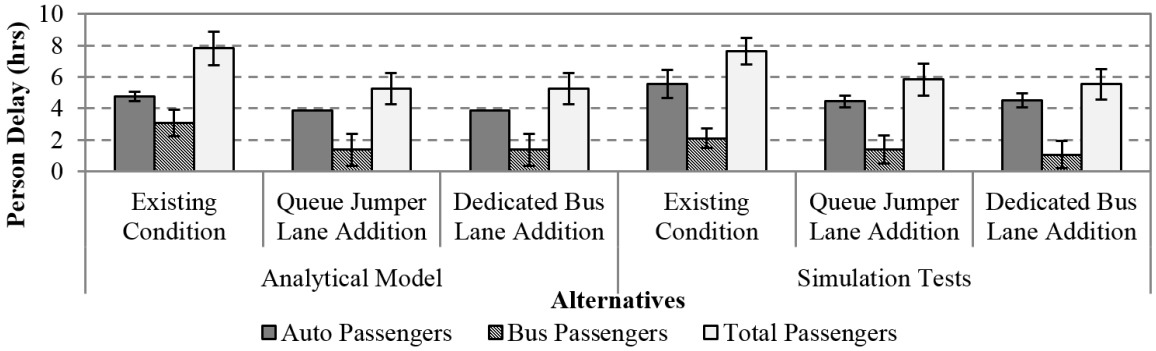

Figure 3.15: Person delay results of the analytical model and simulation tests for San Pablo Avenue northbound direction at the intersection with Cedar Street (with bus stop)

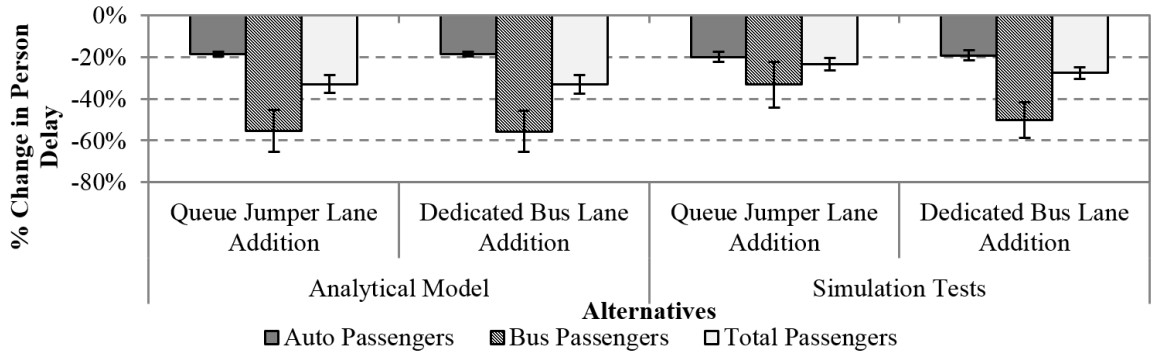

Figure 3.16: Percent change in person delay results of the analytical model and simulation tests for San Pablo Avenue northbound direction at the intersection with Cedar Street (with bus stop)

direction of traffic at the intersection of San Pablo Avenues and Cedar Street. No results are presented for the cross street traffic since there was no negative impact on it when a DBL or a QJL was added, due to no changes in the signal settings for the intersection.

The analytical model results indicate that implementation of space TPTs decreases bus person delay by up to 55%. When QJL and DBL are added, auto person delay is reduced by 18% due to the reduction in lane blockings by the stopped buses. The DBL substitution alternative gridlocks auto vehicles and increases auto person delay by 746%. Since traffic conditions at the test site are undersaturated, discharge

flow remains unchanged in the DBL addition and QJL alternatives. The results of the DBL substitution are not presented in Figures 3.15 and 3.16, because auto person delays of this alternative are very high which makes it difficult to distinguish the differences between the results of other alternatives when plotted in the same graph.

Simulation tests results reveal that bus person delay is reduced by 50% when a DBL is introduced. Auto person delay decreases by about 19% with QJL and DBL addition, but it increases by 142% with the DBL substitution alternative. As before, for the DBL substitution alternative the approach becomes oversaturated and auto person delay increases dramatically. The magnitude of the delay increase in the simulation is much lower than in the analytical model, because the simulation only accounts for the vehicles queued within the link, whereas the analytical model includes delays for vehicles that are blocked by the spillback on upstream links. The QJL and DBL addition alternatives reduce total person delay by 23% and 28% respectively.

The analytical model and simulation results suggest a 55% and 50% reduction in bus person delay respectively when DBL addition is implemented. Using a 5% level of significance, there is not a statistical difference between analytical model and simulation test results, since the p-value is $0.28>0.05$. The DBL addition decreases auto person delay by 18% and 19% according to the analytical model and the simulation test results respectively and these results are not significantly different from each other (p-value $= 0.33>0.05$). The analytical model and simulation results also indicate an 18% and 20% decrease in auto person delay with QJL implementation, and there is not enough evidence to conclude that the results differ from each other as the p-value is $0.19>0.05$. The results for the QJL alternative show that bus person delay is reduced by 55% in the analytical model, while simulation results suggest a 33% reduction. However, there is a significant difference between these results using a 95% confidence interval. The difference is mainly due to the assumption in the

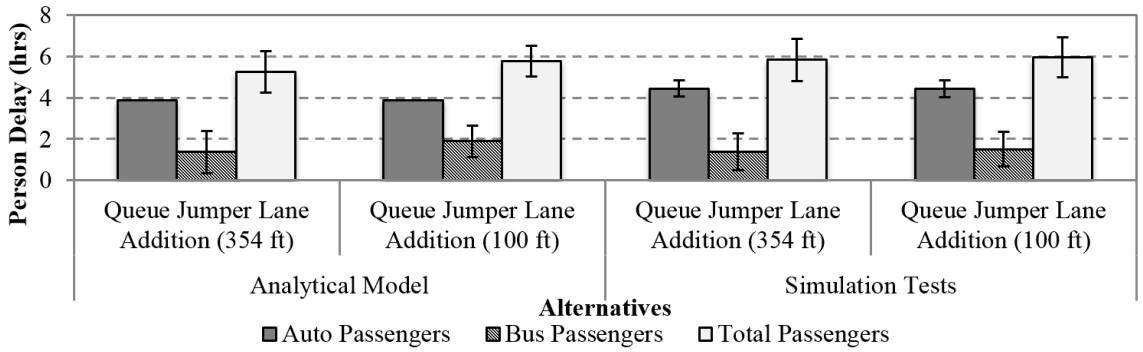

Figure 3.17: Queue jumper length effect on person delay for San Pablo Avenue northbound direction at the intersection with Cedar Street (with bus stop)

analytical model that buses traveling in the QJL merge into the through roadway downstream without experiencing any extra delay.

Since the assumed QJL length (345 ft) is longer than the observed for the specific traffic conditions queue length, buses change freely into the QJL without experiencing extra delay, and consequently bus delays for both QJL and DBL addition alternatives are the same based on the analytical model results. By shortening the QJL, bus delay would increase. To test this, a 100 ft long QJL was modeled. Figure 3.17 shows the results from the analytical model and simulation tests. With a 100 ft QJL bus person delay is 7% and 8% higher than for the 345 ft long queue jumper lane for the analytical model and simulation test results respectively. Total person delay in the DBL addition alternative is 6% less than the delay with a 100 ft long QJL.

3.4 Summary of Findings

The chapter presented an analytical model designed to evaluate the impact of alternative TPTs, in terms of person delay and person discharge flow at signalized both with and without nearside bus stops. The proposed analitycal models can handle both under-saturated on over-saturated conditions; however, in this study only under-saturated conditions have been evaluated. In addition the same TPTs are eval-

uated using a microsimulation model. For the without nearside bus stops condition, the evaluations were performed on a four-intersection signalized arterial located in Berkeley, CA. A total of eight alternative scenarios were evaluated. These scenarios included several space TPTs (DBL addition and substitution, and QJL addition) and a time TPT (green extension). Space and time TPTs were evaluated both individually and in combination. For the with nearside bus stops situation, only space priority strategies were evaluated on the intersection of San Pablo Avenue and Cedar Street.

The results of this study indicate that space TPTs introduce noticeable benefits to transit users. When a QJL or a DBL is added there is no negative impact on auto traffic. However, when a lane is substituted for a bus lane, person discharge flow decreases significantly and auto person delays increase dramatically. This is a result of the oversaturated conditions that the substitution of a lane is likely to cause for high vehicle demand levels. Therefore, DBL substitution is not suitable for high volume approaches, because it reduces the capacity by significant amounts. DBL substitution may be justified for high frequency transit lines, essentially when DBL substitution can serve at least as many people as it does when the lane is available for all vehicles. Implementation of green extension leads to favorable results for total person delay and bus person delay while autos on the priority approach also benefit. In addition, doubling the bus frequency had a positive impact in reducing total and bus person delay when green extension was implemented, while increased bus passenger occupancy had insignificant effect. Finally, a comparison of the analytical with the microsimulation test results indicates that the proposed analytical model can be used to quantitatively assess space and time TPTs.

The person-based analytical model that was presented in this study as well as the insights obtained in this study can be used to provide guidance in the planning and design of TPTs that improve transit reliability while improving overall mobility in urban areas. Developed analytical model can be used to assist decisions on prefer-

ential treatments under various traffic and transit operating conditions. In addition, this study showed that the analytical method could be used for such assessments without the need for expensive microsimulations since the results produced through microsimulation were comparable to the results produced with the analytical model.

CHAPTER 4

BUS TRAVEL TIME PREDICTION

Several applications of intelligent transportation systems (ITS) rely on short-term travel time predictions including advanced traveler information systems (ATIS) and transit signal priority (TSP) strategies. Accurate predictions can improve bus service reliability and traffic signal control efficiency while providing Transit Signal Priority (TSP). Automated Vehicle Location (AVL) systems are widely used by transit agencies; however, low resolution AVL data present a challenge in accurate travel time prediction. A robust parametric model is presented to predict bus travel time along signalized arterials.

The problem is formulated as a mixed-integer quadratic programming (MIQP) model and the unknown parameters are estimated using a robust norm approximation method. The model decomposes total transit travel time into its components including running travel time, dwell time at bus stops, and delays at signalized intersections. It then estimates signal status and predicts individual bus delays at intersections. The outcomes of the MIQP model are compared with the results of a linear regression model.

4.1 Methodology

Bus travel time along a dedicated bus lane in an urban arterial is modeled. In particular, bus travel time is decomposed to free flow travel time, acceleration/deceleration lost time, dwell times at bus stops, and intersection delay. The proposed model can decompose various components only if there are enough data to estimate sig-

nificant parameters. For example, if there is not enough data to estimate acceleration/deceleration lost times significantly, the model cannot distinguish acceleration/deceleration lost times from the free flow travel time. In this case, instead of estimating free flow travel time and acceleration/deceleration lost time separately, average running travel time can be estimated which includes both the free flow travel time and the acceleration/deceleration lost time components. In addition, if there is not enough data to distinguish dwell times at multiple bus stops or delays at multiple intersections, again these components can be aggregated in the average speed estimation of the section. In this case the prediction accuracy will be reduced. With lower data polling frequencies and lower number of buses traveling along the study section, the chance of not having enough data to significantly distinguish various travel time components increases. When there are not enough data to significantly estimate some components, those components must be aggregated in the average speed component.

4.1.1 Travel Time Decomposition

Bus travel time between two records is the time needed to travel from a specific upstream point where a record is obtained to a downstream one that a different record is obtained. The bus travel time includes free flow travel time, acceleration/deceleration lost time, dwell time at bus stops that may be located in-between the two points, and delays at signalized intersections that may exist between the two points. To decompose bus travel time, short segments of an urban arterial where traffic behavior conditions are assumed to be stationary are considered. As a result, it is assumed that the average speed do not vary along the study segment during the prediction period.

To facilitate the description of the model, the following sets, variables and parameters are defined:

- Sets:

- $I_N = \{1, 2, .., N\}$: Set of network intersections,
- $I_B = \{1, 2, .., B\}$: Set of buses traveling through the arterial segment,
- $I_A = \{1, 2, .., i\}$: Set of ordered AVL records,
- $I_K = \{1, 2, , K\}$: Set of bus stops,
- $I_{N_{i,j}}$ is a subset of I_N that includes the signalized intersections between AVL records i and j
- I_b is a subset of I_A that includes the AVL records for bus $b \in I_B$
- $I_{K_{i,j}}$ is a subset of I_K that includes the bus stops between AVL records i and j

- Variables:
  - $\bar{p}$: Average bus pace along a segment (sec/mile),
  - $\bar{v}$: Average bus speed along a segment (miles/sec),
  - t^n_{gr}: Beginning of the green signal indication for the direction of interest at intersection n as measured from the beginning of the cycle (sec),
  - t^n_b: Bus b arrival time at intersection n as measured from the beginning of the cycle (sec),
  - $tt^{u,n}_b$: Bus b travel time from the AVL record reported upstream of the intersection n to the intersection n stop line (sec)
  - $\hat{tt}_{b,i,j}$: Bus b travel time from AVL record i to j,
  - $\bar{w}^k$: Average dwell time at bus stop k (sec/bus),
  - $D^n_{b,1}$, $D^n_{b,2}$, $D^n_{b,3}$, $D^n_{b,4}$: Delay of bus b at intersection n for different cases (sec),
  - $\bar{D}^n$: Average bus delay at intersection n (sec),
  - D^n_b: Delay of bus b at intersection n (sec),

- $\bar{a}^n$: Average lost time at intersection n (sec),
- $\bar{ad}$: Average acceleration/deceleration lost time (sec),
- $x^n_{b,1}$, $x^n_{b,2}$, $x^n_{b,3}$, $x^n_{b,4}$: Binary variables indicating the delay case that bus b at intersection n belongs to.
- $y^n_{b,1}$, $y^n_{b,2}$: Binary variables indicating the bus arrival time case that bus b at intersection n belongs to.

- Parameters:
  - $t_{b,i}$: Bus b AVL record i time stamp (sec),
  - $t^{u,n}_b$: Bus b most recent time stamp upstream of intersection n (sec) as measured from the beginning of a cycle (sec),
  - $l_{b,i,j}$: distance traveled by bus b between records i and j (miles),
  - $l^{u,n}_b$: distance between most recent record of bus b upstream of intersection n and intersection n stop line (miles),
  - $AD_{b,i,j}$: Number of acceleration/deceleration events from AVL record i to j for bus b,
  - M: Big number,
  - C^n: Signal cycle length of intersection n (sec),
  - r^n: Signal red phase duration for the direction of interest at intersection n (sec),
  - g^n: Signal green phase duration for the direction of interest at intersection n (sec).

Figure 4.1 illustrates an urban arterial layout, used to facilitate the description of the models. The network includes multiple signalized intersections. Each AVL record i of a bus b includes geographical location information, i.e., coordinates at time $t_{b,i}$.

The distance a bus travels between two records i and j ($l_{b,i,j}$) can be determined by mapping the records to the roadway. The records stored while loading and alighting passengers or while the bus is stopped at an intersection are dismissed. In Figure 4.1 for instance, record 4 is stored while the bus dwells at the bus stop. Since the proportion of the dwell time component of the travel time from point 3 to 4 and from point 4 to 5 cannot be determined, record 4 is dismissed, and the travel time from point 3 to 5 is analyzed, which includes the total dwell time at bus stop 2. Dwell time is defined as the total time spent from the moment the bus doors open until the bus leaves the bus stop. Highway Capacity Manual defines dwell time as the time required to serve passengers at a stop plus the time required to open and close the doors (HCM, 2010).

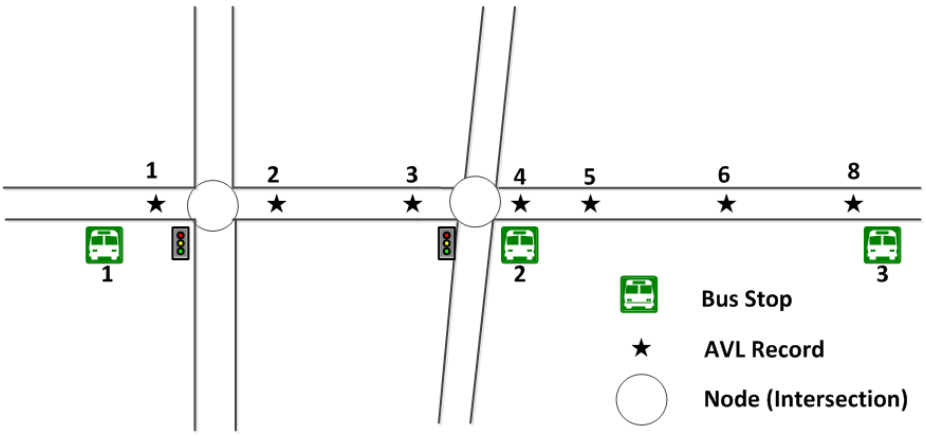

Figure 4.1: Urban arterial layout

The estimate of bus travel time from record $i-1$ to record i, $\hat{tt}_{b,i-1,i}$, can be calculated as free flow travel time between the two consecutive records, acceleration/deceleration lost time, dwell time at the bus stops, and delay at the intersections between $i-1$ and i as follows:

$$\hat{tt}_{b,i-1,i} = \bar{p} * l_{b,i-1,i} + \bar{ad} * AD_{b,i-1,i} + \sum_{k \in I_{K_{i-1,i}}} \bar{w}^k + \sum_{n \in I_{N_{i-1,i}}} \bar{D}^n \quad \forall b \in I_B, \quad i \in I_b, \quad \& \quad i \neq 1 \quad (4.1)$$

The unknown variables in equation (4.1) are $\bar{p}$, $\bar{w}^k \ \forall \ k \in I_K$, and $\bar{D}^n \ \forall \ n \in I_N$ which could be estimated by estimation methods like least-squares method.

4.1.2 Linear Regression

In previous research (Farid et al., 2016) the unknown parameters in equation (4.1) were estimated using the following linear regression model was formulated :

$$\hat{tt}_{b,i-1,i} = \beta_1 * l_{b,i-1,i} + \beta_2 * AD_{b,i-1,i} + \sum_{k \in I_K} \beta_3^k * \lambda_{b,i-1,i}^k + \sum_{n \in I_N} \beta_4^n * \mu_{b,i-1,i}^n \quad \forall b \in I_B, \quad i \in I_b \quad \& \quad i \neq 1 \quad (4.2)$$

where

$$\lambda_{b,i-1,i}^k = \begin{cases} 1 & \text{if bus stop k is between records i-1 and i} \\ 0 & \text{otherwise} \end{cases} \quad (4.3)$$

$$\mu_{b,i-1,i}^n = \begin{cases} 1 & \text{if intersection n is between records i-1 and i} \\ 0 & \text{otherwise} \end{cases} \quad (4.4)$$

β_1 represents expected values for bus pace while β_2 is the expected values for acceleration/deceleration lost time, β_3^k is the expected value of dwell times at bus stop k and β_4^n is expected value of delay at intersection n.

4.1.3 MIQP Model

β_3^n in the linear regression model (equation (4.2)) is the expected value of bus delays at intersection n over all buses; However, determining individual bus intersection

delay is critical since the variation in this type of delay could be large due to some of the buses stopping and some not stopping at the signalized intersection. Therefore, determining individual bus intersection delay could improve the accuracy of travel time predictions. In this regard equation (4.1) becomes:

$$\hat{tt}_{b,i-1,i} = \bar{p} * l_{b,i-1,i} + \bar{ad} * AD_{b,i-1,i} + \sum_{k \in I_{K_{i-1,i}}} \bar{w}^k + \sum_{n \in I_{N_{i-1,i}}} D_b^n \quad \forall b \in I_B, i \in I_b \quad \& \quad i \neq 1 \quad (4.5)$$

Where D_b^n is delay of bus b at intersection n. The difference between equations (4.1) and (4.5) is that in equation (4.1) average intersection delay over all buses, $\bar{D}^n$, is estimated. In equation (4.5), intersection delay for each individual bus at intersections, D_b^n, are estimated. In this regard, the proposed MIQP model estimates signal phases status and by inferring trajectories of the buses, it estimates individual bus delays. Next, individual bus intersection delay is further investigated.

Intersection delay is defined as the difference between the time a bus actually passes the intersection and the time it would have passed if it did not have to stop at the intersection. To calculate the intersection delay, perfect knowledge about the signal settings and signal status during the estimation period is usually required. In this study, no knowledge about the actual signal status of the intersection is assumed. However, we have assumed that signal settings remain constant during each study period and the duration of signal phases is given. In cases where the study period includes multiple periods with constant but different signal settings (e.g. peak and off-peak signal plans), each of those periods should be analyzed separately.

To estimate intersection delay, bus arrival time at the intersection as well as the beginning of the green for the bus approach are needed, both of which are considered unknown and should be estimated. Bus arrival time at the intersection stop line, $\hat{t}_b^n$, can be estimated using the time stamp of the AVL record just upstream of the

intersection, $t_b^{u,n}$, and the bus travel time from the record location to the intersection, $\hat{tt}_b^{u,n}$. The time interval between the beginning of the cycle and the beginning of the green phase, t_{gr}^n, is constant and is less than the cycle length. Federal Highway Administration defines a cycle as the total time to complete one sequence of signalization for all movements at an intersection (Koonce et al., 2008).

The estimated time interval between the bus arrival time at the intersection stop line and the beginning of the cycle is:

$$\hat{t}_b^n = (\hat{tt}_b^{u,n} + t_b^{u,n}) \% C^n = \hat{tt}_b^{u,n} + t_b^{u,n} - \lfloor (\hat{tt}_b^{u,n} + t_b^{u,n} / C^n \rfloor * C^n \quad \forall b \in I_B, \quad n \in I_N \tag{4.6}$$

Since $\hat{tt}_b^{u,n}$ is a variable, the floor operator in equation (4.7) will result in a non-quadratic and non-linear objective function. To determine $\hat{t}_b^n$ using linear inequalities, two cases (Figure 4.2) are considered assuming that bus arrival at the intersection stop line, $\hat{t}_b^n$, occurs during the same or next cycle as the most recent record upstream of the intersection, $t_b^{u,n}$. If not, more cases should be added. In case A1, both $\hat{t}_b^n$ and $t_b^{u,n}$ are in the same cycle and in case A2, $\hat{t}_b^n$ is in the next cycle.

Case A1: $\hat{tt}_b^{u,n} + t_b^{u,n} \leq C^n$

In this case both $\hat{t}_b^n$ and $t_b^{u,n}$ are in the same cycle and as a result, $\hat{t}_b^n = \hat{tt}_b^{u,n} + t_b^{u,n}$.

Case A2: $\hat{tt}_b^{u,n} + t_b^{u,n} > C^n$

In this case $\hat{t}_b^n$ is in the next cycle than the one that the last record for bus b upstream of the intersection was reported. In this case $\hat{t}_b^n = \hat{tt}_b^{u,n} + t_b^{u,n} - C^n$.

Therefore, the bus arrival time at intersection stop line can be expressed as follows:

$$\hat{t}_b^n = \hat{tt}_b^{u,n} + t_b^{u,n} - y_{b,2}^n * C^n \quad \forall b \in I_B, \ n \in I_N \tag{4.7}$$

where $y_{b,2}^n$ is a binary variable which is one if case A2 is true and zero otherwise.

The delay of the buses traveling in the dedicated bus lane depends on the arrival time of the bus at the stop line, t_b^n, the signal status when the bus arrives, and

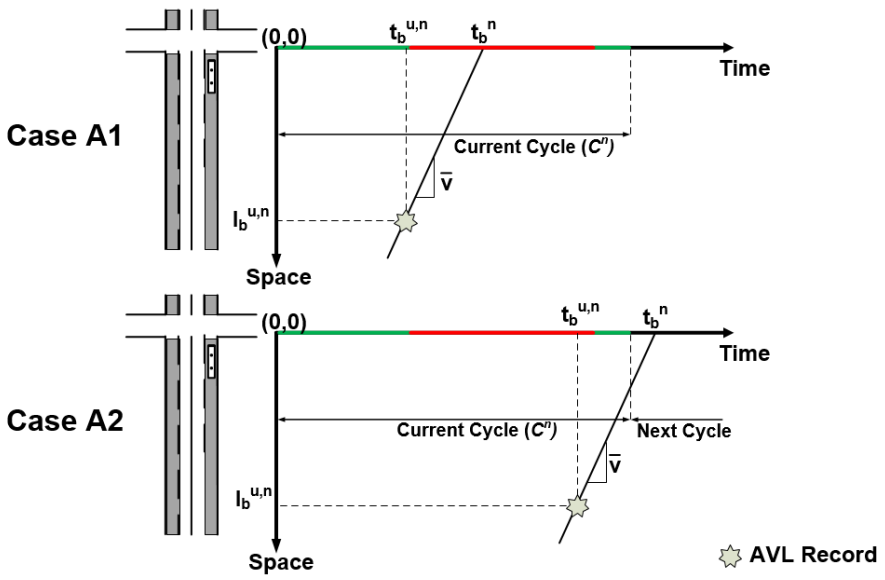

Figure 4.2: Cases of bus arrival times at the intersection stop line.

the duration of the signal phases at the intersection of interest. To estimate the intersection delay as a function of the bus arrival at the intersection stop line, four different cases are considered, which are shown in Figure 4.3. In cases D1 and D2 the phase at the beginning of the cycle is green while for cases D3 and D4 it is red. In cases D1 and D3 the bus arrives at the intersection during the green phase while in cases D2 and D4 the bus arrives during the red phase.

Case D1: $t_b^n \leq t_{gr}^n - r^n$

The bus arrives at the intersection stop line during the green phase and a portion of the green phase precedes the red one in the cycle. The bus passes the intersection without experiencing delay.

$$D_{b,1}^n = 0 \quad \forall b \in I_B,\ n \in I_N \tag{4.8}$$

Case D2: $t_{gr}^n - r^n < t_b^n \leq t_{gr}^n$

The bus arrives at the intersection stop line during the red phase and a portion of the green phase precedes the red one in the cycle. The bus will pass the intersection

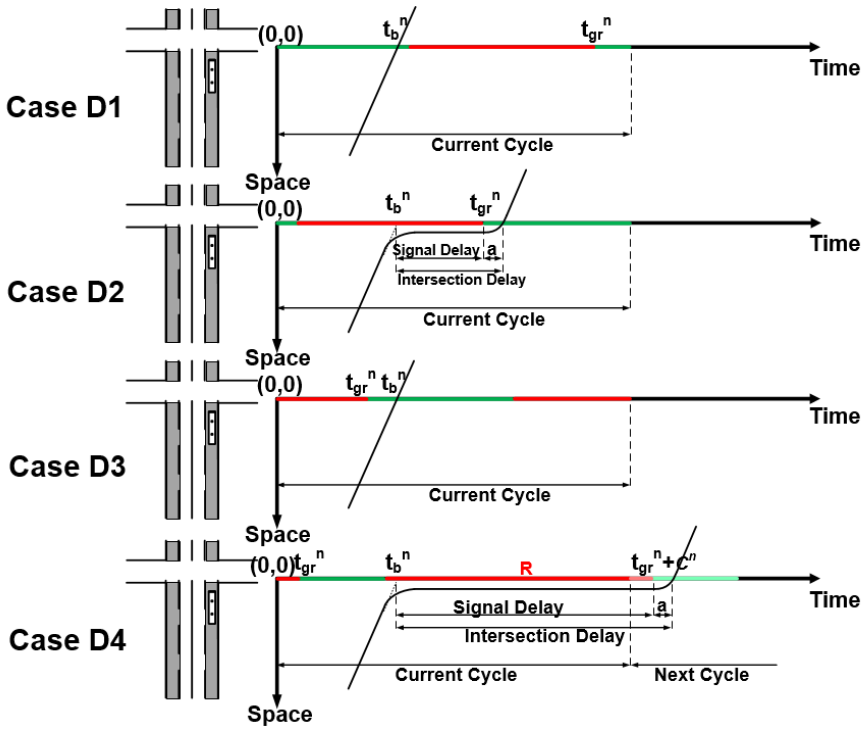

Figure 4.3: Intersection delay cases

when the green phase begins and thus, its delay will be equal to beginning of the green phase, t_{gr}^n, minus the bus arrival time at the intersection stop line, t_b^n, plus the intersection lost time.

$$D_{b,2}^n = t_{gr}^n - t_b^n + \bar{a}^n \quad \forall b \in I_B,\ n \in I_N \tag{4.9}$$

Case D3: $t_{gr}^n < t_b^n \leq t_{gr}^n + g^n$

The bus arrives at the intersection stop line during the green phase and a portion of the red phase precedes the green one in the cycle. The bus experiences no delay.

$$D_{b,3}^n = 0 \quad \forall b \in I_B,\ n \in I_N \tag{4.10}$$

Case D4: $t_{gr}^n + g^n < t_b^n$

The bus arrives at the intersection during the red phase and a portion of the red phase precedes the green one in the cycle. The bus will be served in the next cycle and will experience delay equal to:

$$D^n_{b,4} = t^n_{gr} + C^n - t^n_b + \bar{a}^n \quad \forall b \in I_B,\ n \in I_N \tag{4.11}$$

Four binary variables, $x^n_{b,1}$, $x^n_{b,2}$, $x^n_{b,3}$, $x^n_{b,4}$ are introduced to define the four delay cases for buses. As a result, the intersection delay can be expressed as:

$$D^n_b = x^n_{b,1} * D^n_{b,1} + x^n_{b,2} * D^n_{b,2} + x^n_{b,3} * D^n_{b,3} + x^n_{b,4} * D^n_{b,4} \quad \forall b \in I_B,\ n \in I_N \tag{4.12}$$

Since $D^n_{b,1}$ and $D^n_{b,3}$ are zero, equation (4.12) becomes:

$$D^n_b = x^n_{b,2} * D^n_{b,2} + x^n_{b,4} * D^n_{b,4} \quad \forall b \in I_B,\ n \in I_N \tag{4.13}$$

Using equation (4.5) we have:

$$\begin{aligned} \hat{tt}_{b,i-1,i} = \bar{p} * l_{b,i-1,i} + \bar{ad} * AD_{b,i-1,i} + \sum_{k \in I_{K_{i-1,i}}} \bar{w}^k \\ + \sum_{m \in I_{N_{i-1,i}}} (x^m_{b,2} * D^m_{b,2} + x^m_{b,4} * D^m_{b,4}) \quad \forall b \in I_B,\ i \in I_b\ \&\quad i \neq 1 \end{aligned} \tag{4.14}$$

Note that in equation (4.14), the term $x^n_{b,2} * D^n_{b,2}$ and $x^n_{b,4} * D^n_{b,4}$ are multiplications of the continuous variables $D^n_{b,2}$ and $D^n_{b,4}$ with the binary variables $x^n_{b,2}$ and $x^n_{b,4}$ respectively, which results in a non-quadratic and non-linear function. To avoid these bilinearities,

two new continuous variables, $h^n_{b,1}$ and $h^n_{b,2}$ are introduced for each bus b at each intersection n and are defined as follows:

$$h^n_{b,1} = x^n_{b,2} * D^n_{b,2} \quad \forall b \in I_B,\ n \in I_N \tag{4.15}$$

$$h^n_{b,2} = x^n_{b,4} * D^n_{b,4} \quad \forall b \in I_B,\ n \in I_N \tag{4.16}$$

When $x^n_{b,2}$ is 1, $h^n_{b,1}$ equals to $D^n_{b,2}$, and when $x^n_{b,2}$ is zero, $h^n_{b,1}$ equals to zero. In addition, new linear inequalities are introduced which return $h^n_{b,1}$ and $h^n_{b,2}$ that are consistent with equations (4.15) and (4.16) as shown in (4.17)-(4.22).

$$h^n_{b,1} \leq D^n_{b,2} + M * (1 - x^n_{b,2}) \quad \forall b \in I_B,\ n \in I_N \tag{4.17}$$

$$h^n_{b,1} \geq D^n_{b,2} - M * (1 - x^n_{b,2}) \quad \forall b \in I_B,\ n \in I_N \tag{4.18}$$

$$h^n_{b,1} \leq x^n_{b,2} * M \quad \forall b \in I_B,\ n \in I_N \tag{4.19}$$

$$h^n_{b,2} \leq D^n_{b,4} + M * (1 - x^n_{b,4}) \quad \forall b \in I_B,\ n \in I_N \tag{4.20}$$

$$h^n_{b,2} \geq D^n_{b,4} - M * (1 - x^n_{b,4}) \quad \forall b \in I_B,\ n \in I_N \tag{4.21}$$

$$h^n_{b,2} \leq x^n_{b,4} * M \quad \forall b \in I_B,\ n \in I_N \tag{4.22}$$

4.1.4 Mathematical Program Formulation

To estimate the unknown variables the norm minimization approach is selected. The most common approximation problem involves l_2-norm which results in least-squares approximation problem (Boyd and Vandenberghe, 2004). In the presence of outliers in the data, l_2-norm can result in a poor fit since it penalizes deviations quadratically. Various penalty functions have been introduced to reduce the sensitiv-

ity of the models to the outliers. Huber used a penalty function as follows (Boyd and Vandenberghe, 2004):

$$\phi(u) = \begin{cases} u^2 & |u| \leq \gamma \\ \gamma(2|u| - \gamma) & |u| \geq \gamma \end{cases} \tag{4.23}$$

The Huber penalty function is convex and applies l_2-norm for residuals smaller than γ and l_1-norm-like for the larger residuals. However, since it switches from being quadratic to linear at $|u| = \gamma$, several models have been introduced to reduce the Huber penalty function to a quadratic problem. Mangasarian and Musicant (Mangasarian and Musicant, 2000) proposed the following mathematical program:

$$\begin{aligned} \min \quad & \frac{1}{2}||z||_2^2 + \gamma e\prime(s^+ + s^-) \\ \text{s.t.} \quad & Ax - b - z = s^+ + s^- \\ & s^+, s^- \geq 0 \end{aligned} \tag{4.24}$$

where z, s^+ and s^- are vectors of variables, $Ax - b$ is the vector of residuals and $e\prime$ is the vector of ones of arbitrary dimension. In this chapter, the formulation of Mangasarian and Musicant has been adopted. As a result, the objective function of the mixed-integer quadratic program is formulated as follows:

$$\min \quad \sum_{b \in I_B} \sum_{i \in I_b i \neq 1} \left(\frac{1}{2}||z_{b,i}||_2^2 + \gamma e\prime(s_{b,i}^+ + s_{b,i}^-) \right) \tag{4.25}$$

The constraints of the mathematical program including the ones associated with the Mangasarian and Musicant formulation, bus arrival time cases, intersection delay cases, defeating bilinearity, as well as non-negativity and binary integer constraints are as follows:

$$\min \quad \sum_{b\in I_B}\sum_{i\in I_b i\neq 1}(\frac{1}{2}||z_{b,i}||_2^2+\gamma e\prime(s_{b,i}^+ + s_{b,i}^-)) \tag{4.26}$$

subject to

$$\bar{p}*l_{b,i-1,i}+\bar{ad}*AD_{b,i-1,i}+\sum_{k\in I_{K_{i-1,i}}}\bar{w}^k+\sum_{n\in I_{N_{i-1,i}}}(h_{b,1}^n+h_{b,2}^n)-tt_{b,i}-z_{b,i}$$
$$=s_{b,i}^+ + s_{b,i}^- \quad \forall b\in I_B,\ i\in I_b \tag{4.27}$$

$$\hat{tt}_b^{u,n}=\bar{p}*l_b^{u,n}+\sum_{k\in I_{K_{u,n}}}\bar{w}^k \quad \forall b\in I_B,\ n\in I_N \tag{4.28}$$

$$\hat{tt}_b^{u,n}+t_b^{u,n}\leq C^n+M*(1-y_{b,1}^n) \quad \forall b\in I_B,\ n\in I_N \tag{4.29}$$

$$C^n\leq \hat{tt}_b^{u,n}+t_b^{u,n}+M*(1-y_{b,2}^n) \quad \forall b\in I_B,\ n\in I_N \tag{4.30}$$

$$y_{b,1}^n+y_{b,2}^n=1 \quad \forall b\in I_B,\ n\in I_N \tag{4.31}$$

$$\hat{t}_b^n=\hat{tt}_b^{u,n}+t_b^{u,n}-C^n*y_{b,2}^n \quad \forall b\in I_B,\ n\in I_N \tag{4.32}$$

$$t_b^n\leq t_{gr}^n-r^n+M*(1-x_{b,1}^n) \quad \forall b\in I_B,\ n\in I_N \tag{4.33}$$

$$t_{gr}^n-r^n\leq t_b^n+M*(1-x_{b,2}^n) \quad \forall b\in I_B,\ n\in I_N \tag{4.34}$$

$$t_b^n\leq t_{gr}^n+M*(1-x_{b,2}^n) \quad \forall b\in I_B,\ n\in I_N \tag{4.35}$$

$$t_{gr}^n\leq t_b^n+M*(1-x_{b,3}^n) \quad \forall b\in I_B,\ n\in I_N \tag{4.36}$$

$$t_b^n\leq t_{gr}^n+g^n+M*(1-x_{b,3}^n) \quad \forall b\in I_B,\ n\in I_N \tag{4.37}$$

$$t_{gr}^n+g^n\leq t_b^n+M*(1-x_{b,4}^n) \quad \forall b\in I_B,\ n\in I_N \tag{4.38}$$

$$x_{b,1}^n+x_{b,2}^n+x_{b,3}^n+x_{b,4}^n=1 \quad \forall b\in I_B,\ n\in I_N \tag{4.39}$$

$$h^n_{b,1} \leq t^n_{gr} - t^n_b + \bar{a}^n + M * (1 - x^n_{b,2}) \ \forall b \in I_B, \ n \in I_N \tag{4.40}$$

$$h^n_{b,1} \geq t^n_{gr} - t^n_b + \bar{a}^n - M * (1 - x^n_{b,2}) \quad \forall b \in I_B, \ n \in I_N \tag{4.41}$$

$$h^n_{b,1} \leq x^n_{b,2} * M \quad \forall b \in I_B, \ n \in I_N \tag{4.42}$$

$$h^n_{b,2} \leq t^n_{gr} + C^n - t^n_b + \bar{a}^n + M * (1 - x^n_{b,4}) \quad \forall b \in I_B, \ n \in I_N \tag{4.43}$$

$$h^n_{b,2} \geq t^n_{gr} + C^n - t^n_b + \bar{a}^n - M * (1 - x^n_{b,4}) \quad \forall b \in I_B, \ n \in I_N \tag{4.44}$$

$$h^n_{b,2} \leq x^n_{b,4} * M \quad \forall b \in I_B, \ n \in I_N \tag{4.45}$$

$$h^n_{b,1} \geq 0, h^n_{b,2} \geq 0 \quad \forall b \in I_B, \ n \in I_N \tag{4.46}$$

$$t^n_{gr}, \bar{a}^n \geq 0 \quad \forall n \in I_N \tag{4.47}$$

$$\bar{w}^k \geq 0 \quad \forall k \in I_K \tag{4.48}$$

$$s^+_{b,i}, s^-_{b,i} \geq 0 \quad \forall b \in I_B, \ i \in I_b \tag{4.49}$$

$$\bar{p} \geq 0 \tag{4.50}$$

$$x^n_{b,1}, x^n_{b,2}, x^n_{b,3}, x^n_{b,4}, y^n_{b,1}, y^n_{b,2} \in \{0, 1\} \quad \forall b \in I_B, \ n \in I_N \tag{4.51}$$

The objective function (4.26) and constraint (4.27) represent the reformulated Huber loss function. Constraints (4.28)-(4.32) determine bus arrival time at intersection stop line based on the two cases described in Figure 4.2.

Constraints (4.33)-(4.39) determine the intersection delay case presented in Figure 4.3. When it is case D1 ($t^n_b \leq t^n_{gr} - r^n$), $x^n_{b,1}$ could be either zero or one in constraint (4.33); however, since $x^n_{b,2}$, $x^n_{b,3}$, and $x^n_{b,4}$ must be zero to hold constraints (4.34), (4.36), and (4.38) feasible, based on the constraint (4.39), we have $x^n_{b,1} = 1$. If it is case D2 ($t^n_{gr} - r^n \leq t^n_b \leq t^n_{gr}$), based on constraints (4.34) and (4.35)

$x^n_{b,2}$ could be either zero; but to keep constraints (4.33),(4.36), and (4.38) feasible, $x^n_{b,1}$, $x^n_{b,3}$, and $x^n_{b,4}$ must be zero and thus, based on constraint (4.39), $x^n_{b,2}$ must be one. Similarly other cases can be determined using the constraints.

Constraints (4.40)-(4.46) defeat the bilinearity problem presented in equations (4.17)-(4.22). Constraints (4.47)-(4.51) are non-negativity and binary variable constraints.

4.2 Application

4.2.1 Test Site

The test site is a 1,300 feet long arterial segment of Washington Street in Boston, Massachusetts, between the Newton Street and Massachusetts Avenue bus stops (Figure 4.4). Washington Street is an arterial with one lane for autos and one dedicated bus lane in each direction. On-street parking is permitted and left-turning pockets at intersections are provided. The southbound direction is the direction of interest. The study site includes two bus stops, on Newton Street and Worcester Square, and one signalized intersection, the intersection of Massachusetts Avenue with Washington Street. The intersection is signalized with a fixed-time signal control scheme and a cycle length of 120 seconds during morning (6:00 AM - 10:30 AM) and afternoon (2:30 PM - 7:30 PM) periods and 110 seconds at all other times. The green phases duration serving the approach of interest are 47, 41, and 37 for the morning, afternoon and all other times respectively.

Two major MBTA bus routes, Silver Line 4 (SL4) and Silver Line 5 (SL5), travel through the segment. MBTA Route SL4 runs from South Station, mostly via Washington Street, to Dudley Station in Boston, Massachusetts. The frequency varies from 3 (late night) to 10 (during peak hours) buses per hour. MBTA Route SL5 runs from the Downtown Crossing terminal, via Washington Street, to Dudley Station. The frequency varies from 4 to 11 buses per hour.

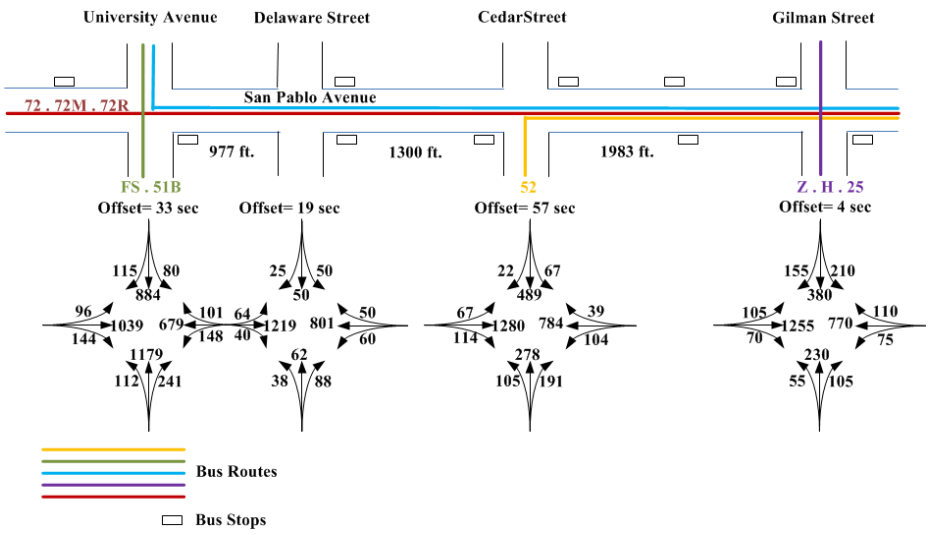

Figure 4.4: Test site

4.2.2 Data

Three AVL data sampling methods are used by MBTA including announcement, heartbeat, and adherence. Announcement is an event-based sampling in which records are polled at internal (e.g. stop request announcement) and external (e.g., announcing destination at bus stop) announcements. Heartbeat is a time-based sampling in which records are polled every 60 seconds and adherence is a location-based sampling where data is polled when a bus crosses a time point (geo nodes).

In this study, announcement and heartbeat data are used. The AVL records from the routes SL4 and SL5 of the MBTA, between 7:00 AM and 10:00 PM on May 4, 2015 are analyzed. Three time periods including morning (6:00 AM – 10:30 AM), midday (10:30 AM – 2:30 PM) and afternoon (2:30 PM – 7:30 PM) are studied separately. The signal control plan is constant during each period. The raw data are processed for the analysis. Records with zero distance from the previous record are dismissed. In cases where there are bus stops or intersections, data is filtered so that the travel time between two consecutive records includes the full length of dwell time or intersection delay. After filtering, 225 (36 buses), 154 (30 buses) and 315 (50 buses) AVL records

are used for morning, midday, and afternoon periods respectively. The data is divided into training (50%) and test data sets (50%). The models are trained on the training data and their performance is tested on the test data. Cross-validation technique is used to estimate γ in the MIQP model.

4.2.3 Results

To estimate various components of the bus travel time, both MIQP and linear regression models were trained using the available training data. However, estimates of some parameters, especially acceleration/deceleration lost times, were insignificant. Therefore, instead of estimating free flow travel time and acceleration/deceleration lost time separately, average running travel time is estimated which includes both the free flow travel time and the acceleration/deceleration lost time components.

The MIQP is solved with CPLEX solver on an Intel(R) Core i5 CPU (3.2 GHz) system with 4 GB installed memory (RAM). The CPLEX output is listed in Table 4.1. The results show that the optimality gap is reached in less than 1 second with 260, 259, and 184 simplex iterations for the morning, midday and afternoon periods respectively.

Table 4.1: CPLEX Output of the MIQP Model

Metric	Morning	Midday	Afternoon
Objective Value	1661	2754	2616
MIP simplex iterations	4939	3285	2939
Branch and Bound Nodes	260	259	184
Run Time (s)	0.30	0.30	0.53

The estimated parameters of the MIQP model using the training dataset are listed in Table 4.2. The average running speed can be calculated as the inverse of the average running pace. Average running speed for the morning, midday, and afternoon periods are 13.67, 12.73, and 12.13 miles per hour respectively. The average running speed includes the free-flow portion of the bus travel time as well as the lost time due to

Table 4.2: MIQP Parameter Estimates

Model	Average Running Pace (sec/mile)	Stop 1 Average Dwell Time (sec)	Stop 2 Average Dwell Time (sec)	Average Lost Time at Intersection (sec)
Morning	263.28	15.74	11.25	24.66
Midday	282.80	15.17	18.95	4.80
Afternoon	296.75	21.14	15.00	16.27

acceleration and deceleration at bus stops. Since all buses are traveling on a dedicated bus lane and therefore, are not affected by general traffic congestion, the fact that average running speeds for all three time periods are similar is not surprising. The lost time at intersections includes the acceleration and deceleration portion at the signal as well as delays other than the ones caused by the signal, e.g., delays due to right-turning vehicles utilizing the dedicated bus lane, delays due to buses dwelling at the downstream of the intersection bus stop, etc. As shown in Table 4.2, the average intersection lost time is higher for the peak morning and afternoon periods. This is likely due to the increased volumes of right-turning vehicles during peak hours that utilize the dedicated bus lanes and delay the buses or due to higher frequency bus service and potentially longer dwell times at the downstream bus stop.

The linear regression model is estimated with the Pandas library in Python using the training data and the results are shown in Table 4.3. All estimated coefficients are significant with 99% confidence assuming a Gaussian distribution of the error terms. The average intersection delay over all vehicles is 51.95, 33.32 and 36.20 seconds and the average running speed 12.81, 12.22, and 12.37 miles per hour, for the morning, midday, and afternoon periods respectively.

Both models are evaluated based on their generalized error on the test data. Bus timestamp at location of record i has been predicted using the timestamp of record $i-1$ and estimated travel time between two records. The predicted timestamps of records are evaluated against the actual timestamps of those records. The prediction results of both models are evaluated in terms of the mean absolute error (MAE), the

Table 4.3: Linear Regression Model Parameter Estimates.

Model		Average Running Pace (sec/mile)	Stop 1 Average Dwell Time (sec)	Stop 2 Average Dwell Time (sec)	Average Intersection Delay (sec)
Morning	Coefficient	281.09	20.2	14.06	51.95
	t statistic	9.61	6.45	4.77	15.2
	P-value	0.0000	0.0000	0.0000	0.0000
Midday	Coefficient	294.51	24.77	31.75	33.32
	t statistic	4.45	3.6	4.97	4.71
	P-value	0.0000	0.0006	0.0000	0.0000
Afternoon	Coefficient	291.00	22.61	21.02	36.20
	t statistic	8.43	6.15	6.21	9.61
	P-value	0.0000	0.0000	0.0000	0.0000

Table 4.4: Generalized Errors of the MIQP and Linear Regression Models.

Model		MAE	MAPE	RMSE
Morning	MIQP	3.85	45.09	6.67
	Linear Regression	7.48	59.38	13.72
Midday	MIQP	4.74	34.36	10.35
	Linear Regression	8.82	56.25	12.74
Afternoon	MIQP	4.55	35.64	8.22
	Linear Regression	8.10	47.95	14.30

mean absolute percentage error (MAPE) and the root mean square error (RMSE) of the travel time estimates. These three measures are presented in Table 4.4. The results show that the MIQP model outperforms the regression model by all measures. In particular, the proposed model can predict bus travel times with less than five seconds average error for all tested time periods compared to linear regression with average errors higher than seven seconds.

Using the estimated beginning of the green phase at each cycle, the signal status at the intersection is estimated. Intersection delay estimates from both the actual records and the MIQP model on the test data are shown in Figures 4.5a, 4.5b, and 4.5c for the morning, midday, and afternoon periods respectively. Intersection delay estimates from the actual records are determined as the total travel time of the bus

passing the intersection obtained from the records just before and after the intersection minus the estimated running travel time. Delay estimates from the MIQP model are determined using the estimated intersection lost time plus the signal delay time. Note that the linear regression model estimates are average values over all buses. The results indicate that the estimated signal phase starting and ending times are reasonable since the MIQP model predicts that the delay decreases as the bus arrival time gets closer to the beginning of the green phase and approaches zero once the green phase has started. These results are in close agreement with the actual AVL records observed. At the same time, the linear regression model predicts a constant intersection delay for all buses independently of their arrival time at the intersection stop line.

Using the decomposed traffic characteristics from both the linear regression and MIQP models, bus trajectories can be inferred. Bus arrival times at downstream bus stop are predicted using the buses' timestamp at the upstream bus stop (stop 1). Figure 4.6 shows two examples of the inferred trajectories. The Figures show that the MIQP inferred bus trajectories are very close to the recorded AVL data, while the linear regression inferred trajectories tend to underestimate intersection delay. Prediction errors of the MIQP and linear regression models for the first sample bus (Figure 4.6a) are 1 and 20 seconds respectively. Prediction errors of the MIQP and linear regression models for the second sample bus (Figure 4.6b) are 1 and 26 seconds respectively. As mentioned before this is due to the fact that the MIQP model estimates the status of the signal, and as a result, it can estimate individual bus delay, while the linear regression model estimates an average intersection delay for all buses.

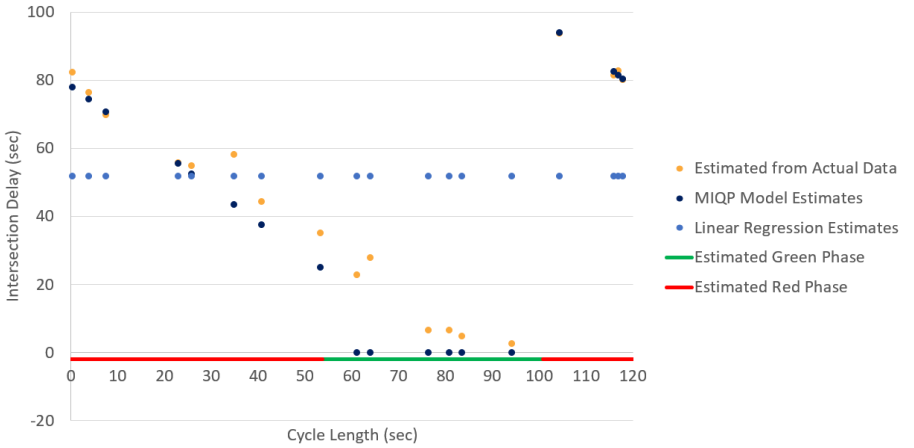

(a) Intersection delay on the morning test dataset

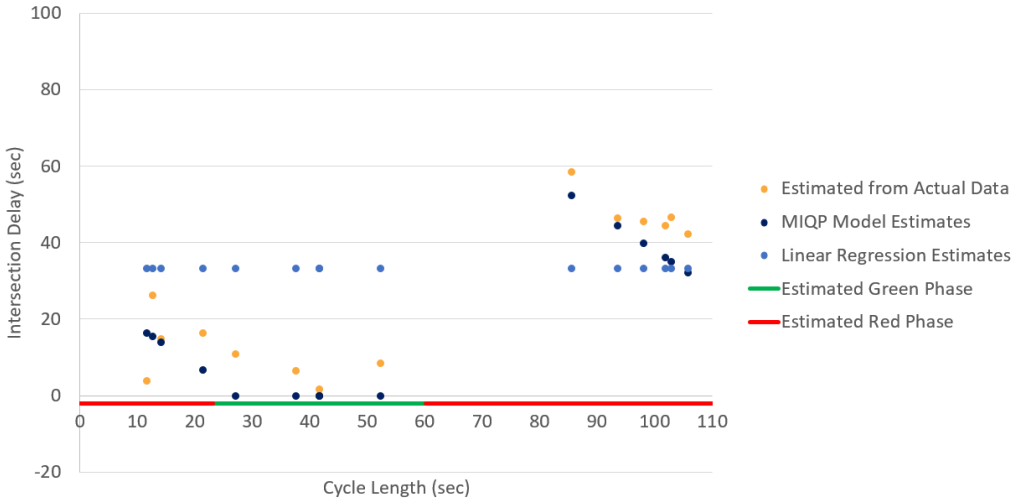

(b) Intersection delay on the midday test dataset

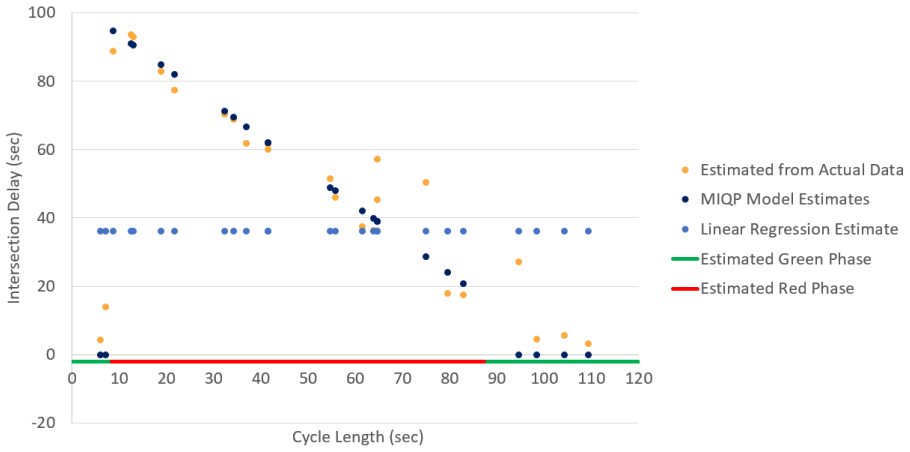

(c) Intersection delay on the afternoon test dataset

Figure 4.5: Intersection delay for the morning, midday, and afternoon periods

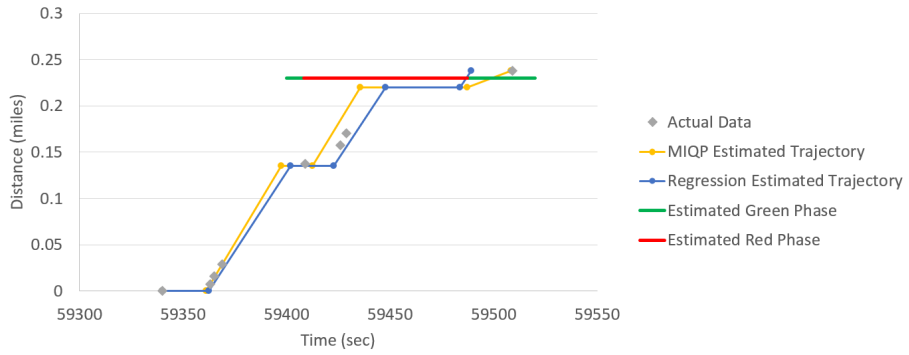

(a) Sample Bus 1

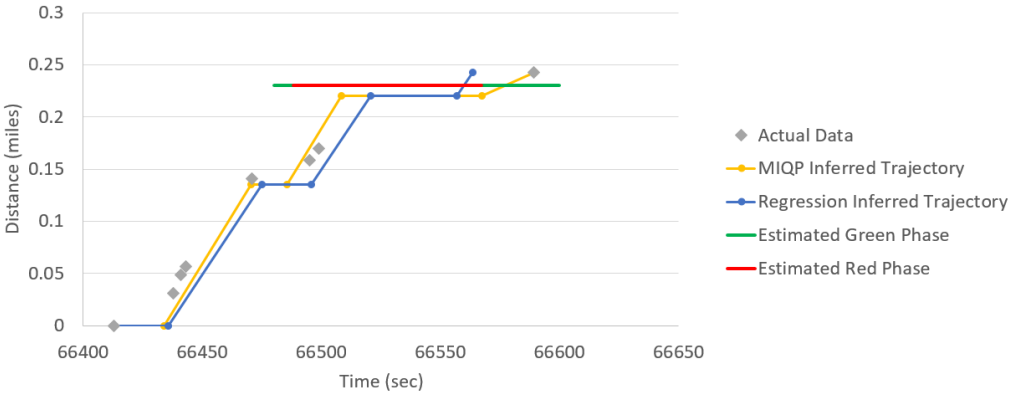

(b) Sample Bus 2

Figure 4.6: Estimated trajectories of two sample buses

4.3 Summary of Findings

This chapter developed a mixed-integer quadratic programming model (MIQP) to obtain estimates of dwell time at bus stops, average speed, acceleration/deceleration lost time, and intersection delay that can be used to predict bus travel time along a signalized arterial. The model learns these components using historical low resolution AVL data (i.e. one record every 60 seconds) without requiring information about the dwell times at bus stops, the signal status, or traffic conditions. The MIQP model is robust since it has been developed using the Huber loss function that ensures low sensitivity to the outliers. The results of this model are compared against the ones obtained with a linear regression model. This study addresses shortcomings of previous studies by estimating individual bus delays at intersections rather than estimating an average value over all buses. Another advantage is that the only signal settings required are the phase durations.

The proposed method improves prediction accuracy of bus arrival times at any point along the study segment. Accurate predictions are especially crucial in TSP systems. Inaccurate bus arrival predictions at signalized intersections implementing TSP could increase intersection delay for conflicting vehicles while not benefiting the bus (i.e., wasted priority). Although the main purpose of the model is to be used in TSP systems, it can also be used for other applications including advanced passenger information systems.

Both the linear regression and MIQP models are tested in a segment of the Washington Street in Boston, Massachusetts. The MIQP model is solved using CPLEX and the linear regression is estimated using the Panda library in Python. The results indicate that the MIQP model outperforms linear regression model in terms of generalized error measures including MAE, MAPE, and RMSE. In particular, the MIQP model is capable of predicting bus travel time with an average error of less

than five seconds, which is sufficient for implementation of TSP strategies and traveler information systems.

Implementation of the proposed model is expected to lead to enhanced traveler information systems and efficient TSP provision, consequently improving transit reliability and ridership. Future work will improve the model to account for cases where buses travel on mixed-use lanes and actuated signal control plans. In a mixed-traffic lane case, the position of buses in queue at intersections should be estimated to determine bus delay at the intersections. Furthermore, future research will relax the assumption that information about the duration of the signal phases is available.

CHAPTER 5

REAL-TIME TRAFFIC SIGNAL CONTROL

While traditional traffic signal control systems rely on historical data to develop optimal signal timing plans, recent systems increasingly rely on real-time data to provide real-time control that automatically adapts to changes in traffic conditions. Adjustments of signal timings to in traffic conditions can potentially improve system efficiency. In this chapter, a person-based real-time signal control system that accounts for stochasticity in transit vehicles' arrival time is presented. The system evaluates person delay measure using the analytical models developed in chapter 3 and takes into account the randomness in bus arrival time predictions.

5.1 Methodology

A real-time signal control system is developed to minimize total person delay while accounting for stochasticity in bus arrival times. Auto vehicle arrivals are assumed to be deterministic while bus arrivals at intersection stopline are assumed to be stochastic. It is assumed that cycle length, as well as the sequence of the phases are constant. The model optimizes signal phase splits by minimizing the total person delay at the intersection. Auto and bus delays are determined using methods described in Chapter 3. The case where buses are traveling in a mixed traffic lane is modeled. The mathematical program is formulated under assumptions consistent with those made in Chapter 3 including: Shockwave theory holds true, there is negligible platoon dispersion, and traffic conditions are under-saturated.

5.2 Mathematical Model

The mathematical model that is developed minimizes total person delay of both autos and transit vehicles at intersections that are part of a signalized arterial corridor while providing a priority window equal to one standard deviation lower and one higher than the expected transit arrival time at the intersection. Since the intersection is part of a signalized arterial, it is assumed that vehicles arrive in platoons. It is further assumed that traffic operations can be modeled by the Kinematic Wave Theory (Lighthill and Whitham, 1955, Richards, 1956) and saturation flows are constant. The auto arrivals and platoon sizes are deterministic and it is assumed that there is no platoon dispersion. The mathematical model is developed to describe a variety of traffic conditions but while it does not account for queue spillbacks, saturation flows can be easily adjusted to describe this phenomenon occurring during times of oversaturated conditions. Transit vehicle arrivals at the intersection stopline are assumed to be stochastic an following a exponential distribution. Finally, it is assumed that the cycle length as well as the phase sequence are constant. Transit vehicles and autos travel in mixed use lanes and the impact of transit stops on traffic and transit operations has been ignored.

The mathematical program optimizes the green times for the intersection by minimizing the summation of the auto and transit vehicle person delays. Auto delays for both autos and transit vehicles are estimated based on the KWT as functions of the auto arrival times, platoon sizes, sizes of the residual queue, transit vehicle arrival times, and signal settings and are then weighted by their respective passenger occupancies. Since the focus is on one signalized intersection, which is however influenced by upstream intersections, the offsets remain constant. The proposed real-time signal control system minimizes total person delay by changing the phase green times at the intersection while ensuring the provision of a priority window for transit vehicles arriving from a certain direction.

To facilitate the description of the model, the following sets, variables and parameters are defined:

- Sets:
  - $M_a = \{1, 2, .., 6\}$: Set of auto delay cases,
  - $M_b = \{1, 2, .., 16\}$: Set of transit delay cases,
  - $J = \{1, 2, .., j\}$: Set of lane groups,
  - $I = \{1, 2, .., i\}$: Set of signal phases,
  - $B = \{1, 2, .., b\}$: Set of total transit vehicles during cycle T,
  - $B_j = \{1, 2, .., b_j\}$Set of the transit vehicles traveling on the lane group j during cycle T.
- Variables:
  - G_j^e: effective green time for the phase that serves lane group j [sec];
  - za_j^m: variable introduced to defeat bilinearity in determining delay of autos traveling in lane group j for case m;
  - $zb_{j,b}^m$: variable introduced to defeat bilinearity in determining delay of transit vehicle b traveling in lane group j for case m;
  - x_j^m: Binary variable indicating the delay case that autos in lane group j belong to;
  - $y_{j,b}^m$: Binary variable indicating the transit vehicle sub-case that transit vehicle b in lane group j belongs to.
  - E_b^1, E_b^2, and E_b^3: Binary variable indicating the transit vehicle case (i.e., within, ahead, or behind the platoon) that transit vehicle b in lane group j belongs to.

- Parameters:
  - C: cycle length [sec];
  - $N_{j,T-1}$: residual queue size of lane group j at the end of the previous cycle T -1 [veh];
  - $P_{j,T}$: total platoon size of lane group j during cycle T;
  - s_j: total saturation flow of lane group j [vpm];
  - $tb_{b,T}$: arrival time of transit vehicle b at the intersection during cycle T [sec];
  - $t_{j,T}$: platoon arrival time at the intersection of lane group j during cycle T [sec];
  - t_T: beginning of the cycle [sec];
  - $\bar{o}_a$ average auto occupancy [passenger/car];
  - $\bar{o}_b$ average transit vehicle occupancy [passenger/transit vehicle];
  - $Z_{\alpha/2}$ = the value from the standard normal distribution for the confidence level $(1-\alpha)\%$;
  - σ = standard deviation of transit arrival time predictions;
- Others
  - $Da_{j,T}$: total delay of autos in lane group j during cycle T [veh-sec];
  - $Da^s mj, T$: delay of autos in lane group j during cycle T for delay case m $m \in M_a$[veh-sec];
  - $Db_{j,T}$: total delay of transit vehicles in lane group j during cycle T [veh-sec];

- $Db^m_{j,T}$: delay of transit vehicles in lane group j during cycle T for delay case m $m \in M_b$ [veh-sec];
- $R^{(1)}_j$: component of the red time from the beginning of the cycle until the start of the green time for lane group j [sec];
- $R^{(2)}_j$: component of the red time from end of the green until end of the cycle for lane group j [sec];
- T: signal cycle index.

5.2.1 Auto delay estimation

Auto delay is estimated as a function of the platoon arrival time, platoon size, residual queue length, and signal timing. As shown in Figure 5.1 six cases for auto delay estimation are considered as follows:

- Case $N1$: Platoon arrival before residual queue served, entire platoon served in green

  The corresponding constraints are:

$$t_{j,T} \leq t_T + R^{(1)}_j + \frac{N_{j,T-1}}{s_j} \quad \forall j \in J \tag{5.1}$$

$$P_{j,T} \leq G_j s_j - N_{j,T-1} \quad \forall j \in J \tag{5.2}$$

  The auto delay function is:

$$Da^1_{j,T} = P_{j,T}\left((T-1)C + R^{(1)}_j + \frac{N_{j,T-1}}{s_j} - t_{j,T}\right) + N_{j,T-1}R^{(1)}_j \tag{5.3}$$

- Case $N2$: Platoon arrival before residual queue served, insufficient green to serve entire platoon

  The corresponding constraints are:

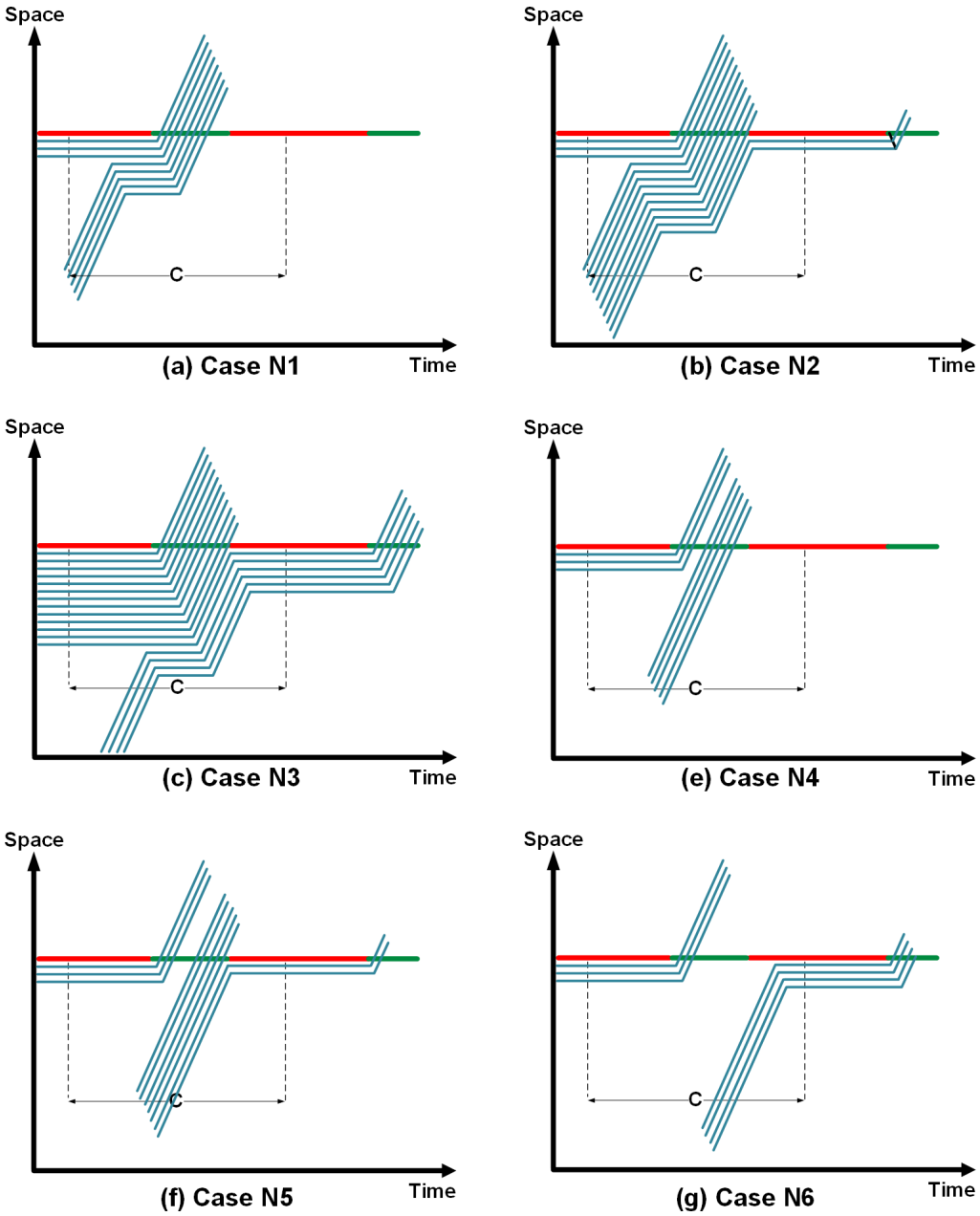

Figure 5.1: Auto delay cases

$$t_{j,T} \leq t_T + R_j^{(1)} + \frac{N_{j,T-1}}{s_j} \quad \forall j \in J \tag{5.4}$$

$$P_{j,T} \geq G_j s_j - N_{j,T-1} \quad \forall j \in J \tag{5.5}$$

The auto delay function is:

$$Da_{j,T}^2 = P_{j,T}\left((T-1)C + R_j^{(1)} + \frac{N_{j,T-1}}{s_j} - t_{j,T}\right) + (P_{j,T} + N_{j,T-1} - G_j^e s_j)(R_j^{(2)} + R_j^{(1)}) + N_{j,T-1}R_j^{(1)} \tag{5.6}$$

- Case $N3$: Insufficient green to serve residual queue

  The corresponding constraint is:

$$N_{j,T-1} \geq G_j s_j \quad \forall j \in J \tag{5.7}$$

  The auto delay function is:

$$Da_{j,T}^3 = P_{j,T}\left((TC + R_j^{(1)} + \frac{N_{j,T-1} - G_j^e s_j}{s_j} - t_{j,T}\right) + N_{j,T-1}R_j^{(1)} \tag{5.8}$$

- Case $N4$: Platoon arrival after residual queue served, entire platoon served in green

  The corresponding constraints are:

$$t_{j,T} \geq t_T + R_j^{(1)} + \frac{N_{j,T-1}}{s_j} \quad \forall j \in J \tag{5.9}$$

$$P_{j,T} \leq (t_T + R_j^{(1)} + G_j - t_{j,T})s_j \quad \forall j \in J \tag{5.10}$$

  The auto delay function is:

$$Da^4_{j,T} = N_{j,T-1} R^{(1)}_j \tag{5.11}$$

- Case $N5$: Arrival after residual queue served, insufficient green to serve entire platoon

  The corresponding constraints are:

$$t_{j,T} \geq t_T + R^{(1)}_j + \frac{N_{j,T-1}}{s_j} \quad \forall j \in J \tag{5.12}$$

$$t_{j,T} \leq t_T + R^{(1)}_j + G_j \quad \forall j \in J \tag{5.13}$$

$$P_{j,T} \geq (t_T + R^{(1)}_j + G_j - t_{j,T}) s_j \quad \forall j \in J \tag{5.14}$$

  The auto delay function is:

$$Da^5_{j,T} = \left(P_{j,T} - ((T-1)C + R^{(1)}_j + G^e_j - t_{j,T}) s_j\right) (R^{(2)}_j + R^{(1)}_j) + N_{j,T-1} R^{(1)}_j \tag{5.15}$$

- Case $N6$: Arrival after the green, entire residual queue is served

  The corresponding constraint is:

$$t_{j,T} \geq t_T + R^{(1)}_j + G_j \quad \forall j \in J \tag{5.16}$$

  The auto delay function is:

$$Da^6_{j,T} = P_{j,T}(TC + R^{(1)}_j - t_{j,T}) + N_{j,T-1} R^{(1)}_j \tag{5.17}$$

5.2.2 Transit delay estimation

Transit vehicles traveling in mixed-traffic lanes are traveling either within the auto platoon or outside of it. Therefore, two cases are defined to capture whether transit vehicles are within the auto platoons (cases TW) or not (cases TO). For each case, several sub-cases are considered.Constraints to determine transit vehicle position cases are as follows:

Case TW

$$tb_b \leq t_{j,T} + \frac{P_{j,T}}{s_j} + M(1 - E_b^1) \quad \forall j \in J \& \forall b \in B_j \tag{5.18}$$

$$tb_b \geq t_{j,T} + M(E_b^1 - 1) \quad \forall j \in J \& \forall b \in B_j \tag{5.19}$$

Case TO - Ahead of the Auto platoon

$$tb_b \leq t_{j,T} + M(1 - E_b^2) \quad \forall j \in J \& \forall b \in B_j \tag{5.20}$$

Case TO - After the Auto platoon

$$tb_b \geq t_{j,T} + \frac{P_{j,T}}{s_j} + M(E_b^3 - 1) \quad \forall j \in J \& \forall b \in B_j \tag{5.21}$$

$$E_b^1 + E_b^2 + E_b^3 = 1 \quad \forall \forall b \in B \tag{5.22}$$

5.2.2.1 Case TW

In this case, transit vehicles travel within the platoon. Vehicles experience delay as the autos in the platoon except for cases N2 and N5. In N2 and N5, a portion of the platoon passes the intersection during the green phase and the rest of the platoon will wait until the next cycle to discharge. As a result, eight different sub-cases (Figure 5.2) are considered as follows:

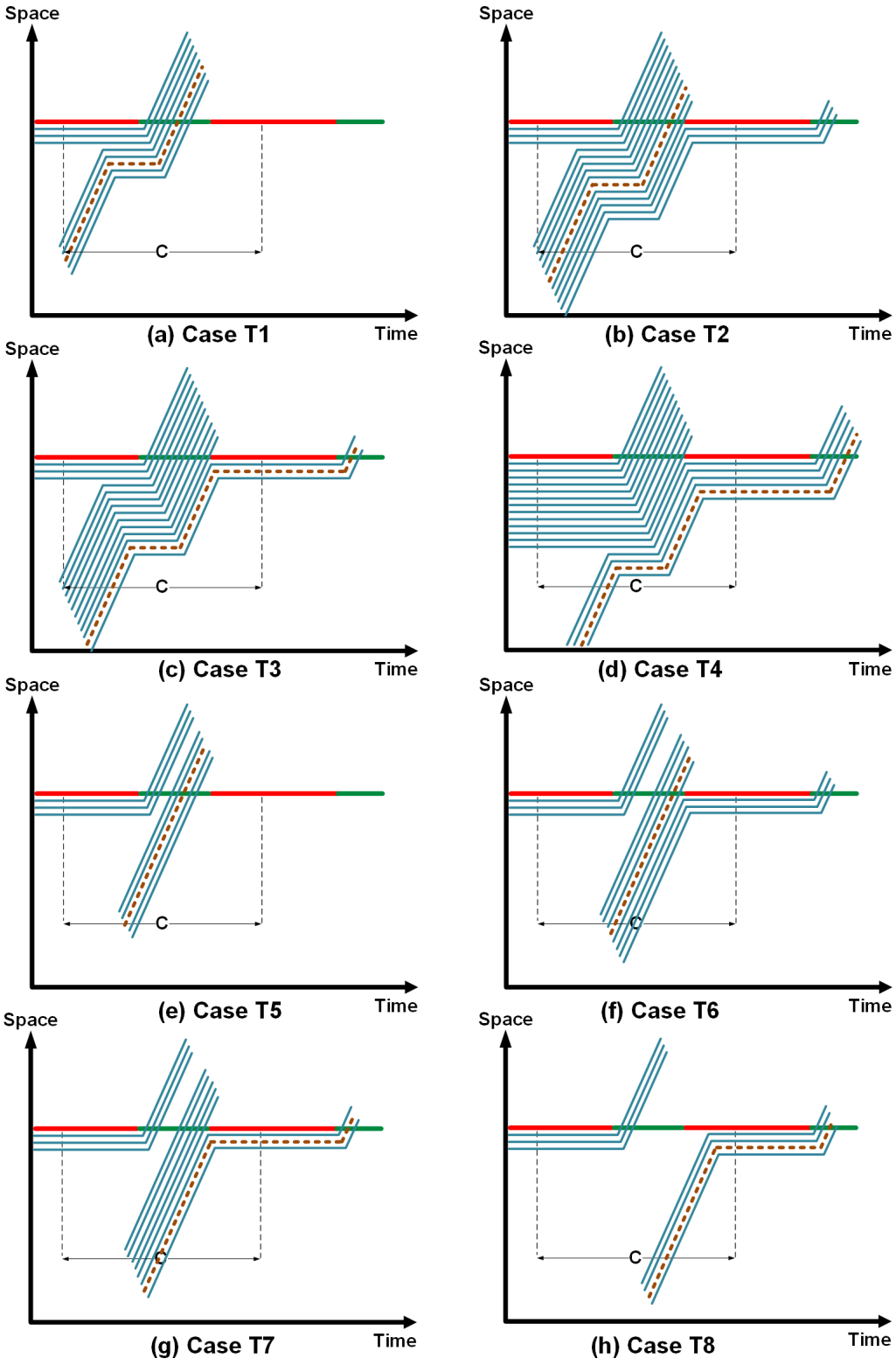

Figure 5.2: Transit delay cases: transit vehicle traveling within the platoon

- Case $T1$: Platoon arrival before residual queue served, entire platoon served in green, transit vehicle also served in green

  The Corresponding constraints are as follows:

$$t_{j,T} \leq t_T + R_j^{(1)} + \frac{N_{j,T-1}}{s_j} + M(1 - y_{j,b}^1) \quad \forall j \in J \& \forall b \in B_j \tag{5.23}$$

$$P_{j,T} \leq G_j s_j - N_{j,T-1} + M(1 - y_{j,b}^1) \quad \forall j \in J \& \forall b \in B_j \tag{5.24}$$

$$y_{j,b}^1 \leq E_b^1 \quad \forall j \in J \& \forall b \in B_j \tag{5.25}$$

  This case corresponds to case $N1$ for auto delay. The transit vehicle delay function is:

$$db_{b,T}^1 = (T-1)C + R_j^{(1)} + \frac{N_{j,T-1}}{s_j^N} - t_{j,T} \tag{5.26}$$

- Case $T2$: Platoon arrival before residual queue served, insufficient green to serve entire platoon, transit vehicle also served in green

  The Corresponding constraints are as follows:

$$tb_b - t_{j,T} \leq G_j^e - \frac{N_{j,T-1}}{s_j} + M(1 - y_{j,b}^2) \quad \forall j \in J \& \forall b \in B_j \tag{5.27}$$

$$y_{j,b}^2 \leq E_b^1 \quad \forall j \in J \& \forall b \in B_j \tag{5.28}$$

  This case corresponds to case $N2$ for auto delay. The transit vehicle delay function is:

$$db_{b,T}^2 = (T-1)C + R_j^{(1)} + \frac{N_{j,T-1}^N}{s_j} - t_{j,T} \tag{5.29}$$

- Case $T3$: Platoon arrival before residual queue served, insufficient green to serve entire platoon, transit vehicle can not get served in green

The Corresponding constraints are as follows:

$$tb_b - t_{j,T} \leq G_j^e - \frac{N_{j,T-1}}{s_j} + M(y_{j,b}^3) - 1) \quad \forall j \in J \& \forall b \in B_j \tag{5.30}$$

$$y_{j,b}^3 \leq E_b^1 \quad \forall j \in J \& \forall b \in B_j \tag{5.31}$$

This case corresponds to case $N2$ for auto delay. The transit vehicle delay function is:

$$db_{j,T}^3 = (T-1)C + R_j^{(1)} + \frac{N_{j,T-1}}{s_j} - t_{j,T} + (R_j^{(2)} + R_j^{(1)}) \tag{5.32}$$

- Case $T4$: Insufficient green to serve residual queue, transit vehicle cannot served in green

  The Corresponding constraints are as follows:

$$N_{j,T-1} \geq G_j s_j + M(y_{j,b}^4 - 1) \quad \forall j \in J \& \forall b \in B_j \tag{5.33}$$

$$y_{j,b}^4 \leq E_b^1 \quad \forall j \in J \& \forall b \in B_j \tag{5.34}$$

  This case corresponds to case $N3$ for auto delay. The transit vehicle delay function is:

$$db_{b,T}^4 = TC + R_j^{(1)} + \frac{N_{j,T-1} - G_j^e s_j}{s_j} - t_{j,T} \tag{5.35}$$

- Case $T5$: Platoon arrival after residual queue served, entire platoon served in green, transit vehicle served in green

The Corresponding constraints are as follows:

$$t_{j,T} \geq t_T + R_j^{(1)} + \frac{N_{j,T-1}}{s_j} + M(y_{j,b}^5 - 1) \quad \forall j \in J \& \forall b \in B_j \tag{5.36}$$

$$P_{j,T} \leq (t_T + R_j^{(1)} + G_j - t_{j,T})s_j + M(1 - y_{j,b}^5) \quad \forall j \in J \& \forall b \in B_j \tag{5.37}$$

$$y_{j,b}^5 \leq E_b^1 \quad \forall j \in J \& \forall b \in B_j \tag{5.38}$$

This case corresponds to case $N4$ for auto delay. The transit vehicle delay function is:

$$db_{j,T}^4 = 0 \tag{5.39}$$

- Case $T6$: Arrival after residual queue served, insufficient green to serve entire platoon, transit vehicle served in green

  The Corresponding constraints are as follows:

$$tb_b \leq (T-1)C + R_j^{(1)} + G_j^e + M(1 - y_{j,b}^6) \quad \forall j \in J \& \forall b \in B_j \tag{5.40}$$

$$y_{j,b}^5 \leq E_b^1 \quad \forall j \in J \& \forall b \in B_j \tag{5.41}$$

  This case corresponds to case $N5$ for auto delay. The transit vehicle delay function is:

$$db_{b,T}^6 = 0 \tag{5.42}$$

- Case $T7$: Arrival after residual queue served, insufficient green to serve entire platoon, transit vehicle cannot get served in green

The Corresponding constraints are as follows:

$$tb_b \geq (T-1)C + R_j^{(1)} + G_j^e + M(y_{j,b}^7 - 1) \quad \forall j \in J \& \forall b \in B_j \tag{5.43}$$

$$y_{j,b}^5 \leq E_b^1 \quad \forall j \in J \& \forall b \in B_j \tag{5.44}$$

This case corresponds to case $N5$ for auto delay. The transit vehicle delay function is:

$$db_{b,T}^7 = R_j^{(2)} + R_j^{(1)} \tag{5.45}$$

- Case $T8$: Arrival after the green, entire residual queue is served, transit vehicle served in green

  The Corresponding constraints are as follows:

$$t_{j,T} \geq t_T + R_j^{(1)} + G_j + M(y_{j,b}^8 - 1) \quad \forall j \in J \& \forall b \in B_j \tag{5.46}$$

$$y_{j,b}^8 \leq E_b^1 \quad \forall j \in J \& \forall b \in B_j \tag{5.47}$$

  This case corresponds to case $N6$ for auto delay. The transit vehicle delay function is:

$$db_{b,T}^8 = TC + R_j^{(1)} - t_{j,T} \tag{5.48}$$

5.2.2.2 Case TO

In this case, the buses travel outside the platoon either ahead of it or after and the bus can be modeled as a platoon of size one. If the bus travels ahead of the platoon the residual queue for determining bus delay is the residual queue from the previous cycle (cases $T9$-$T12$). If the bus travels behind the platoon, the residual queue is

the residual queue from the previous cycle plus the platoon size of the current cycle (cases $T13$-$T16$). Eight different sub-cases (Figure 5.3) are considered as follows:

- Case $T9$: Transit vehicle arrival before residual queue served, sufficient green to serve entire residual queue, transit vehicle passes the intersection during the green phase of the current cycle

  The Corresponding constraints are as follows:

$$tb_b \leq t_T + R_j^{(1)} + \frac{N_{j,T-1}}{s_j} + M(1 - y_{j,b}^9) \quad \forall j \in J \& \forall b \in B_j \tag{5.49}$$

$$y_{j,b}^9 \leq E_b^2 \quad \forall j \in J \& \forall b \in B_j \tag{5.50}$$

  The transit vehicle will experience delay which is:

$$db_{b,T}^9 = (T-1)C + R_j^{(1)} + \frac{N_{j,T-1}}{s_j} - tb_{b,T} \tag{5.51}$$

- Case $T10$: Insufficient green to serve entire residual queue, transit vehicle passes the intersection during the green phase of the next cycle

  The Corresponding constraints are as follows:

$$N_{j,T-1} \geq G_j s_j + M(y_{j,b}^1 0 - 1) \quad \forall j \in J \& \forall b \in B_j \tag{5.52}$$

$$y_{j,b}^1 0 \leq E_b^2 \quad \forall j \in J \& \forall b \in B_j \tag{5.53}$$

  The transit vehicle will experience delay which is:

$$db_{b,T}^{10} = TC + R_j^{(1)} + \frac{N_{j,T-1}}{s_j} - G_j^e - tb_{b,T} \tag{5.54}$$

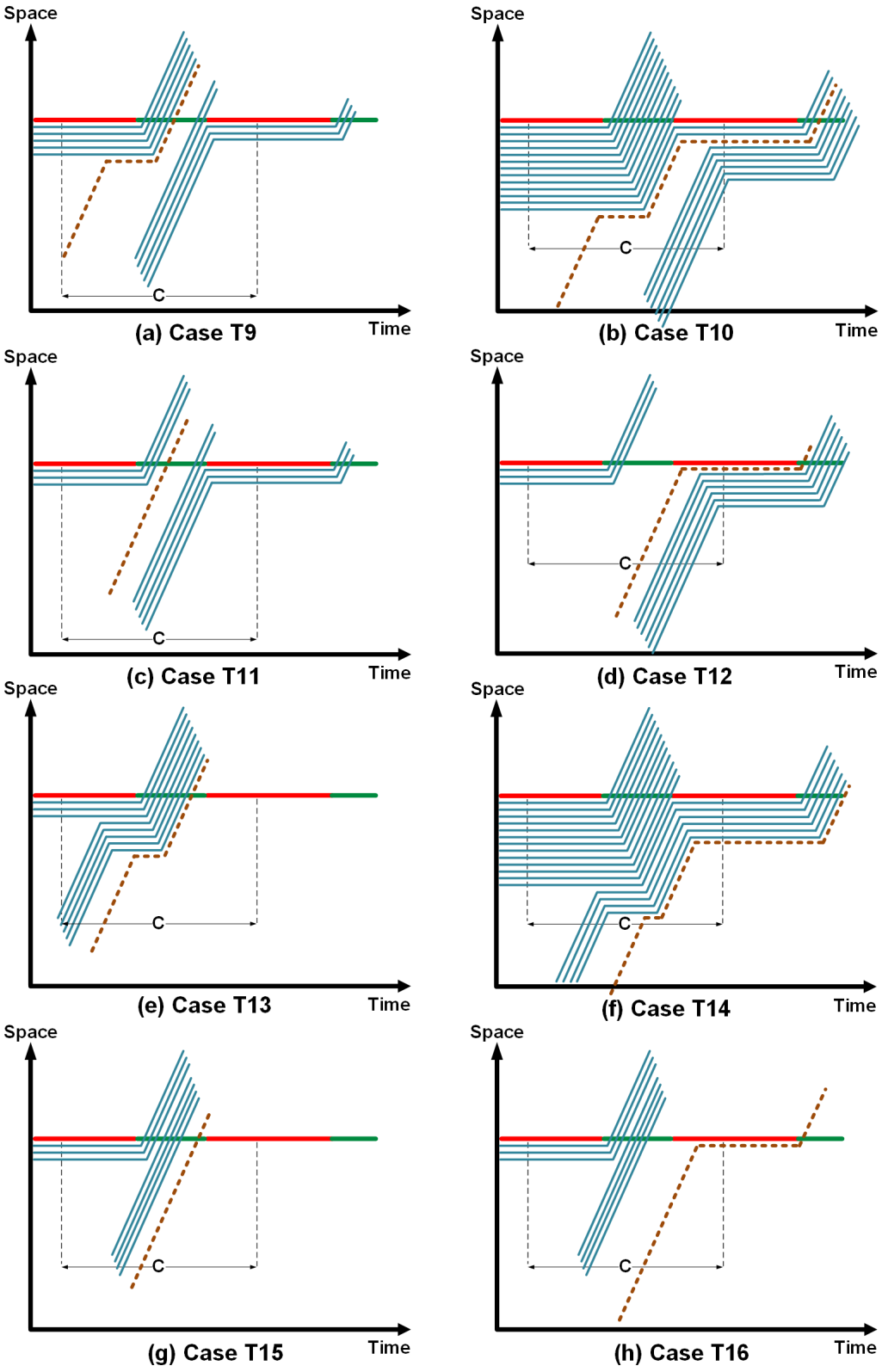

Figure 5.3: Transit delay cases: transit vehicle traveling outside the auto platoon

- Case $T11$: Transit vehicle arrival during the green phase before residual queue served, transit vehicle passes the intersection without delay

  The Corresponding constraints are as follows:

$$tb_b \geq t_T + R_j^{(1)} + \frac{N_{j,T-1}}{s_j} + M(y_{j,b}^1 1 - 1) \quad \forall j \in J \& \forall b \in B_j \tag{5.55}$$

$$tb_b \leq t_T + R_j^{(1)} + G_j + M(1 - y_{j,b}^1 1) \quad \forall j \in J \& \forall b \in B_j \tag{5.56}$$

$$y_{j,b}^1 1 \leq E_b^2 \quad \forall j \in J \& \forall b \in B_j \tag{5.57}$$

  The transit vehicle delay is zero:

$$db_{b,T}^{11} = 0 \tag{5.58}$$

- Case $T12$: Transit vehicle arrival after the green, entire residual queue is served, transit vehicle passes the intersection during the green phase of the next cycle

  The Corresponding constraints are as follows:

$$tb_b \geq t_T + R_j^{(1)} + G_j + M(y_{j,b}^1 2 - 1) \quad \forall j \in J \& \forall b \in B_j \tag{5.59}$$

$$y_{j,b}^1 2 \leq E_b^2 \quad \forall j \in J \& \forall b \in B_j \tag{5.60}$$

  The transit vehicle delay is:

$$Db_{b,T}^{12} = TC + R_j^{(1)} - tb_{b,T} \tag{5.61}$$

Cases $T13$, $T14$, $T15$, $T16$ are similar to cases $T9$, $T10$, $T11$, $T12$ respectively and just $N_{j,T-1}$ must be replaced with $N_{j,T-1} + P_{j,T}$.

5.2.3 Mathematical Program Formulation

The mathematical program objective function consists of the auto and transit person delays for all vehicles arriving at the intersection during two cycles.

5.2.4 Objective Function

$$min \sum_{j=1}^{J} \bar{o}_a Da_{j,T} + \sum_{j=1}^{J} \sum_{b=1}^{B_j} \bar{o_b} Db_{j,b,T} \tag{5.62}$$

where:

$$Da_{j,T} = \sum_{m=1}^{M_a} (x_j^m \times Da_{j,T}^m) \quad \forall j \in J \tag{5.63}$$

$$Db_{j,b,T} = \sum_{m=1}^{M_b} (y_b^m \times Db_{j,b,T}^m) \quad \forall j \in J, \forall b \in B_T \tag{5.64}$$

So, the objective function becomes:

$$min \sum_{j=1}^{J} \sum_{m=1}^{M_a} \bar{o}_a (x_j^m \times Da_{j,T}^m) + \sum_{j=1}^{J} \sum_{b=1}^{B_T} \sum_{m=1}^{M_b} \bar{o_b} (y_b^m \times Db_{b,T}^m) \tag{5.65}$$

In the objective function (equation (5.65)), the binary variables x_j^m and $y_{j,b}^m$ are multiplied by the continuous variables Da_j^m and $Db_{j,b}^m$ respectively, which make it non-linear. To defeat these bilinearities, the objective function is reformulated and new variables za_j^m and $zb_{j,b}^m$ are introduced, which are defined as follows:

$$za_j^m = x_j^m \times Da_j^m \quad \forall j \in J \& \forall m \in M_a \tag{5.66}$$

$$zb_{j,b}^m = y_{j,b}^m \times Db_{j,b}^m \quad \forall j \in J \& \forall b \in B_j \& \forall m \in M_b \tag{5.67}$$

5.2.5 Constraints

$$tb_b \leq t_{j,T} + \frac{P_{j,T}}{s_j} + M(1 - E_b^1) \quad \forall j \in J \& \forall b \in B_j \tag{5.68}$$

$$tb_b \geq t_{j,T} + M(E_b^1 - 1) \quad \forall j \in J \& \forall b \in B_j \tag{5.69}$$

$$tb_b \leq t_{j,T} + M(1 - E_b^2) \quad \forall j \in J \& \forall b \in B_j \tag{5.70}$$

$$tb_b \geq t_{j,T} + \frac{P_{j,T}}{s_j} + M(E_b^3 - 1) \quad \forall j \in J \& \forall b \in B_j \tag{5.71}$$

$$E_b^1 + E_b^2 + E_b^3 = 1 \quad \forall b \in B \tag{5.72}$$

$$za_j^m \leq Da_j^m + M \times (1 - x_j^m) \quad \forall j \in J \& \forall m \in M_a \tag{5.73}$$

$$za_j^m \geq Da_j^m - M \times (1 - x_j^m) \quad \forall j \in J \& \forall m \in M_a \tag{5.74}$$

$$za_j^m \leq M \times x_j^m \quad \forall j \in J \& \forall m \in M_a \tag{5.75}$$

$$zb_{j,b}^m \leq Db_{j,b}^m + M \times (1 - y_{j,b}^m) \quad \forall j \in J \& \forall b \in B_j \& \forall m \in M_b \tag{5.76}$$

$$zb_{j,b}^m \geq Db_{j,b}^m - M \times (1 - y_{j,b}^m) \quad \forall j \in J \& \forall b \in B_j \& \forall m \in M_b \tag{5.77}$$

$$zb_{j,b}^m \leq M \times y_{j,b}^m \quad \forall j \in J \& \forall b \in B_j \& \forall m \in M_b \tag{5.78}$$

$$\sum_{i=1}^{I} g_{i,T} + \sum_{i=1}^{I} y_i = C \tag{5.79}$$

$$g_{i,T} \geq g_{i,min} \quad \forall i \in I \tag{5.80}$$

$$g_{i,T} \leq g_{i,max} \quad \forall i \in I \tag{5.81}$$

$$g_{i,T} \geq 0 \quad \forall i \in I \tag{5.82}$$

$$za_j^m \geq 0 \quad \forall j \in J \& \forall m \in M_a \tag{5.83}$$

$$zb_{j,b}^m \geq 0 \quad \forall j \in J \& \forall b \in B_j \& \forall m \in M_b \tag{5.84}$$

$$x_j^m \in \{0,1\} \quad \forall j \in J \& \forall m \in M_a \tag{5.85}$$

$$y_{j,b}^m \in \{0,1\} \quad \forall j \in J \& \forall b \in B_j \& \forall m \in M_b \tag{5.86}$$

Constraints (5.68) to (5.72) are used to determine the case that a transit vehicle falls under, meaning whether it is traveling within, ahead, or after the vehicle platoon. Constraints (5.73) to (5.78) are added in the mathematical program formulation with the introduction of the auxiliary variables to treat the bilinearities originally existing in the objective function. Constraint (5.79) ensures that the optimal green times add up to the cycle length, and constraints (5.80) and (5.81) provide the lower and upper bounds of the green times respectively. Finally, (5.82) and (5.86) determine the feasible domain for all decision variables.

Additional constraints are introduced to determine the six different auto delay and 16 transit vehicle delay cases, but are omitted here for brevity. An example of constraints for case $N1$ of auto delays are:

$$t_{j,T} \leq t_T + R_j^{(1)} + \frac{N_{j,T-1}}{s_j} + M(1 - x_j^1) \quad \forall j \in J \tag{5.87}$$

$$P_{j,T} \leq G_j s_j - N_{j,T-1} + M(1 - x_j^1) \quad \forall j \in J \tag{5.88}$$

Finally, to provide the priority window, at first optimum green times are determined without applying it. Then, using the optimum green times, if the estimated transit arrival times are within the confidence intervals of the beginning or the end of green, two additional constraints are activated and the optimum green times are recalculated using these additional constraints. If the time between the estimated transit arrival time and the end of the calculated optimum green, g_j^{opt}, is less than one confidence interval, constraint (5.89) ensures that there will be at least one confidence interval from the estimated transit arrival time to the end of the green. Also

constraint (5.90) ensures that the there will be at least one confidence interval from the beginning of the green to the estimated transit arrival time.

$$L_{upper} \leq (T-1)C + R_j^{(1)} + g_j^{opt} \quad \forall j \in J \& \forall b \in B_j \tag{5.89}$$

$$L_{lower} \geq (T-1)C + R_j^{(1)} \quad \forall j \in J \& \forall b \in B_j \tag{5.90}$$

where:

$$L_{upper} = tb_b + Z_{\alpha/2} \times \frac{\sigma}{\sqrt{n}} \tag{5.91}$$

$$L_{lower} = tb_b - Z_{\alpha/2} \times \frac{\sigma}{\sqrt{n}} \tag{5.92}$$

assuming a normal distribution of transit arrival times. Applying these constraints requires careful consideration to avoid infeasibility in solutions. For instance, if the first phase is serving a transit vehicle, applying constraint (5.90) will result in an infeasible solution space.

5.3 Application

The real-time signal control system has been tested with the use of the microsimulation software AIMSUN through Emulation-In-the-Loop Simulation (EILS). In particular, five different scenarios are tested and their results are compared:

- **Scenario 1: SYNCHRO**: signal timings are designed based on the optimum signal timings obtained from SYNCHRO.
- **Scenario 2: Vehicle-based Optimization without Priority Window**: signal timings are optimized by minimizing total vehicle delay. In other words, passenger occupancy of both transit vehicles and autos are one. Priority window is not applied.

- **Scenario 3: Vehicle-based Optimization with Priority Window**: signal timings are optimized by minimizing total vehicle delay and priority window is applied.

- **Scenario 4: Person-based Optimization without Priority Window**: signal timings are optimized by minimizing total person delay. Passenger occupancy of autos and transit vehicles are 1.25 and 40 passengers per vehicle respectively. Priority window is not applied.

- **Scenario 5: Person-based Optimization with Priority Window**: signal timings are optimized by minimizing total person delay and priority window is applied.

5.3.1 Test Site

The developed real-time TSP control is tested on a single intersection. The intersection of San Pablo Avenue and University Avenue is selected as the test site to study the performance of the real-time signal control system. Existing conditions at this intersection indicate traffic condition close to saturation. The selected intersection layout and the lane groups, phasing, and green times for the intersection during the evening peak are shown in Figure 5.4. The intersection flow ratio during evening peak hour (4-5pm) is 0.73. The cycle length is $C = 80$ seconds and the lost time is $L = 12$ seconds. The heaviest direction during the evening peak hour is the northbound through movement and for that reason it has been selected for the analysis by including only buses for that direction. Traffic flow of the northbound through movement includes three bus lines (72, 72M, and 72R) with 10 buses per hour. Buses are considered only in the north bound direction. The frequency of buses are increased to one dispatch in every 5 minutes for each of the bus lines 72, 72M, and 72R.

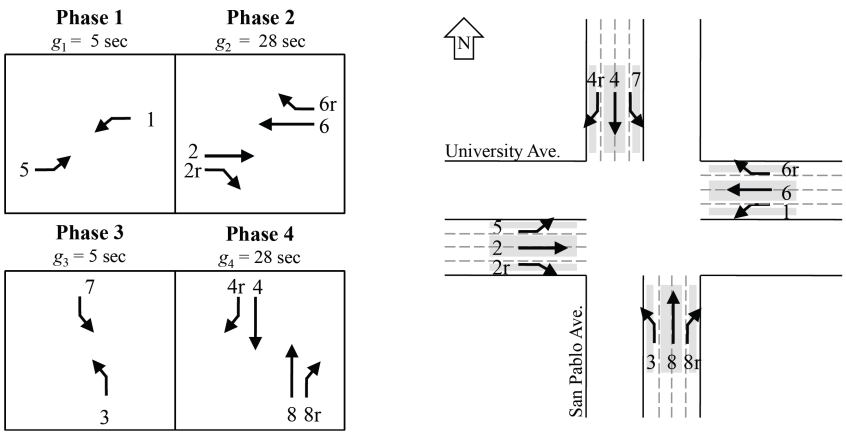

Figure 5.4: Test Site: Lane Groups, Phasing, and Green Times

5.3.2 Simulation Tests

The AIMSUN micro-simulation software (TSS, 2006) is used to develop the simulation model. 30 replications are used to overcome the stochastic nature of auto and bus arrivals. Each replication includes 5 minutes of warm-up period and is run for one hour. The auto inter-arrival times on the incoming links are set to follow an exponential distribution at upstream intersections. Due to the existence of upstream intersections vehicles arrive in platoons at the University Avenue intersection with San Pablo Avenue, however the platoon size may vary from cycle to cycle since the vehicle arrivals at the upstream intersection are random.

Detectors are placed 1400 feet upstream of the upstream intersections to make sure that travel time from the detectors to the upstream intersections is more than one cycle length. The detectors are used to estimate the platoon size of each lane group during the next cycles. Based on the speed of the detected vehicles, their travel time to the upstream intersection are estimated. Based on the estimated arrival time of each vehicle and signal plan of the upstream intersection, platoon sizes for the next cycle are estimated. Theses detectors are also used to predict bus arrival times at the intersection stopline.

Residual queues for each lane group are determined using the exit and entering detectors. The entering detectors are located at the far-side of the links and detect the actual number of vehicles entering the link. The exit detectors are located at the University intersection stoplines and are used to determine the number of vehicles discharging from the intersection. Residual queues are calculated as the difference between entered and discharged vehicles during the previous cycle.

5.3.3 Results

The mathematical program is a Mixed Integer Linear Program (MILP) modeled in C++ and solved using ILOG CPLEX Concert package and is simulated in Aimsun using application programming interface (API) provided by Aimsun. A separate micro-simulation test were run to determine error in predicting bus arrival times. Ten replications for an hour were run and estimated bus arrivals and actual arrivals were collected. Bus arrival estimates were calculated using upstream detectors and actual arrival times were collected using the detectors at intersection stopline. The average error in predicting bus arrivals was -0.4 seconds with a standard deviation of 7.6 seconds. Using the standard normal table, the confidence interval for $\alpha = 0.5$ is 4.7 seconds. Therefore, in the priority window constraints, a 5-second confidence interval is considered. The results of the vehicle delay and person delay for auto passengers, bus passengers, and total passengers for the five scenarios as well as their standard deviation are listed in Tables 5.1 and 5.2 respectively.

The results indicate that the vehicle-based optimization without applying priority window significantly reduces bus person delay by 32% in comparison to the base case (SYNCHRO) (Figure 5.5). Person-based optimization reduces bus person delay by 54% and increases car person delay by 20%. This increase is due to the fact that in person-based optimization higher weight is given to the buses. Although car person delay is increased, total person delay has not been changed in comparison to the

Table 5.1: Vehicle Delays

	Bus Delay (sec)	SD	Auto Delay (sec)	SD	Total Delay (sec)	SD
SYNCHRO	27.84	7.87	18.57	2.73	18.64	2.75
Vehicle-Based - No Priority Window	18.79	4.49	19.63	3.83	19.62	3.81
Vehicle-Based - With Priority Window	15.62	3.95	20.12	3.64	20.08	3.63
Person-Based - No Priority Window	12.52	3.95	22.35	4.83	22.27	4.79
Person-Based - With Priority Window	6.88	3.22	26.09	7.87	25.95	7.81

Table 5.2: Person Delays

	Bus Person Delay (pax-sec)	SD	Auto Person Delay (pax-sec)	SD	Total Person Delay (pax-sec)	SD
SYNCHRO	11.01	3.06	30.46	4.75	41.47	7.23
Vehicle-Based - No Priority Window	7.52	1.79	32.21	6.54	39.73	7.11
Vehicle-Based - With Priority Window	6.25	1.58	33.00	6.22	39.25	7.05
Person-Based - No Priority Window	5.01	1.58	36.65	8.28	41.66	8.22
Person-Based - With Priority Window	2.75	1.29	42.71	13.17	45.46	13.31

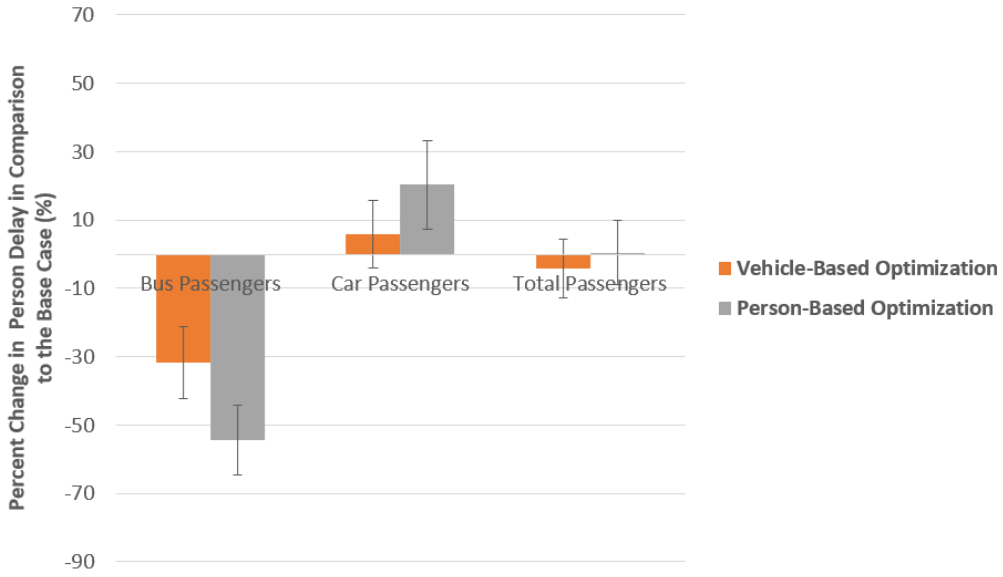

Figure 5.5: Percent change in person delay without priority window

base case. By applying 5 seconds priority window, results (Figure 5.6) show that additional 11% and 21% reduction in bus person delay is achieved by vehicle-bases and person-based optimization methods respectively. Person-based optimization with priority window increases car person delay by 40% while total person delay increased 10%.

Applying priority window in vehicle-based optimization reduces bus person delay by 43% which is 11% higher than the scenario without priority window (Figure 5.7). With the person-based optimization, applying priority window achieves 21% higher reduction in person delay in comparison to the scenario without priority window (Figure 5.8).

5.4 Summary of Findings

This chapter developed a real-time signal control plan which minimizes total person delay of an intersection along a signalized corridor while accounting for stochasticity in transit vehicle arrival time by ensuring a priority window for them. An analytical

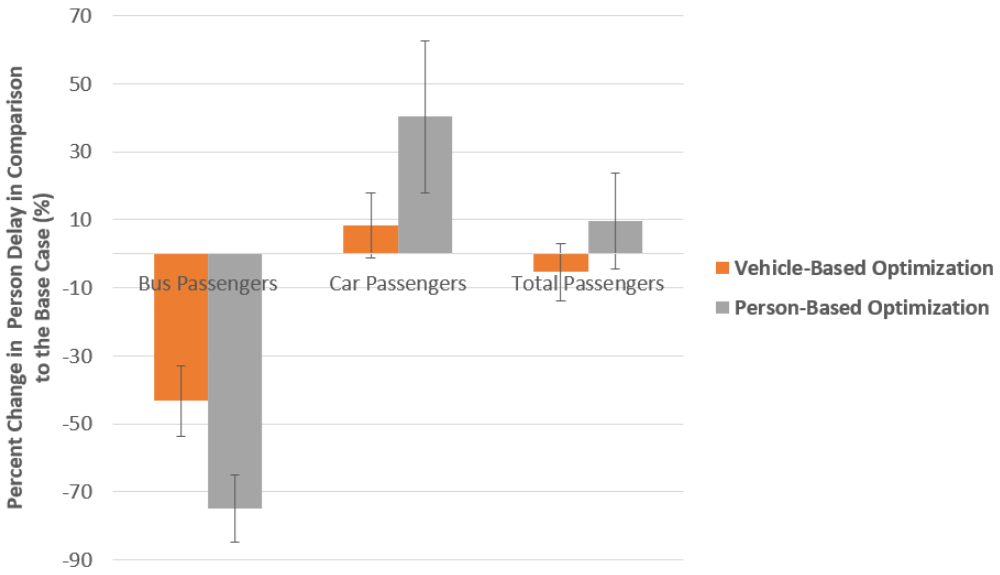

Figure 5.6: Percent change in person delay with priority window

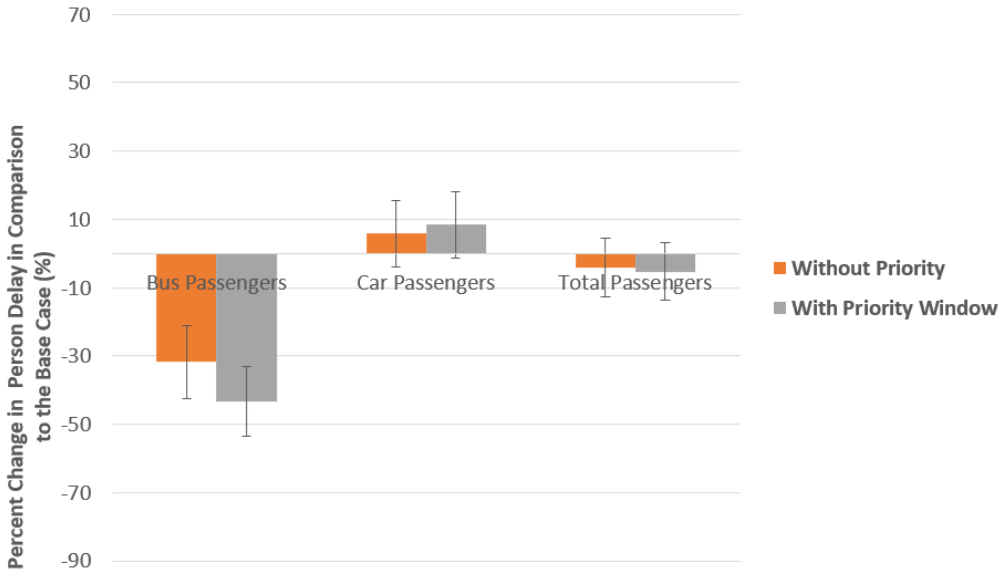

Figure 5.7: Percent change in person delay with vehicle-based optimization

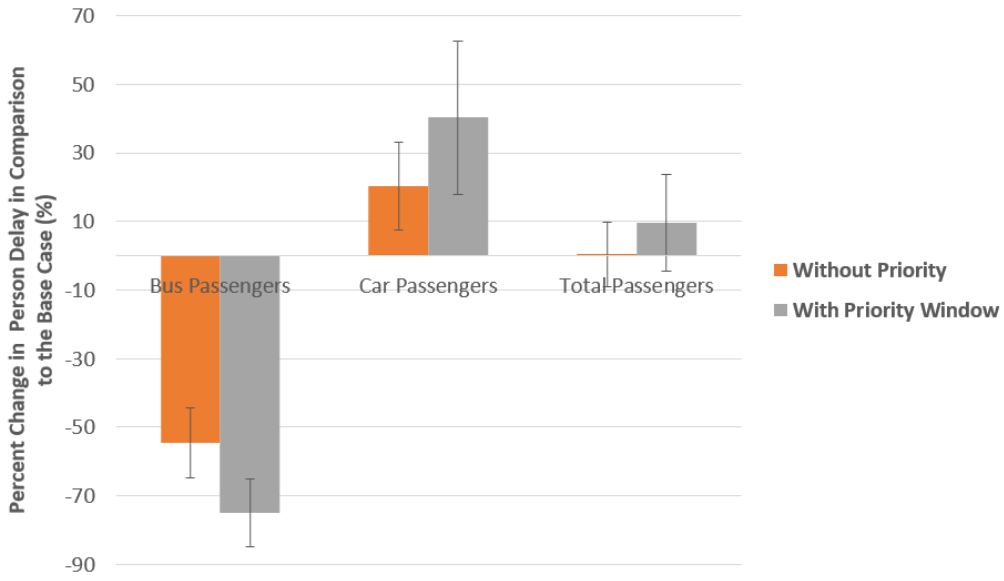

Figure 5.8: Percent change in person delay with person-based optimization

model based on Kinematic Wave Theory is used to estimate auto and transit vehicle delays. The optimization model is formulated as a mixed-integer programming model. The mathematical program is modeled in C++ and solved using the CPLEX Concert package. Results from the AIMSUN micro-simulation tests indicate that the proposed mathematical program with and without priority window, significantly reduces bus person delay in comparison to the base scenario. By applying 5 seconds priority window, results show that an additional significant reduction in bus person delay is achieved by both vehicle-based and person-based optimization methods.

Future work will focus on expanding the model to accommodate varying cycle lengths and phase sequences. In addition, the impact of bus stops as well as queue spillbacks will be incorporated. The mathematical program will be also updated to account for multiple transit lines arriving at the even from conflicting approaches. Finally, additional work will extend this model to multiple intersections along the arterial following a pair-wise optimization as in (Christofa et al., 2016).

CHAPTER 6

CONCLUSION

The objective of this dissertation is threefold: 1) to perform a person-based evaluation of alternative TPTs when considered individually and in combination, 2) to estimate bus arrival time at intersection stopline and 3) to develop a real-time traffic signal control plan accounting for stochastic bus arrivals at the intersection stopline.

6.1 Summary of Findings

6.1.1 TPT Evaluation

This dissertation first (Chapter 3) presented an analytical model to evaluate the impact of alternative TPTs, in terms of person delay and person discharge flow at signalized arterials both with and without nearside bus stops. The model assumes vehicles arrive in platoons and using Kinematic Wave Theory, it determines person delay performance measures of both auto vehicles and buses traveling at each lane group. TPTs are also evaluated using a microsimulation model in Aimsun. The proposed analytical models can handle both under-saturated on over-saturated conditions; however, in this study only under-saturated conditions have been evaluated. For the without nearside bus stops case, the evaluations were performed on a four-intersection signalized arterial located in Berkeley, CA. A total of eight alternative scenarios were evaluated. These scenarios included several space TPTs (dedicated bus lane addition and substitution, and queue jumper lane addition) and a time TPT (green extension). Space and time TPTs were evaluated both individually and in

combination. For the with nearside bus stops situation, only space priority strategies were evaluated on the intersection of San Pablo Avenue and Cedar Street.

The results of this chapter indicate that space TPTs introduce noticeable benefits to transit users. When a QJL or a DBL is added there is no negative impact on auto traffic. However, when a lane is substituted for a bus lane, person discharge flow decreases significantly and auto person delays increase dramatically. This is a result of the oversaturated conditions that the substitution of a lane is likely to cause for high vehicle demand levels. Therefore, DBL substitution is not suitable for high volume approaches, because it reduces the capacity by significant amounts. DBL substitution may be justified for high frequency transit lines, essentially when DBL substitution can serve at least as many people as it does when the lane is available for all vehicles. Implementation of green extension leads to favorable results for total person delay and bus person delay while autos on the priority approach also benefit. In addition, doubling the bus frequency had a positive impact in reducing total and bus person delay when green extension was implemented, while increased bus passenger occupancy had insignificant effect. Finally, a comparison of the analytical with the microsimulation test results indicates that the proposed analytical model can be used to quantitatively assess space and time TPTs.

The person-based analytical model that was presented in this study as well as the insights obtained in this study can be used to provide guidance in the planning and design of TPTs that improve transit reliability while improving overall mobility in urban areas. The developed analytical models can be used to assist decisions on preferential treatments under various traffic and transit operating conditions. In addition, this study showed that the analytical method could be used for such assessments without the need for expensive microsimulations since the results produced through microsimulation were comparable to the results produced with the analytical model.

6.1.2 Bus Arrival Prediction

The second part of this dissertation (Chapter 4) presented a a mixed-integer quadratic programming model (MIQP) to estimate bus travel time along a signalized arterial using data obtained from low resolution Automated Vehicle Location (AVL) data. A model is developed to decompose bus travel time into its components including dwell time at bus stops, average speed, acceleration/deceleration lost time, and intersection delay. The model learns these components using historical low resolution AVL data (i.e. one record every 60 seconds) without requiring information about the dwell times at bus stops, the signal status, or traffic conditions. The model estimates signal status and infers trajectories of the buses. The problem was formulated as a mixed-integer quadratic programming model (MIQP) and was solved using CPLEX solver.

The results of the MIQP model and a linear regression model are compared. Both the linear regression and MIQP models are tested in a segment of the Washington Street in Boston, Massachusetts. Results indicate that the MIQP model outperforms linear regression model in terms of generalized error measures including MAE, MAPE, and RMSE. In particular, the MIQP model is capable of predicting bus travel time with an average error of less than five seconds, which is sufficient for implementation of TSP strategies and traveler information systems.

6.1.3 Real-time Traffic Signal Control Plan

The third part of this dissertation (Chapter 5) presented a real-time signal control plan which minimizes total person delay of an intersection along a signalized corridor while providing a priority window for transit vehicles. The program uses the analytical models developed in Chapter 3 to evaluate person delay of an intersection and arrival time of the buses at the intersection stopline are predicted. Taking into account the stochasticity in transit vehicles' arrival time, a mathematical program is formulated to minimize total person delay while providing priority window for buses to make sure

that 95% of the buses arriving during the green phase can be served. The optimization model is formulated as mixed-integer programming model and is solved using CPLEX Concert package. Results from the Aimsun micro-simulation test showed that the proposed mathematical program significantly reduces bus, car and total person delays in caparison to the base scenario.

6.2 Research Contributions

- Development of analytical models to evaluate various space (e.g., queue jumper lane and dedicated bus lane) and time (e.g., transit signal priority) priority strategies along signalized arterials with and without nearside bus stops. The analytical models evaluate person-based performance measures including person delay and person discharge flow using Kinematic Wave Theory. Vehicles approaching the signalized intersection are considered to travel within platoons.

- Development of a bus travel time prediction model using data obtained from AVL systems. The proposed model estimates traffic signal status using the AVL records of buses and provides more accurate predictions in comparison to a simple linear regression model. The proposed model decomposes bus travel time into its components including running travel time, dwell times at bus stops, and delays at intersections. Unlike other studies, the developed model in this research estimates intersection delay for individual buses rather than estimating an average delay over all buses thus, improves prediction accuracy.

- Development of a real-time traffic signal control with TSP which takes into account stochasticity in bus arrivals and provides a priority window for buses. The control system minimizes total person delay at an intersection. The person delay measures are determined using the analytical models developed for the TPT evaluation. This study is unique since the developed control system

provides a priority window to make sure that buses can pass the intersection (if arriving during the green phase) considering a certain confidence level to overcome the randomness in the bus arrival time predictions.

6.3 Future Work

6.3.1 TPT Evaluation

Future work will improve the analytical models to account for platoon dispersion and stochasticity in auto arrivals. Future work will extend the analytical model to evaluate other TPT strategies including intermittent bus lanes. In addition, future research will focus on testing the proposed analytical and simulation models at test sites that present oversaturated traffic conditions. Finally, future research will investigate a variety of traffic and transit conditions to determine domains where certain TPTs should be implemented to minimize person delay.

6.3.2 Bus Arrival Prediction

Future work will improve the model to account for cases where buses travel on mixed-use lanes and actuated signal control plans. In a mixed-traffic lane case, the position of buses in queue at intersections should be estimated to determine bus delay at the intersections. Furthermore, future research will relax the assumption that information about the duration of the signal phases is available.

6.3.3 Real-time Traffic Signal Control Plan

Future work will expand the model to accommodate varying cycle lengths and phase sequences. In addition, the impact of bus stops as well as queue spillbacks will be incorporated. The mathematical program will be also updated to account for multiple transit lines arriving at the even from conflicting approaches. Finally, additional work

will extend this model to multiple intersections along the arterial following a pair-wise optimization as in Christofa et al. (2016).

BIBLIOGRAPHY

Abdy, Z. R. and B. R. Hellinga (2011). Analytical method for estimating the impact of transit signal priority on vehicle delay. *Journal of Transportation Engineering 137*(8), 589–600.

ACTransit (2014). Ac transit, alameda-contra costa transit district, http://www.actransit.org.

Arasan, V. T. and P. Vedagiri (2010). Study of the impact of exclusive bus lane under highly heterogeneous traffic condition. *Public Transport 2*(1-2), 135–155.

Baptista, A. T., E. P. Bouillet, and P. Pompey (2012). Towards an uncertainty aware short-term travel time prediction using GPS bus data: Case study in Dublin. In *Intelligent Transportation Systems (ITSC), 2012 15th International IEEE Conference on*, pp. 1620–1625. IEEE.

Bie, Y., D. Wang, and H. Qi (2011). Prediction model of bus arrival time at signalized intersection using GPS data. *Journal of Transportation Engineering 138*(1), 12–20.

Bielefeldt, C. and F. Busch (1994). Motion-a new on-line traffic signal network control system motion. In *Seventh International Conference on Road Traffic Monitoring and Control*. IET.

Boyd, S. and L. Vandenberghe (2004). *Convex optimization*. Cambridge University Press.

Bretherton, D., G. Bowen, and K. Wood (2002). Effective urban traffic management and control-scoot version 4.4. *Publication of: Association for European Transport*.

Busch, F. and G. Kruse (2001). Motion for sitraffic-a modern approach to urban traffic control. In *Intelligent Transportation Systems, 2001. Proceedings. 2001 IEEE*, pp. 61–64. IEEE.

Carey, G., T. Bauer, and K. Giese (2009). Bus lane with intermittent priority (blimp) concept simulation analysis. Technical report.

Cathey, F. and D. Dailey (2003). A prescription for transit arrival/departure prediction using automatic vehicle location data. *Transportation Research Part C: Emerging Technologies 11*(3), 241–264.

Chang, J., J. Collura, F. Dion, and H. Rakha (2003). Evaluation of service reliability impacts of traffic signal priority strategies for bus transit. *Transportation Research Record: Journal of the Transportation Research Board 1841*(1), 23–31.

Chen, M., X. Liu, and J. Xia (2005). Dynamic prediction method with schedule recovery impact for bus arrival time. *Transportation Research Record: Journal of the Transportation Research Board* (1923), 208–217.

Chiabaut, N., X. Xie, and L. Leclercq (2012). Road capacity and travel times with bus lanes and intermittent priority activation. *Transportation Research Record: Journal of the Transportation Research Board 2315*(1), 182–190.

Chien, S. I.-J., Y. Ding, and C. Wei (2002). Dynamic bus arrival time prediction with artificial neural networks. *Journal of Transportation Engineering 128*(5), 429–438.

Christofa, E. (2012). *Traffic Signal Optimization with Transit Priority: A Person-based Approach*. Ph. D. thesis, University of California, Berkeley.

Christofa, E., K. Aboudolas, and A. Skabardonis (2013). Arterial traffic signal optimization: A person-based approach. In *Transportation Research Board 92nd Annual Meeting*, Number 13-3395.

Christofa, E., K. Ampountolas, and A. Skabardonis (2016). Arterial traffic signal optimization: a person-based approach. *Transportation Research Part C: Emerging Technologies 66*, 27–47.

Christofa, E., I. Papamichail, and A. Skabardonis (2013). Person-based traffic responsive signal control optimization. *IEEE Transactions on Intelligent Transportation Systems 14*(3), 1278–1289.

Currie, G., K. C. K. Goh, and M. Sarvi (2013). An analytical approach to measuring the impacts of transit priority. In *Transportation Research Board 92nd Annual Meeting*.

Currie, G. and H. Lai (2008). Intermittent and dynamic transit lanes: melbourne, australia, experience. *Transportation Research Record: Journal of the Transportation Research Board 2072*(1), 49–56.

Danaher, A. R., K. Blume, H. Levinson, and S. Zimmerman (2007). Tcrp report 118: Bus rapid transit practitioners guide. *Transportation Research Board of the National Academies, Washington, DC*.

Dion, F., H. Rakha, and Y. Zhang (2004). Evaluation of potential transit signal priority benefits along a fixed-time signalized arterial. *Journal of transportation engineering 130*(3), 294–303.

Donati, F., V. Mauro, G. Roncolini, and M. Vallauri (1984). A hierarchical decentralised traffic light control system. the first realisation:progetto torino. In *IFAC 9th World Congress*, Volume 2.

Eichler, M. and C. F. Daganzo (2006). Bus lanes with intermittent priority: Strategy formulae and an evaluation. *Transportation Research Part B: Methodological 40*(9), 731–744.

Ekeila, W., T. Sayed, and M. El Esawey (2009). Development of dynamic transit signal priority strategy. *Transportation Research Record: Journal of the Transportation Research Board 2111*(1), 1–9.

Farid, Y. Z., E. Christofa, and L. Paget-Seekins (2016). Short-term bus travel time estimation using low-resolution automated vehicle location data. *Transportation Research Record: Journal of the Transportation Research Board, No. 2539*(DOI 10.3141/2539-13).

Fitzpatrick, K., K. Hall, D. Perkinson, L. Nowlin, and R. Koppa (1996). Guidelines for the location and design of bus stops. Technical Report Report No. 19, TCRP.

Fitzpatrick, K. and R. L. Nowlin (1997). Effects of bus stop design on suburban arterial operations. *Transportation Research Record: Journal of the Transportation Research Board 1571*(1), 31–41.

Furth, P. G., B. Cesme, and T. Rima (2010). Signal priority near major bus terminal, case study of ruggles station, boston, massachusetts. *Transportation Research Record: Journal of the Transportation Research Board 2192*(1), 89–96.

Furth, P. G. and J. L. SanClemente (2006). Near side, far side, uphill, downhill: impact of bus stop location on bus delay. *Transportation Research Record: Journal of the Transportation Research Board 1971*(1), 66–73.

Garrow, M. and R. Machemehl (1997). Development and evaluation of transit signal priority strategies. Technical report, Center for Transportation Research, The University of Texas at Austin.

Gayah, V. V., Z. Yu, and J. S. Wood (2016). Estimating uncertainty of bus arrival times and passenger occupancies. *Mineta Transportation Institute Publications*.

Gibson, J., M. Munizaga, C. Schneider, and A. Tirachini (2015). Median busways versus mixed-traffic: Estimation of bus travel time under different priority conditions with explicit modelling of delay at traffic signals. In *Transportation Research Board 94th Annual Meeting, Washington, DC.¡ http://docs. trb. org/prp/15-1260. pdf*.

Gu, W., M. J. Cassidy, V. V. Gayah, and Y. Ouyang (2013). Mitigating negative impacts of near-side bus stops on cars. *Transportation Research Part B: Methodological 47*, 42–56.

Gujarati, D. N. (2003). *Basic Econometrics. 4th.* New York: McGraw-Hill.

Guler, S. I. and M. J. Cassidy (2012). Strategies for sharing bottleneck capacity among buses and cars. *Transportation Research Part B: Methodological 46*(10), 1334–1345.

Hans, E., N. Chiabaut, and L. Leclercq (2014). Real-time forecasting the bus route state by data assimilation process. *Transportation Research Arena, Paris, France*, 14–17.

HCM (2010). *Highway Capacity Manual*. Transportation Research Board.

He, Q., K. L. Head, and J. Ding (2012). PAMSCOD: Platoon-based arterial multi-modal signal control with online data. *Transportation Research Part C: Emerging Technologies 20*(1), 164–184.

Hellinga, B., P. Izadpanah, H. Takada, and L. Fu (2008). Decomposing travel times measured by probe-based traffic monitoring systems to individual road segments. *Transportation Research Part C: Emerging Technologies 16*(6), 768–782.

Hernandez, T. (2014). Flex scheduling for bus arrival time prediction. *Transportation Research Record: Journal of the Transportation Research Board* (2418), 110–115.

Hofleitner, A., R. Herring, P. Abbeel, and A. Bayen (2012). Learning the dynamics of arterial traffic from probe data using a dynamic Bayesian network. *Intelligent Transportation Systems, IEEE Transactions on 13*(4), 1679–1693.

Hu, W., L. Yan, K. Liu, and H. Wang (2016). A short-term traffic flow forecasting method based on the hybrid PSO-SVR. *Neural Processing Letters 43*(1), 155–172.

Hunt, P., D. Robertson, R. Bretherton, and M. Royle (1982). The scoot on-line traffic signal optimisation technique. *Traffic Engineering & Control 23*(4), 190–192.

Idé, T. and S. Kato (2009). Travel-time prediction using Gaussian Process regression: A trajectory-based approach. In *SDM*, pp. 1185–1196. SIAM.

Iswalt, M., C. Wong, and K. Connolly (2011). Innovative operating solutions for bus rapid transit through a congested segment of san jose, california. *Transportation Research Record: Journal of the Transportation Research Board 2218*(1), 27–38.

Jacobson, J. and Y. Sheffi (1981). Analytical model of traffic delays under bus signal preemption: theory and application. *Transportation Research Part B: Methodological 15*(2), 127–138.

James, G., D. Witten, T. Hastie, and R. Tibshirani (2013). *An introduction to statistical learning*, Volume 112. Springer.

Jenelius, E. and H. Koutsopoulos (2012). Impact of sampling protocol on bias and consistency in travel time estimation on probe vehicle data. Technical report, Royal Institute of Technology, Stockholm, Sweden.

Jenelius, E. and H. N. Koutsopoulos, H.s (2013). Travel time estimation for urban road networks using low frequency probe vehicle data. *Transportation Research Part B: Methodological 53*, 64–81.

Jeong, R. and L. Rilett (2005). Prediction model of bus arrival time for real-time applications. *Transportation Research Record: Journal of the Transportation Research Board* (1927), 195–204.

Jeong, R. and L. R. Rilett (2004). Bus arrival time prediction using artificial neural network model. In *Intelligent Transportation Systems, 2004. Proceedings. The 7th International IEEE Conference on*, pp. 988–993. IEEE.

Kamdar, V. (2004). Evaluating the transit signal priority impacts along the us 1 corridor in northern virginia. Master's thesis, Virginia Polytechnic Institute and State University.

Khosravi, A., E. Mazloumi, S. Nahavandi, D. Creighton, and J. Van Lint (2011). A genetic algorithm-based method for improving quality of travel time prediction intervals. *Transportation Research Part C: Emerging Technologies 19*(6), 1364–1376.

Kim, W. and L. Rilett (2005). Improved transit signal priority system for networks with nearside bus stops. *Transportation Research Record: Journal of the Transportation Research Board 1925*(1), 205–214.

Kimpel, T. J., J. Strathman, R. L. Bertini, and S. Callas (2005). Analysis of transit signal priority using archived trimet bus dispatch system data. *Transportation Research Record: Journal of the Transportation Research Board 1925*(1), 156–166.

Kittelson, W., J. Ringert, P. Koonce, K. Giese, and S. Beaird (2003). Portland signal priority, technical report, tea-21 signal priority. Technical report, Kittelson & Associates, Inc, Portland, Oregon.

Kloos, W. C., A. R. Danaher, and K. M. Hunter-Zaworski (1994). Bus priority at traffic signals in portland: the powell boulevard pilot project. In *ITE Compendium of Technical Papers*, Number 1503, pp. 420–424. National Research Council.

Koonce, P., L. Rodegerdts, K. Lee, S. Quayle, S. Beaird, C. Braud, J. Bonneson, P. Tarnoff, and T. Urbanik (2008). Traffic signal timing manual. Technical report.

Kormaksson, M., L. Barbosa, M. R. Vieira, and B. Zadrozny (2014). Bus travel time predictions using additive models. In *Data Mining (ICDM), 2014 IEEE International Conference on*, pp. 875–880. IEEE.

Kumar, B. A., S. Mothukuri, L. Vanajakshi, and S. C. Subramanian (2015). An analytical approach to identify the optimum inputs for a bus travel time prediction method. In *Transportation Research Board 94th Annual Meeting*, Number 15-2088.

Lahon, D. (2011). Modeling transit signal priority and queue jumpers for brt. *ITE Journal*, 20–24.

Lehtonen, M. and R. Kulmala (2002). Benefits of pilot implementation of public transport signal priorities and real-time passenger information. *Transportation Research Record: Journal of the Transportation Research Board 1799*(1), 18–25.

Li, J.-Q., M. K. Song, M. Li, and W.-B. Zhang (2009). Planning for bus rapid transit in single dedicated bus lane. *Transportation Research Record: Journal of the Transportation Research Board 2111*(1), 76–82.

Liao, C.-F. and G. A. Davis (2007). Simulation study of bus signal priority strategy: Taking advantage of global positioning system, automated vehicle location system, and wireless communications. *Transportation Research Record: Journal of the Transportation Research Board 2034*(1), 82–91.

Lighthill, M. J. and G. B. Whitham (1955). On kinematic waves. ii. a theory of traffic flow on long crowded roads. *Proceedings of the Royal Society of London. Series A. Mathematical and Physical Sciences 229*(1178), 317–345.

Lin, Y., X. Yang, N. Zou, and L. Jia (2013). Real-time bus arrival time prediction: Case study for Jinan, China. *Journal of Transportation Engineering 139*(11), 1133–1140.

Liu, H., W.-H. Lin, and C.-w. Tan (2007). Operational strategy for advanced vehicle location system–based transit signal priority. *Journal of Transportation Engineering 133*(9), 513–522.

Liu, H., J. Zhang, and D. Cheng (2008). Analytical approach to evaluating transit signal priority. *Journal of Transportation systems engineering and information technology 8*(2), 48–57.

Liu, J., W. Wang, X. Gong, X. Que, and H. Yang (2012). A hybrid model based on kalman filter and neutral network for traffic prediction. In *Cloud Computing and Intelligent Systems (CCIS), 2012 IEEE 2nd International Conference on*, Volume 2, pp. 533–536. IEEE.

Ma, X., Z. Tao, Y. Wang, H. Yu, and Y. Wang (2015). Long short-term memory neural network for traffic speed prediction using remote microwave sensor data. *Transportation Research Part C: Emerging Technologies 54*, 187–197.

Mangasarian, O. L. and D. R. Musicant (2000). Robust linear and support vector regression. *Pattern Analysis and Machine Intelligence, IEEE Transactions on 22*(9), 950–955.

Mazloumi, E., S. Moridpour, G. Currie, and G. Rose (2011). Exploring the value of traffic flow data in bus travel time prediction. *Journal of Transportation Engineering 138*(4), 436–446.

Mirchandani, P. and L. Head (2001). A real-time traffic signal control system: architecture, algorithms, and analysis. *Transportation Research Part C: Emerging Technologies 9*(6), 415–432.

Mirchandani, P. B. and D. E. Lucas (2001). Rhodes-itms tempe field test project: Implementation and field testing of rhodes, a real-time traffic adaptive control system. Technical report.

Mirchandani, P. B. and D. E. Lucas (2004). Integrated transit priority and rail/emergency preemption in real-time traffic adaptive signal control. *Journal of Intelligent Transportation Systems 8*(2), 101–115.

Myung, J., D.-K. Kim, S.-Y. Kho, and C.-H. Park (2011). Travel time prediction using k nearest neighbor method with combined data from vehicle detector system and automatic toll collection system. *Transportation Research Record: Journal of the Transportation Research Board* (2256), 51–59.

Nikovski, D., N. Nishiuma, Y. Goto, and H. Kumazawa (2005). Univariate short-term prediction of road travel times. In *Intelligent Transportation Systems, 2005. Proceedings. 2005 IEEE*, pp. 1074–1079. IEEE.

Noonan, J. and O. Shearer (1998). Intelligent transportation systems field operational test cross-cutting study: Advance traveler information systems. Technical report.

Oliveira-Neto, F. M., C. F. G. Loureiro, and L. D. Han (2009). Active and passive bus priority strategies in mixed traffic arterials controlled by scoot adaptive signal system. *Transportation Research Record: Journal of the Transportation Research Board 2128*(1), 58–65.

Pessaro, B. and C. Van Nostrand (2011). Miami urban partnership agreement (upa) pines boulevard transit signal priority evaluation report. Technical report, Center for Urban Transportation Research, University of South Florida.

Rakha, H. A. and K. Ahn (2006). Transit signal priority project-phase ii: Field and simulation evaluation results. Technical report, Virginia Department of Transportation.

Richards, P. I. (1956). Shock waves on the highway. *Operations research 4*(1), 42–51.

Sakamoto, K., C. Abhayantha, and H. Kubota (2007). Effectiveness of bus priority lane as countermeasure for congestion. *Transportation Research Record: Journal of the Transportation Research Board 2034*(1), 103–111.

Schrank, D., B. Eisele, and T. Lomax (2012). Ttis 2012 urban mobility report. Technical report, Texas A&M Transportation Institute.

SCOOT (2015). Scoot website, url: http://www.scoot-utc.com.

Shepherd, S. (1992). A review of traffic signal control.

Sims, A. G. and K. Dobinson (1980). The sydney coordinated adaptive traffic (scat) system philosophy and benefits. *Vehicular Technology, IEEE Transactions on 29*(2), 130–137.

Sinn, M., J. W. Yoon, F. Calabrese, and E. Bouillet (2012). Predicting arrival times of buses using real-time GPS measurements. In *Intelligent Transportation Systems (ITSC), 2012 15th International IEEE Conference on*, pp. 1227–1232. IEEE.

Skabardonis, A. (2000). Control strategies for transit priority. *Transportation Research Record: Journal of the Transportation Research Board 1727*(1), 20–26.

Slavin, C., W. Feng, M. Figliozzi, and P. Koonce (2013). Statistical study of the impact of adaptive traffic signal control on traffic and transit performance. *Transportation Research Record: Journal of the Transportation Research Board 2356*(1), 117–126.

Smith, H. R., B. Hemily, and M. Ivanovic (2005, May). *Transit signal priority (TSP): A planning and implementation handbook*. 1100 17th Street, NW, 12th Floor Washington, DC 20036 USA 1200 New Jersey Avenue, SE Washington, DC 20590 USA: ITS America and Department of Transportation.

Surprenant-Legault, J. and A. M. El-Geneidy (2011). Introduction of reserved bus lane. *Transportation Research Record: Journal of the Transportation Research Board 2218*(1), 10–18.

Tak, S., S. Kim, K. Jang, and H. Yeo (2014). Real-time travel time prediction using multi-level k-nearest neighbor algorithm and data fusion method. *Computing in civil and building engineering*, 1861–1868.

Tan, C.-W., S. Park, H. Liu, Q. Xu, and P. Lau (2008). Prediction of transit vehicle arrival time for signal priority control: algorithm and performance. *Intelligent Transportation Systems, IEEE Transactions on 9*(4), 688–696.

Tan, C.-W., S. Park, K. Zhou, H. Liu, P. Lau, M. Li, and W.-B. Zhang (2006). Prediction of transit vehicle arrival times at signalised intersections for signal priority control. In *Intelligent Transportation Systems Conference, 2006. ITSC'06. IEEE*, pp. 1477–1482. IEEE.

TSS (2006). *TSS-Transport Simulation System*. TSS.

van Hinsbergen, C. I., J. Van Lint, and H. Van Zuylen (2009). Bayesian committee of neural networks to predict travel times with confidence intervals. *Transportation Research Part C: Emerging Technologies 17*(5), 498–509.

Viegas, J. and B. Lu (2004). The intermittent bus lane signals setting within an area. *Transportation Research Part C: Emerging Technologies 12*(6), 453–469.

Viegas, J. M., R. Roque, B. Lu, and J. Vieira (2007). The intermittent bus lane system: Demonstration in lisbon. In *Proceedings of the 86th Annual Meeting of the Transportation Research Board*.

Vlachou, K., J. Collura, and A. Mermelstein (2010). Planning and deploying transit signal priority in small and medium-sized cities: Burlington, vermont, case study. *Journal of Public Transportation 13*(3), 101–123.

Vlahogianni, E. I., M. G. Karlaftis, and J. C. Golias (2014). Short-term traffic forecasting: Where we are and where were going. *Transportation Research Part C: Emerging Technologies 43*, 3–19.

Wadjas, Y. and P. G. Furth (2003). Transit signal priority along arterials using advanced detection. *Transportation Research Record: Journal of the Transportation Research Board 1856*(1), 220–230.

Wahlstedt, J. (2013). Evaluation of different bus priority functions in coordinated traffic signals. In *Transportation Research Board 92nd Annual Meeting*, Number 13-0818.

Wen, Y., L. Zhang, and Z. Huang (2012). Coordination of connected vehicle and transit signal priority in transit evacuations. In *Transportation Research Board 91st Annual Meeting*.

Wong, S., H. Yang, W. A. Yeung, S. Cheuk, and M. Lo (1998). Delay at signal-controlled intersection with bus stop upstream. *Journal of transportation engineering 124*(3), 229–234.

Yagar, S. and B. Han (1994). A procedure for real-time signal control that considers transit interference and priority. *Transportation Research Part B: Methodological 28*(4), 315–331.

Yu, B., W. H. Lam, and M. L. Tam (2011). Bus arrival time prediction at bus stop with multiple routes. *Transportation Research Part C: Emerging Technologies 19*(6), 1157–1170.

Yu, B., T. Ye, X.-M. Tian, G.-B. Ning, and S.-Q. Zhong (2012). Bus travel-time prediction with a forgetting factor. *Journal of Computing in Civil Engineering 28*(3), 06014002.

Zhang, Y. and A. Haghani (2015). A gradient boosting method to improve travel time prediction. *Transportation Research Part C: Emerging Technologies 58*, 308–324.

Zhao, X.-m., Z.-y. Gao, and B. Jia (2007). The capacity drop caused by the combined effect of the intersection and the bus stop in a ca model. *Physica A: Statistical Mechanics and its Applications 385*(2), 645–658.

Zheng, J., G. Zhang, Y. Wang, and P. M. Briglia Jr (2009). Evaluation of transit signal priority using observed and simulated data. *ITE Journal 79*(11).

Zhu, H. (2010). Numerical study of urban traffic flow with dedicated bus lane and intermittent bus lane. *Physica A: Statistical Mechanics and its Applications 389*(16), 3134–3139.

Zlatkovic, M., A. Stevanovic, P. T. Martin, and I. Tasic (2012). Evaluation of transit signal priority options for future bus rapid transit line in west valley city, utah. *Transportation Research Record: Journal of the Transportation Research Board 2311*(1), 176–185.

Zlatkovic, M., A. Stevanovic, and R. Reza (2013). Effects of queue jumpers and transit signal priority on bus rapid transit. In *Transportation Research Board 92nd Annual Meeting*, Number 13-0483.

Zyryanov, V. and A. Mironchuk (2012). Simulation study of intermittent bus lane and bus signal priority strategy. *Procedia-Social and Behavioral Sciences 48*, 1464–1471.